CONTENTS

Scientific/Technical Articles

Department of Veterans Affairs

Vol. 30 No. 2
1993

Journal of Rehabilitation Research and Development

CONTENTS

Veterans Health Administration
Rehabilitation Research and Development Service

CALL FOR PAPERS

We would welcome submission of manuscripts in the fields of Prosthetics and Orthotics; Spinal Cord Injury and Related Neurological Disorders; Communication, Sensory and Cognitive Aids; and, Gerontology. Guidelines for submission of manuscripts may be located on page ii.

Editor
Tamara T. Sowell

EXPANSION OF THE LETTERS TO THE EDITOR SECTION

Interested readers are encouraged to engage in an exchange of information through this Section.

Letters should relate specifically to material published in the *Journal of Rehabilitation Research and Development.*

Authors of the article(s) in question will be asked to respond.

Journal of
Rehabilitation
Research and Development

VOL. 30 NO. 2 1993

For sale by:

Superintendent of Documents, U.S. Government Printing Office (GPO)
Washington, DC 20402.
Available in microfilm from University Microfilms International, Inc.

Indexed by:

- Engineering Index (Bioengineering Abstracts)
- Excerpta Medica
- Index Medicus
- The BLDOC System (French)
- Index to U.S. Government Periodicals (Infordata Int., Inc.)
- Social Science Index, WILSONDISC Databases (H.W. Wilson Co.)
- SPORT Database / SPORT Discus (Canadian)

Library of Congress Catalog Card No. 6.60273
ISSN 0007-506X

The *Journal of Rehabilitation Research and Development* is a quarterly publication of the Rehabilitation Research and Development Service, Department of Veterans Affairs. The opinions of contributors are their own and are not necessarily those of the Department of Veterans Affairs. Address correspondence to: Editor, *Journal of Rehabilitation Research and Development*, Scientific and Technical Publications Section, VA Rehabilitation Research and Development Service, 103 South Gay Street, Baltimore, MD 21202-4051.

The *Journal of Rehabilitation Research and Development* and its supplements are printed on acid-free paper, as of Vol. 25 No. 2 (Spring 1988).

Journal of Rehabilitation Research and Development

NOTICE TO CONTRIBUTORS

Purpose and Scope

The *Journal of Rehabilitation Research and Development*, published quarterly, is a scientific rehabilitation engineering, research and development publication in the multidisciplinary field of disability rehabilitation. General priority areas are: Prosthetics and Orthotics; Spinal Cord Injury and Related Neurological Disorders; Communication, Sensory and Cognitive Aids; and, Gerontology. The *Journal* receives submissions from sources within the United States and throughout the world.

Only original scientific rehabilitation engineering papers will be accepted. Technical Notes describing preliminary techniques, procedures, or findings of original scientific research may also be submitted. Letters to the Editor are encouraged. Books for review may be sent by authors or publishers. The Editor will select reviewers.

Review Process

All scientific papers submitted to the *Journal* are subject to critical peer review by at least two referees, either editorial board members or ad hoc consultants, who have special expertise in a particular subject. To ensure objectivity, anonymity will be maintained between the author(s) and the referees. The final decision as to the paper's suitability for publication rests with the Editor of the *Journal*.

Originality

Authors must confirm that the contribution has not already been published by or submitted to another journal. The submission letter must be signed by all authors.

Instructions to Contributors

Manuscripts should meet these requirements: 1) Papers must be original and written in English. 2) Manuscripts must contain an Abstract, Introduction, Method, Results, Discussion, Conclusion, and References. 3) Manuscripts are to be typewritten on good quality 8½ x 11 inch white paper double-spaced, with liberal margins. 4) A 3½ or 5¼ inch floppy disk (nonreturnable) preferably in IBM-PC format—generic ASCII text (if using other software version, label disk accordingly) should accompany the hard copy. If using Macintosh, please so advise in cover letter. The length of a manuscript will vary, but generally should not exceed 20 double-spaced typed pages.

Abstracts: An Abstract of 150 words or less must be provided with the submitted manuscript. It should give the factual essence of the article and be suitable for separate publication in index journals.

Key Words: Three to ten key words, preferably terms from the Medical Subject headings from Index Medicus should be provided.

Illustrations: In preparing original drawings or graphs, authors should use black or India ink. Professional lettering is required. Lettering should be large enough to be read when drawings are reduced. Black and white computer-generated graphics are acceptable. Five-by-seven-inch glossy print photographs are preferred; good black and white contrast is essential. Color photographs cannot be accepted. All figures should have legends, listed on a separate sheet. The number of illustrations should be limited to six. The same holds true for tables. These should be used with the sole intent of clarifying or amplifying the text.

References should be cited in the Vancouver style. They should be typed separately, double-spaced, and numbered consecutively in the order in which they are first mentioned in the text, with only one reference per number. The number appropriate to each reference should be included in parentheses at the proper point in the text. "Unpublished observations" or "personal communications," in which the author has secured the permission of the person cited, should be treated as footnotes and not be included in the numbering of references. Authors are responsible for the accuracy of their references. Please follow these sample formats:

Article. Gilsdorf P, Patterson R, Fisher S. Thirty-minute continuous sitting force measurements with different support surfaces in the spinal cord injured and able-bodied. J Rehabil Res Dev 1991;28:33-8.

Chapter in a Book. Wagner KA. Outcome analysis in comprehensive rehabilitation. In: Fuhrer MJ, ed. Rehabilitation outcomes. Baltimore: Brookes Publishing Co., 1987:233-9.

Published Proceedings Paper. Hammel JM, Van der Loos M. A vocational assessment model for use of robotics technology. In: Presperin JJ, ed. Proceedings of the 13th Annual RESNA Conference, 1990:327-8.

Tables should not duplicate material in text or illustrations. They should be numbered consecutively with Arabic numerals cited in the text. Each table should be typed double-spaced on a separate sheet and should have a brief title. Short or abbreviated column heads should be used and explained, if necessary, in footnotes.

Mathematical Formulas and Specialized Nomenclature: Traditional mathematical treatments should be extended by adding brief narrative notes of explanation and definitions of terms, as appropriate, to ensure that readers of other disciplines gain the fullest understanding of the material presented. The International System of Units (SI) are requested for use in all quantities in text, tables, and figures.

Permissions and Copyright

Articles published and their original illustrations (unless borrowed from copyrighted sources) are in the public domain. Borrowed illustrations must contain full information about previous publication and credit to be given. Authors must obtain permission to reproduce figures, signed release forms for use of photographs containing identifiable persons, and submit originals of those signed documents with the manuscript.

Review of Proofs

Galley proofs will be sent to the first-named author, unless otherwise requested. To avoid delays in publication, galleys should be checked immediately and returned to the publishers by express mail within five working days.

Reprints Policy/Procedures

The VA will provide 100 reprints free of charge to the first-named author (or other designated corresponding author) of published articles at the time of *Journal* distribution.

Manuscripts should be submitted to:

Editor, *Journal of Rehabilitation Research and Development*
Scientific and Technical Publications Section (117A)
103 South Gay Street — 5th floor
Baltimore, MD 21202-4051
Telephone: (410)962-1800
Fax: (410)962-9670

Department of Veterans Affairs

Journal of Rehabilitation Research and Development

Volume 30, Number 2, 1993

The *Journal of Rehabilitation Research and Development* is a publication of the Rehabilitation Research and Development Service, Scientific and Technical Publications Section, Veterans Health Administration, Department of Veterans Affairs, Baltimore, MD

Department of Veterans Affairs

Journal of Rehabilitation Research and Development
Vol. 30, No. 2 1993

CONTENTS

EDITOR'S NOTE

Dudley S. Childress, PhD, is an internationally recognized electrical/biomedical engineer in the field of motor control mechanisms that power both above- and below-elbow prostheses. He was a pioneer in the development of myoelectric prosthetic hand replacements and designed the Northwestern Supracondylar Socket design for the below-elbow amputee. His most recent design is the (soon to be commercially available), myoelectric NU/VA Synergetic Prehensor for the upper-limb amputee. In the area of lower-limb prosthetic development, Dr. Childress is well-known for his recent work in the Automated Fabrication of Mobility Aids (AFMA) program, developed by his team at the Rehabilitation Engineering Center, Northwestern University, Chicago, IL, along with, and in partnership with, Ernest Burgess, MD, world-renowned surgeon, Seattle, WA and H. Richard Lehneis, PhD, CPO, international expert in lower limb prosthetic design and development, of New York University Medical Center, New York, NY.

Throughout the years Dr. Childress has been awarded many honors, far too many to list in their entirety. They include the Distinguished Service Award from the Congress of Organizations for the Physically Handicapped (1980); Fellow, at the RESNA International Conference (1988); Fellow of the International Society of Prosthetics and Orthotics (ISPO, 1990); and in 1993, he was appointed an honorary member of the American Academy of Orthotists and Prosthetists. He is a founding Fellow of the American Institute of Medical and Biological Engineers (AIMBE), 1992. Dr. Childress has been and is a prolific writer and has contributed more than his share to the scientific literature in peer-reviewed journals, text books on principles of rehabilitation medicine, amputation, prosthetics, and an orthopedic atlas.

Above all, Dr. Childress has been a technical/scientific advisor to the Department of Veterans Affairs Rehabilitation Research and Development Service for many years. His knowledge of the service-connected-injury amputee and their rehabilitation needs is exemplary. He is a man of great vision who is truly concerned with the quality of life of the veteran population. We are proud that he has agreed to write an editorial for the *Journal of Rehabilitation Research and Development.*

The field of rehabilitation research and development thank you, Dr. Childress, for your ongoing dedication to the needs of our nation's veterans.

Tamara T. Sowell
Editor

GUEST EDITORIAL

Medical/Technical Collaboration in Prosthetics Research and Development

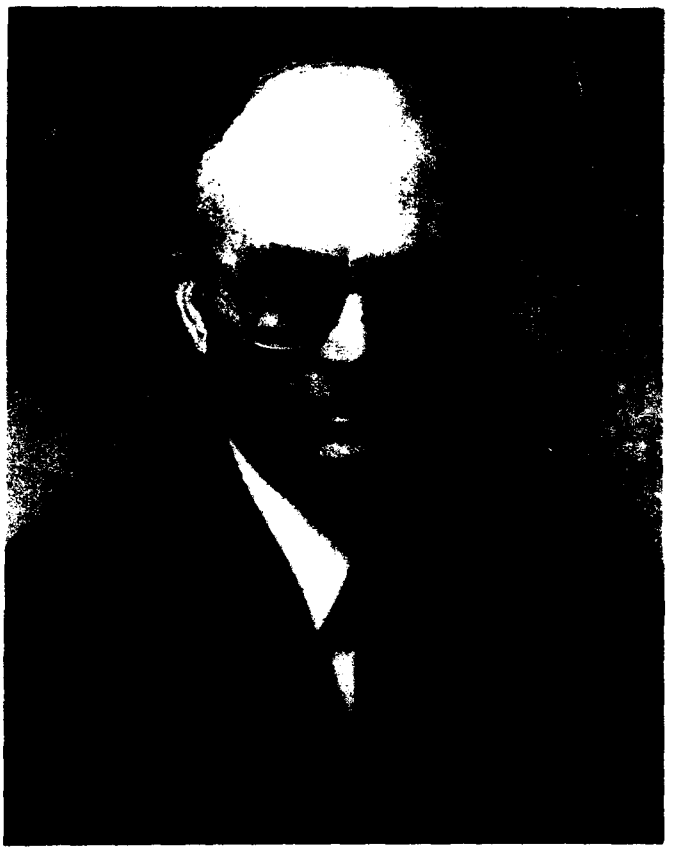

Dudley S. Childress, Ph.D.

Director, Northwestern University, Prosthetics Research Laboratory, Chicago, IL; Director of Prosthetic Research, VA Medical Center, Lakeside, Chicago, IL

The recent successes of Professor Per-Ingvar Brånemark and his team in Göteborg, Sweden with human direct skeletal attachments for arm and leg prostheses may herald a new era in the field of limb prosthetics. Direct skeletal attachment has long been a hope of practitioners in the limb prosthetics field. It is too early at this point to know what the long-range impact of the preliminary Swedish work in this area may be. Nevertheless, the group in Sweden is well-advanced with this potentially valuable technique and their previous successes with dental implants in the jaw to support artificial teeth and with attachments to the skull for support of maxillofacial prostheses indicates that the approach is well-founded. One thing is apparent, direct skeletal attachment of limb prostheses exemplifies the possibilities that can come about through interdisciplinary research and development activities.

Interdisciplinary research and interdisciplinary clinical care have long been hallmarks of the limb prosthetics field and of the rehabilitation field in general. However, over the last 10 to 15 years, a gap seems to have developed between people in limb prosthetics and those in the biomedical/surgical community. The probable causes of this gap are multifactorial and are not addressed here. The result of this gap has been that the field of prosthetics has been technology-driven for more than a decade. While an obsession with technology can be beneficial, the focus of the field should not be so narrow that it reduces input by surgeons or that it reduces input from the general biomedical community. In the long run, diminished interaction between the technical side of prosthetics and the biomedical/surgical side is likely to be detrimental to the advancement of the limb prosthetics field. It is time for investigators from various disciplines to build new relationships, or to rebuild old ones; to develop new approaches to problems of body prosthesis integration.

Historically, physicians/surgeons have been heavily involved in the prosthetics field not only in amputation but also with other function-enhancing procedures. The work of Sauerbruch, Lebsche, Kessler, and others on tunnel cineplasty comes quickly to mind. Also, we are aware of the effectiveness of the Krukenberg procedure when it is needed. Marquardt's development of the angle osteotomy is an example of more recent vintage. The work of Burgess in the USA, and many other orthopaedic surgeons here and abroad, in the appropriate surgical management of amputations is well-known. Nonetheless, it seems that the most recent surgical advances of vascular surgery, plastic surgery, neurosurgery, hand surgery, and general

Journal of Rehabilitation Research and Development Vol. 30 No. 2 1993

orthopaedic surgery have not, in recent years, influenced limb prosthetics to the extent that might be expected. There have been few systematic team efforts to integrate available prosthetics technology with new surgical possibilities. Furthermore, few new technologies are being developed to complement new surgical capabilities.

It is interesting to speculate about the possibilities of direct muscular attachment being used in combination with direct bone attachment. The first skeletally attached below-elbow prosthesis, fitted in Sweden, used myoelectric control, but improved control might be possible though more direct means. Robert Beasley, MD, a hand surgeon associated with New York University, has demonstrated the feasibility of exteriorized tendons, which, like tunnel cineplasties, make it possible to bring muscle forces directly outside the body. This kind of control has the potential of considerably enhanced proprioception through direct muscle connections. The intimate integration of bone and muscle with prosthesis structure and control has considerable potential to move human/prosthesis function to a new level of performance, but the development of such systems requires collaborative efforts.

Many persons with hand loss inquire about the future possibilities of control of individual artificial fingers in meaningful, coordinated ways. Intimate connections with muscles in such a way as to take advantage of their natural proprioception is one way such control may be brought about. These ideas may also be of considerable benefit for persons with high-level arm loss, particularly bilateral high-level loss.

This editorial is a call for new—or for renewed—collaboration between people in the limb prosthetics field and people in biomedical/surgical fields. Many possibilities exist beyond the examples already cited. It is hoped that increased collaboration of the kind proposed will result in deft prostheses that have natural proprioception. The objective of this kind of collaborative work should be limb prostheses that permit persons to make meaningful, multifunctional, coordinated movements with little mental effort and with minimal visual supervision.

Dudley S. Childress, Ph.D.

Clinical Relevance for the Veteran

SUMMARY OF SCIENTIFIC/TECHNICAL PAPERS IN THIS ISSUE

Normal and Shear Stresses on a Residual Limb in a Prosthetic Socket During Ambulation: Comparison of Finite Element Results with Experimental Measurements. Joan E. Sanders, PhD and Colin H. Daly, PhD *(p. 191)*

Purpose of the Work. The mechanical stress at the interface of the residual limb and prosthetic socket is a cause of skin breakdown in lower-limb amputees. The purpose of this study was to develop and evaluate a computer-based model of the residual limb and socket to predict interface normal stresses and shear stresses on below-knee amputees during ambulation, a potentially useful prosthetic design and fitting tool. **Subjects and Procedures.** To develop the model, data from a single male unilateral amputee subject was used, and the ANSYS® (Swanson Analysis System, Houston, PA) finite element code was employed. **Results.** Results were encouraging in that at some sites the shapes of analytical and experimental interface stress waveforms were similar in that they were double-peaked with some distinct features apparent. However, quantitative comparisons indicate that further model development is needed and suggest that primary attention should be concentrated on more accurate mathematical descriptions of the stump-socket interface region and tissue material properties. **Relevance to Veteran Population.** Being able to predict the sites on a prosthetic socket which might cause shear on the skin when a veteran amputee is walking, could eliminate potential skin breakdown in that area which could prevent the client from being able to continue walking.
Joan E. Sanders, PhD

A Technical Brief: Modelling the Mechanics of Narrowly Contained Soft Tissues: The Effect of Specification of Poisson's Ratio. William M. Vannah, PhD and Dudley S. Childress, PhD *(p. 205)*

Purpose of the Work. The purpose of this study is to demonstrate that the mechanics of soft tissue held in a narrow space (such as a residual limb in a prosthetic socket) are strongly sensitive to small changes in compressibility. **Subjects.** None. **Procedures.** A series of finite element models (having definite limits or boundaries) using differing Poisson's ratios (the ratio of transverse to longitudinal strain in a material under strain) is employed to illustrate the sensitivity effect. **Results.** For the case of a simplified above-knee socket model, changing Poisson's ratio from 0.45 to 0.50, results in a two-fold and five-fold change in the calculated reaction force and tissue stresses, respectively. **Conclusion.** Small changes in Poisson's ratio can strongly affect the results of mechanical analyses of narrowly contained soft tissues, such as a residual limb in a prosthetic socket. **Relevance to Veteran Population.** Relevant examples of narrowly contained soft tissues are those in prosthetic sockets, wheelchair seating, and orthotic footwear. Use of the more accurate analytical technique by researchers may enable us to more clearly understand the mechanics of soft tissue support, leading to fundamentally improved, better fitting, and more comfortable designs in the aforementioned prosthetic sockets, orthotic footwear, and wheelchair seating.
William M. Vannah, PhD

Basic Gait Parameters. Reference Data for Normal Subjects 10-79 Years of Age. Tommy Öberg, MD, PhD; Alek Karsznia, PT, PhD; Kurt Öberg, PhD *(p. 210)*

Purpose of the Work. The basic gait parameters most frequently used are gait speed, step length and step frequency. If such measurements are used for evaluation of pathological gait, the results must be compared with reference data from healthy subjects. The aim of this study was to provide such reference data. **Subjects.** 233 healthy subjects, 116 men and 117 women, 10-79 years of age. **Procedures.** Gait was tested on a 10 m walkway in a gait laboratory. Gait parameters were calculated for the middle 5.5 m, acceleration and deceleration distances were

excluded at the ends. **Results.** Mean, standard deviation, coefficient of variation, 95% confidence intervals and 95% prediction intervals are presented in an appendix. Significant sex differences exist in all gait parameters. In a two-way analysis of variance model there was a statistically significant age variability for gait speed and step length at normal and fast gait, but not for step frequency. In the step length parameter, there was a significant interaction effect of age and sex at normal and fast gait. **Relevance to Veteran Population.** The reference data are considered valid in an indoor laboratory situation. If gait analysis is used for evaluation of gait ability in disabled veterans, and in the disabled community in general, comparison must be made with data from healthy people. This study provides such normative data which makes it easier for the clinician to evaluate what is different about the veteran's gait. The gait evaluation must be done in a gait laboratory to insure validity.
Tommy Öberg, MD, PhD

Characterization of the Dynamic Stress Response of Manual and Powered Wheelchair Frames. J.D. Baldwin, MS and J.G. Thacker, PhD *(p. 224)*

Purpose of the Work. A common thought in random fatigue analysis is that the stress history in a structure matches a consistent statistical assumption. This statistical assumption is known as a stationary narrow band Gaussian random process (SNG). This investigation sought to determine the validity of the SNG assumption for dynamically loaded wheelchairs. **Subjects.** One nondisabled male. **Procedures.** Two folding wheelchairs, one manual, one electrically powered, were instrumented with strain gages near the cross tube pin and operated over four different laboratory terrains. The stresses were computed and statistical hypothesis tests were performed to determine whether the stresses were consistent with the SNG process. **Results.** Summary data for two strain gage locations on each wheelchair suggest that the stress can be considered stationary, but neither narrow-banded nor Gaussian distributed. **Conclusion and Discussion.** These findings indicate that the SNG model for random fatigue testing may not be valid for the wheelchairs and terrains investigated here. These results should caution designers about using the SNG assumption in fatigue analyses. **Relevance to Veteran Population.** The veteran is concerned about how long his wheelchair will last and under what conditions will certain areas fail (such as near the cross pin). Some of the fatigue testing figures being given in laboratories are not valid for certain terrains. The veteran would like to know, before he or she purchases a chair, under what conditions/terrains the chair will or will not hold up.
J.D. Baldwin, MS

Design of a Composite Monocoque Frame Racing Wheelchair. Michael S. MacLeish, MS; Rory A. Cooper, PhD et al. *(p. 233)*

Purpose of the Work. Monocoque shapes may improve the performance of racing wheelchairs. Monocoque is a type of construction in which the outer skin carries all or a major part of the stresses. A monocoque vehicle is one in which the body is integral with the chassis. The purpose of this study was to design a unibody frame racing wheelchair through the use of engineering technology. **Subjects.** One subject was used to represent the racing chair pilot. **Procedures.** A finite element analysis model created with the help of a computer helped point out problems in the design of unibody frame racing wheelchairs. Slight modifications can be made to the model to try different shapes, to see how much weight it could carry, or to use different materials in its construction. **Results.** A prototype was built and tested. While repeated use in racing competitions is still to be done, it has been indicated through this study that the application of engineering technology can improve the design of racing wheelchairs. **Relevance to Veteran Population.** Many veterans participate in and enjoy the sport of wheelchair racing. The sport has been instrumental in promoting the abilities and potential of people with disabilities. Racing wheelchair design has made significant contributions to the improvement of nearly all wheelchairs in use today. By seeking to further improve performance in the racing chairs, wheelchairs designed for daily use may also benefit.
Rory A. Cooper, PhD

The Analysis of Sweat During Soft Tissue Breakdown Following Pressure Ischemia. Adrian Polliack, BS; Richard Taylor, PhD; Dan Bader, PhD *(p. 250)*

Purpose of the Work. This paper examines the nature of sweat by-products collected from soft tissues subjected to mechanical loading for long periods of time. **Procedures.** This loading was produced by 1) external application on the forearm and 2) buttocks support when seated in a wheelchair and sacral support when lying on an examination bed. Sweat pads were attached to the supported tissue areas of a group of able-bodied subjects. After a prescribed period the pads were removed and a quantitative analysis of the biochemical composition of sweat was performed. **Results.** Tissues subjected to pressure, which cut off blood supply to the body part, produced a general increase in concentrations of by-products such as lactate, chloride, ureas and urate, all associated with a decreased sweat rate which are noxious to the body if they are not flushed away. In the refilling of blood to the part when the load was relieved, some of these by-products were washed away. It is proposed that specific biochemical by-products remaining in the area too long may be used as an indicator of soft tissue damage. **Relevance to Veteran Population.** This technique may provide a simple means of identifying veterans and others in the disabled community who are at risk of developing pressure sores by analyzing the sweat content produced at at-risk areas of the body, such as the buttocks and/or sacrum. This is one of the primary reasons why it is important for those people who have lost sensation and motion in parts of their body subjected to mechanical loading to periodically change position (e.g., when sitting in a chair or lying in bed) so as not to keep pressure on any one area of the body for too long a time.

Dan Bader, PhD

Department of Veterans Affairs

Journal of Rehabilitation Research and Development Vol. 30 No. 2 1993
Pages 191-204

Normal and shear stresses on a residual limb in a prosthetic socket during ambulation: Comparison of finite element results with experimental measurements

Joan E. Sanders, PhD and Colin H. Daly, PhD
Center for Bioengineering and Department of Mechanical Engineering, University of Washington, Seattle, WA 98195; Prosthetics Research Study, Seattle, WA 98122

Abstract—Interface stresses on a below-knee amputee residual limb during the stance phase of gait calculated using an analytical finite element model were compared with experimental interface stress measurements. The model was quasi-static and linear. Qualitatively, shapes of analytical and experimental interface stress waveforms were similar in that they were double-peaked with some distinct features apparent. However, quantitatively analytical resultant shear stress magnitudes were less than experimental values at all transducer measurement sites. Analytical normal stresses were less than experimental values at postero-proximal, postero-distal, and antero-medial proximal sites, but were greater than experimental values at antero-lateral distal and antero-lateral proximal sites. Anterior resultant shear angles were directed more distally in the model than in clinical data, an expected result since there was no relief for the tibial crest in the model. Model sensitivity analyses to shank loads showed interface normal and resultant shear stresses were most sensitive to axial force, sagittal bending moment, or sagittal shear force. The finite element model presented in this paper is significant because it contributes toward development of an analytical modeling technique to predict interface stress distributions for proposed prosthetic designs, provides insight into physical explanations of features apparent in interface stress waveforms (thereby enhancing understanding of interface mechanics), and provides insight into nonlinear characteristics that need to be added to improve the model.

Keywords: *amputee interface, finite element modeling, interface stress, prosthetics.*

INTRODUCTION

A prosthetic limb is a common rehabilitation treatment to replace function lost as a result of lower-limb amputation. This treatment places heavy demands on residual limb soft tissues. Rather than supporting the body weight load on the plantar surface of the foot, an amputee is forced to tolerate the entire load of body weight at the interface of the residual limb and the prosthetic socket, an area of skin tissue that is not usually subjected to such intensive magnitudes of normal and shear stress. Possible skin responses to these high stresses are: 1) an inflammatory response followed by necrosis and ulceration; or, 2) an adaptation process in which skin becomes durable and load-tolerant. Thus, tissue response to ambulation with a prosthesis can be separated into a two-step process. First, normal and shear stresses are generated at the interface of the residual limb and the prosthetic socket. Second, residual limb tissues respond to interface stresses by either adapting to become load-tolerant or else undergoing an inflammatory response and breaking down.

Address all correspondence and requests for reprints to: J.E. Sanders, PhD, Assistant Professor, Center for Bioengineering, WD-12, University of Washington, Seattle, WA 98195.

This investigation was supported by the Department of Veterans Affairs Rehabilitation Research and Development Service, Washington, DC; the Whitaker Foundation; and the University of Washington.

Journal of Rehabilitation Research and Development Vol. 30 No. 2 1993

The first part of this two-step process is addressed in this paper. We have developed an analytical model using the finite element (FE) method that predicts interface normal and shear stresses during ambulation based on characteristics of the amputee, as well as shape and mechanical properties of the prosthesis made by the prosthetist.

The model is an extension of models previously reported in the literature. Linear static models have been developed in order to investigate interface stress distributions during standing and their sensitivity to prosthesis and residual limb characteristics. Pearson's (1) conically-shaped below-knee model analysis used rigid body mechanics to demonstrate that distal cavity pressure was highly sensitive to the interface coefficient of friction. Nissan's (2) short-below-knee stump model was based on cadaver bone geometry measurements and static equilibrium equations. Results from this analysis showed that interface forces were highly sensitive to stump length and socket recesses. More recently, Silver-Thorn (3) found that, under the specific conditions she tested, interface pressure errors determined with a generic geometry FE model were of similar magnitude to those determined from a model with a more accurate representation of residual limb geometry (plaster casts and computer tomography scans), suggesting that model errors were not due to geometric factors, but instead, to material property or boundary condition assumptions. Mak (4) evaluated the adequacy of an elliptical model and an axisymmetric model by comparing interface stress results with those from a 3-dimensional model. Results for the elliptical and axisymmetric models were similar. Quesada (5) developed a finite element model of a below-knee prosthesis of patellar-tendon-bearing design and showed that a 14 percent reduction in interface normal stress at antero-distal and posterior sites was possible with a 10 times reduction in the elastic modulus of the liner material. Winarski (6) demonstrated that there existed a flexion-extension alignment angle that minimized amputee mechanical energy expenditure. Using two test subjects, the investigators demonstrated that this optimal adjustment was very close to the design point set by certified prosthetists.

Krouskop (7), Steege (8), and Torres-Moreno (9) pursued research methodologies that were directed toward incorporating FE models directly into prosthetic design. For Krouskop (for above-knee amputees), and Steege (for below-knee amputees), a user would specify a desired pressure pattern on a residual limb for static alignment conditions, and then a FE model would calculate the socket shape necessary to induce that pressure pattern. Krouskop reported that his model was used 'effectively' to fit two above-knee amputee subjects. Steege's model used constant dilatation elements for tissue as described in detail by Silver-Thorn (10). An iterative removal of constraints was used on surface elements that went into tension. Steege noted that model results were sensitive to tissue stiffness and to underlying tendinous and bony structures of the residual limb. Steege's model is still in a developmental stage; it has not yet undergone clinical evaluation on a population of amputee patients. Torres-Moreno has an above-knee amputee model at a similar developmental stage that shows good correlation between measured standing pressures and model predictions.

The FE model presented in this paper is an extension from previous models in that it addresses interface stresses during ambulation. Ambulation-induced interface stresses are of primary clinical interest because tissue breakdown and the subsequent functional impairment occur more often as a result of ambulation than from standing. Two important simplifying assumptions are made in the model described in this paper: it is quasi-static and it is linear. These assumptions reduce computational intensity, and make it possible to superpose model results for different shank load vectors to generate waveforms for the entire stance phase. Stance phase model results are then compared with stance phase experimental measurements and the following hypotheses are tested:

(i) The model accurately predicts, within instrumentation error, interface stress magnitudes and waveform shapes;

(ii) Model interface stresses are significantly different for a skin moduli of 3.5 kPa compared with a skin moduli of 6.9 kPa;

(iii) Model interface stresses are most sensitive to prosthetic shank axial force, sagittal shear force, and sagittal bending moment, and are relatively insensitive to other force directions in the shank.

By addressing these hypotheses, the model is evaluated, physical understanding of interface me-

chanics is improved, and model characteristics that need or do not need further specification are identified, setting directions for further model development. The long-term goal is an analytical tool that can be used to predict interface stress distributions for proposed socket designs for use in both clinical treatment and prosthetics research.

METHODS

A FE model was developed for one unilateral below-knee amputee subject who underwent interface stress measurement studies at approximately the same time. The subject was 23 years of age, 178 cm tall, 65.9 kg in weight, and had suffered a traumatic injury as the cause of his amputation. He had been an amputee for 4 years and was using a total contact socket of patellar-tendon-bearing design along with Seattle™ System (Model and Instrument Development, Seattle, WA) shank, ankle, and foot components at the time of the study. He regularly used a latex sleeve suspension. By putting a thin layer of powder in the bottom of the socket and then having the subject ambulate, it was demonstrated that he did not distal end-bear: there was no powder transfer to the residual limb. By clinical examination, he had a very bony stump with little soft tissue, especially distally.

The three inputs required for FE model development were determined as follows:

1. *Geometries.* Magnetic resonance (MR) imaging was conducted to determine residual limb tissue geometries. The subject was positioned supine in a 1.5 Tesla magnet (Signa, General Electric) with his residual limb in the same socket used for interface stress measurement. His legs were positioned parallel to each other, and his knees were put in approximately 5 degrees of flexion. The posterior socket surface was supported laterally and posteriorly with foam blocks, taking care to ensure that the supporting load was well-distributed over the posterior socket surface so that minimal bending moment was induced on the residual limb within the socket. Nineteen axial cross-sectional images at 10 mm intervals and 15 coronal images at 12 mm intervals were collected in a 20-minute session. Though only axial images were used for mesh generation, coronal slices were used to ensure that there were not any gross bone or soft tissue abnormalities that were not apparent in axial images. The resolution of the system in the plane being sampled was 1 mm.

Contours at Pelite™/skin, skin/fat, skin/bone, skin/muscle, and muscle/bone interfaces were digitized from each axial cross-sectional image. The Pelite/hard socket interface was added to the model by generating contours outward normal to the Pelite/skin interface except at the distal end which was left as a free surface since the subject did not distal end-bear. The femur, tibia, and joint capsule were connected together and modeled as a single rigid body. The model was extended proximally partway up the thigh to ensure interface stress results were not affected by conditions at the edge of the model.

A FE mesh totaling 795 nodes and 840 elements was generated. Eight-node isoparametric brick elements were used for skin and fat (SF), muscle, and Pelite materials. Quadrilateral shell elements were used for the socket while beam elements were used for the shank. The bone and knee joint were assumed to be zero displacement surfaces; thus, no elements were generated for them. Evaluation runs were conducted to ensure element edge angles and element face warping were within acceptable levels. Element edge angles were within a 45° to 135° range. Warping factor, defined as (on an element face: distance from the first node to the fourth node parallel to the element normal)/(average thickness of the element) was less than 0.1 for most of the elements and less than 1.0 for all elements. Where necessary, brick elements were degenerated to wedges to ensure acceptable face angles and warping factors. Attempts were made to keep wedge elements to the central muscle region. In high stress gradient regions, evaluation runs with smaller element sizes were conducted to ensure convergence.

2. *Boundary Conditions.* Shank forces and moments were measured using an instrumented pylon (11) at the same time that interface normal and shear stress data were collected. The pylon was a 15.2 cm long 4.1 cm outer diameter aluminum tube with 20 strain-gages mounted in the central 4.5 cm to measure axial force, shear forces, bending moments, and torsional moment. During data collection sessions a 16-channel data acquisition system was used. Twelve channels were used for interface stress measurements (three channels for each of four transducers), leaving four channels available for shank force and moment measurement. In a data

collection session, either the two bending moments or the two shear forces were measured with axial force and torsional moment.

At the proximal end of the model, which was partway up the thigh, zero displacement conditions were specified for bone in the cross-section of the thigh. Soft tissues rested on elastic foundations. Because the proximal end of the model was far from the socket, stump/socket interface stresses were not affected by the zero displacement proximal boundary conditions. Zero displacement conditions were also specified on the surfaces of the tibia, femur, and joint capsule which, as described above, were connected together and specified as a single rigid body. Thus, the knee joint was not allowed to flex or extend over the course of stance phase. This was considered acceptable because the force boundary conditions were specified on the distal end of the model instead of on the proximal end; thus the direction of the applied load relative to the socket was not affected by the lack of knee flexion, and soft tissues were extended sufficiently proximally to avoid edge effects.

3. *Material Properties.* Material properties for SF and muscle were taken from the literature (12,13). Skin has been shown to be nonlinear and anisotropic, with a mechanical response that depends nonlinearly on changes in temperature, humidity, and stress history (12). These nonlinearities, however, were not accounted for in the current model, since computing time limitations required the model to be quasi-static and linear. All materials were assumed linear, homogeneous, and isotropic. A modulus of 5.2 kPa was specified for skin, while a modulus of 131 kPa was specified for muscle. A Poisson ratio of 0.49 was used for all soft tissues.

Material properties of vacuum-formed Pelite were measured experimentally under uniaxial compression. Load-deformation curves were nonlinear at low stress values, but an approximately constant slope of 1.8 MPa was measured at stresses between 20 kPa and 200 kPa. Since interface normal stress measurements were typically between 20 kPa and 200 kPa, a modulus of 1.8 MPa was used in the FE model. A Poisson ratio of 0.39 which was from handbook data was used.

Using the ANSYS® finite element package (Swanson Analysis Systems, Houston, PA), the model was run under unit loads for each of the six shank force and moment directions. Quasi-static waveforms of the stance phase of gait were generated by superposition. At time t in each waveform:

$$S_{jk}(t) = \sum_{i=1}^{6} (P_i(t))\,(U_{ijk})$$

where $S_{jk}(t)$ is stress in direction j at transducer site k, i is one of the six prosthetic shank loading directions, $P_i(t)$ is the measured prosthetic shank load in direction i, and U_{ijk} is interface stress per unit load in direction j at transducer site k for a unit shank load in direction i.

Details of the experimental data collection sessions with which model results in this paper are compared are described in detail elsewhere (14,15). Briefly, interface normal and shear stresses at four sites and four shank forces and moments were measured during walking trials on below-knee amputee subjects. The transducers were custom-designed by the investigators. They measured forces in three orthogonal directions applied to a 6.35 mm diameter sensing surface. The measured forces were divided by the transducer surface area to determine stresses. For biaxial force measurement in the plane of the transducer surface, a 1.5 mm square cross-section beam was instrumented with strain-gages to measure the difference in bending moment between gage sites (**Figure 1**). The beam supported a two-part

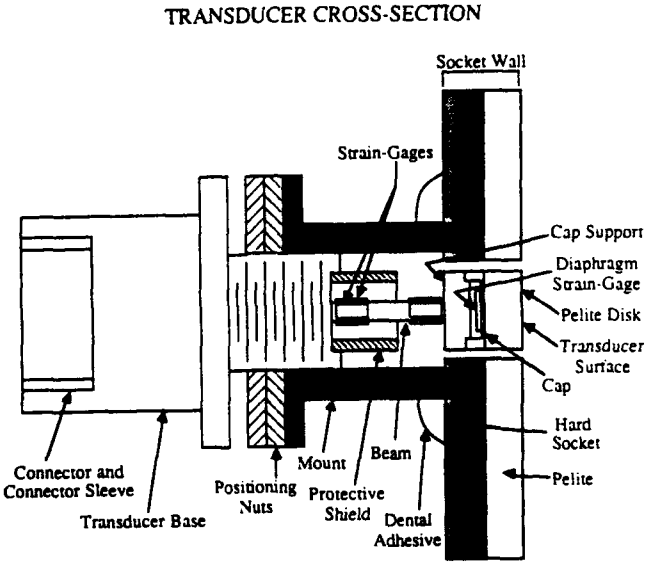

Figure 1.
A cross-sectional view of the transducer used to measure interface stresses in three orthogonal directions in data collection sessions.

short cylinder that was instrumented on its inside top surface with a diaphragm strain-gage. A 6.35 mm diameter disk of Pelite was affixed to the top of the transducer so that no foreign material was introduced to the residual limb. Instrumentation error for the transducers was 4.2 percent full-scale output for the normal direction, and 0.9 percent full-scale output for the shear directions (15).

For the subject data reported in this paper, two data collection sessions were conducted. For the first session, transducers were positioned at antero-lateral proximal, antero-lateral distal, antero-medial proximal, and postero-proximal sites, and prosthetic shank frontal shear force, sagittal shear force, axial force, and torsional moment were measured. In the second session, transducers were positioned at antero-lateral proximal, antero-lateral distal, antero-medial proximal, and postero-distal sites, and prosthetic shank frontal bending moment, sagittal bending moment, axial force, and torsional moment were measured. Subjects walked the length of an 18 m × 1.2 m pathway during a trial to the cadence of a metronome, and data were collected for 8 seconds during each trial. Only steps for which the subject achieved a cadence consistent with the metronome were used in analysis. Typically, the four or five central steps in a trial met this criterion. At least four trials were conducted at each of three angular alignment settings of the socket relative to the shank in the sagittal plane: 'plantarflexion,' 'zero,' and 'dorsiflexion.' The angular adjustments at the alignment jig were 12° for plantarflexion and 4° for dorsiflexion. No translational adjustment was made to accommodate foot displacement.

When comparing analytical data and experimental results, individual steps were analyzed rather than average steps. Because only four shank forces and moment waveforms were collected during a step, however, two shank waveforms needed to be added to each step to achieve a full set of force boundary conditions for the model. Each of the two missing shank waveforms was the average waveform for all steps at the same alignment collected in a different session. Average shank sagittal shear force waveforms for each of three alignments are shown in **Figure 2a**. As shown in the power spectra (**Figure 2b**), the standard deviations were greater for the higher frequency part of the waveform than the lower frequency components, a result found in all six force directions.

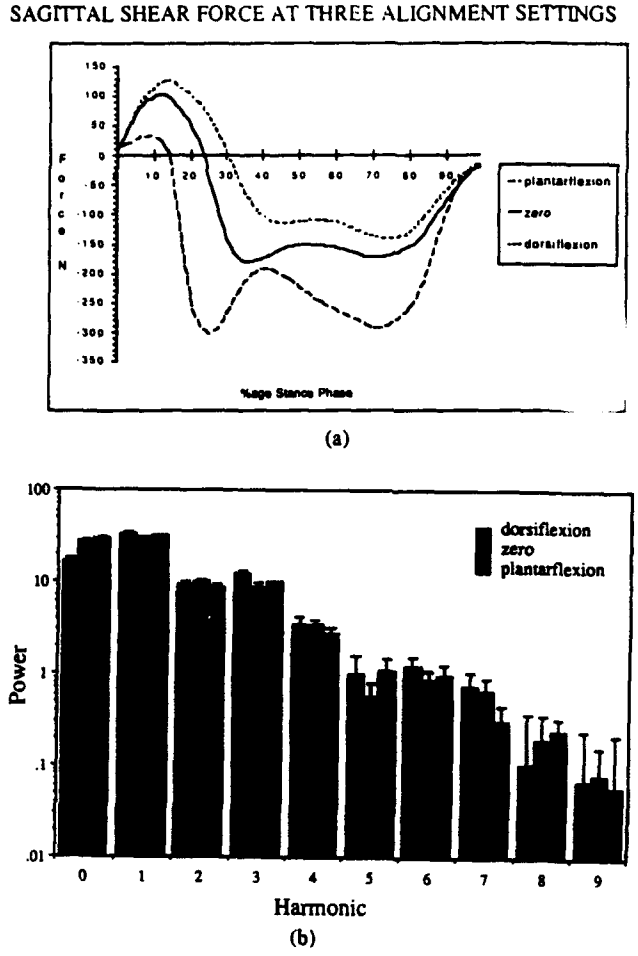

Figure 2.
(a) Sagittal shear force in the prosthetic shank for three alignment settings: dorsiflexion, zero, and plantarflexion; and *(b)* the corresponding power spectra. Three trials (five steps in each trial) are included for each of the three alignment settings.

Sensitivity Analyses

To evaluate sensitivity to prosthetic shank loading direction, interface stresses were calculated for each shank loading direction separately: *(i)* frontal shear force; *(ii)* sagittal shear force; *(iii)* frontal bending moment; *(iv)* sagittal bending moment; *(v)* axial force; and, *(vi)* torsional moment. Average peak maxima or minima, whichever had a greater absolute magnitude during stance phase, were used for each of the shank loading directions. Those values were −74.3 N, −180.3 N, 7.8 N-m, 55.4 N-m, 818.7 N, and 4.95 N-m for shank loading direction *(i)* to *(vi)* respectively. The coordinate system sign conventions are shown in **Figure 3a** and described below. Thus, the calculation provided an assessment of which shank loading directions most

significantly affected each transducer measurement direction, given the assumption that only maximal magnitude shank loads during stance phase were considered.

To evaluate model sensitivity to tissue material properties, model fits to experimental data were compared for different material property combinations. Model runs were carried out with E and G specifications listed in **Table 1**, which reflect ranges from the literature (12,13).

RESULTS

The following sign conventions are used for presentation of results. For the prosthesis coordinate system, axial force (z-direction) is positive when directed in the proximal direction, while sagittal shear force (y-direction), and frontal shear force (x-direction) are in the pylon cross-section in sagittal and frontal planes, respectively (**Figure 3a**). An anteriorly directed sagittal shear force on the foot is positive in sign and a laterally directed (right-legged amputee) frontal shear force on the foot is positive in sign. Sagittal bending moment and frontal bending moment are specified with respect to the center of the alignment jig in a sagittal and frontal plane, respectively. Torsional moment is about the shank axis. All moments are positive by a right-hand rule sign convention.

For each transducer, four stresses are defined (**Figure 3b**). 'Normal stress' is perpendicular to the interface, and 'resultant shear stress' is in the plane of the interface. Resultant shear stress is the resultant vector of two components: 1) 'horizontal shear' is in a transverse plane and is positive in the clockwise direction when viewing a socket from above; 2) 'vertical shear' is perpendicular to horizontal shear in the plane of the interface. It is positive when directed distally. Shear stresses applied to the transducers, as opposed to stresses applied to the residual limb, are positive in sign, and compressive stress on the skin is positive.

Comparison of Analytical and Experimental Data

Analytical interface stress curves were usually double-peaked, matching the general trend in clinical data. However, correlation within individual steps varied in quality among sites. Qualitatively, best matches were achieved at postero-distal and antero-proximal sites. Consistent mismatches were seen in antero-lateral distal normal stress waveforms, which became negative partway through stance, and postero-proximal normal stress waveforms, which showed minima instead of maxima at axial force and sagittal shear force first peaks.

Experimental and analytical (Model Case #1, **Table 1**) peak interface stress magnitudes during stance phase were compared. At the zero alignment, the model significantly ($p<0.05$, *t* test) underestimated posterior normal stress, antero-medial proximal normal stress, and all resultant shear stresses, except antero-medial proximal resultant shear stress. It significantly ($p<0.05$) overestimated antero-lateral distal normal stress and antero-lateral proximal normal stress. Differences between peak stress magnitudes for analytical vs. experimental results are shown in **Table 2**. Closest fits were achieved at postero-distal and antero-medial proximal sites. Instrumentation error, which was 4.2 percent full-scale output (FSO) for normal stress and 0.9 percent FSO for shear stress (15), was included in the above significance calculations.

Unlike clinical data (16), analytical data at all sites (except posterior normal stresses), showed significantly ($p<0.05$) different peak magnitude interface stresses for plantarflexion alignment setting results compared to zero alignment setting results. For dorsiflexion compared to zero alignment set-

Table 1.
Tissue material property combinations used in the analytical model.

MODEL CASE	E_{skin} (kPa)	G_{skin} (kPa)	E_{muscle} (kPa)	G_{muscle} (kPa)
1	5.2	1.7	131	44.0
2	6.9	2.3	131	44.0
3	3.5	1.2	131	44.0

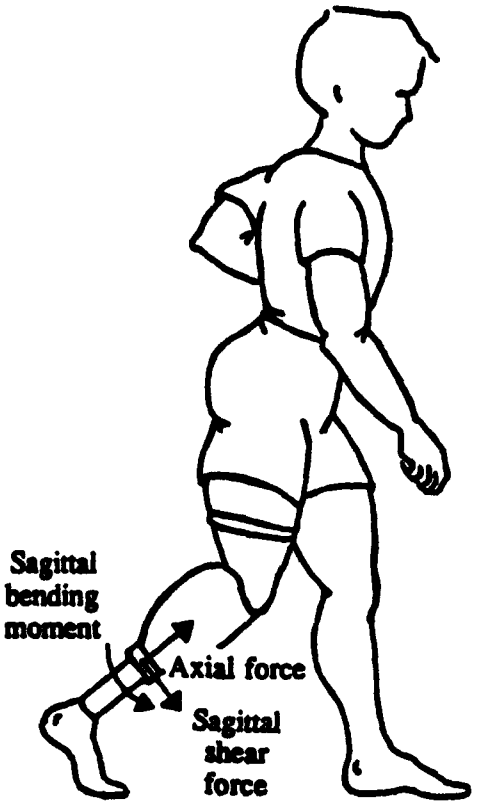

Figure 3a.
Sign conventions for prosthetic shank sagittal plane shear force, axial force, and sagittal bending moment are shown. The center of the alignment jig is the origin of the coordinate system.

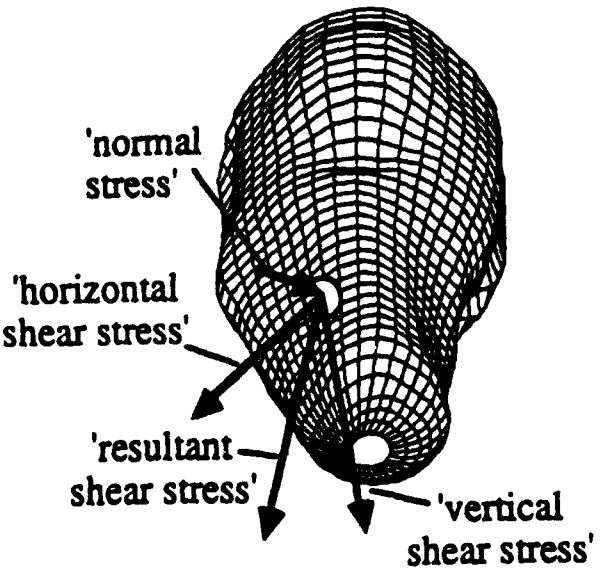

Figure 3b.
Sign conventions for normal stress, horizontal shear stress, vertical shear stress, and resultant shear stress are shown at an antero-lateral distal site. Note that the grid density for this figure is not the FE mesh size.

tings, antero-medial proximal normal stress and antero-lateral proximal resultant shear stress demonstrated significantly ($p<0.05$) different peak magnitudes, unlike clinical data where no significant difference was demonstrated for any site.

A comparison of resultant shear angles during mid-stance is shown in **Figure 4**. Resultant shear angles were directed more distally in analytical data than in clinical data at all sites. Analytically, the antero-lateral proximal site was the only anterior site not directed toward the midline of the tibia.

Though resultant shear angles did not match quantitatively, changes in resultant shear angle waveform shapes over the course of stance phase were similar in shape for clinical and analytical data (**Figure 5**). Resultant shear angle directions did not show consistent changes for different alignments in either clinical or analytical datasets.

In interface stress results from data collection sessions, there were characteristics in the waveforms that were repeated from one step to the next (17). Analytical matches with some of the characteristics of waveform shape are described below.

Loading Delays. 'Loading delays' were times of zero stress at the beginning of interface stress curves (**Figure 6**, first 12 percent of stance phase). They were due to a source other than low shank force and moment magnitudes. At 12 percent into stance phase in the steps shown in **Figure 6**, axial force is at approximately 300 N, more than 30 percent of its maximal value.

FE model data showed loading delays approximately of equal length to those found in clinical data in the same step (**Figure 6**). Exceptions were posterior normal stresses and antero-proximal resultant shear stresses which showed minimal or no loading delays in analytical data, though loading delays were present in experimental results. Also, antero-medial proximal normal stresses in analytical data were often negative during the loading delay phase, a result not found in experimental data.

In the model, loading delays were a result of the shank resultant force being directed antero-proximally. When sagittal shear force and axial force were both positive in sign (which was the case during loading delays, but not later in stance phase),

Table 2.
Comparison of analytical results with experimental data: 'under X%' = underestimated by X%; 'over Y%' = overestimated by Y%.

NORMAL STRESS					
	site				
alignment	postero-proximal	antero-medial proximal	antero-lateral proximal	antero-lateral distal	postero-distal
plantarflexion	under 90%	over 49%	over 95%	over 550%	under 16%
zero	under 89%	under 29%	over 63%	over 221%	under 25%
dorsiflexion	under 86%	under 83%	over 52%	over 197%	under 19%

RESULTANT SHEAR STRESS					
	site				
alignment	postero-proximal	antero-medial proximal	antero-lateral proximal	antero-lateral distal	postero-distal
plantarflexion	under 82%	under 19%	under 49%	under 51%	under 44%
zero	under 87%	under 11%	under 53%	under 74%	under 51%
dorsiflexion	under 88%	under 1%	under 57%	under 75%	under 54%

sagittal shear force contributed positively, and axial force contributed negatively to all normal stresses except those at posterior sites. Posterior sites were the only sites that did not show analytical normal stress loading delays. Thus, interface stress contributions from sagittal shear force and axial force on anterior interface stresses summed to zero during loading delay phases.

High Frequency Events. High frequency events (HFEs) were maxima or inflection points occurring partway up the rising parts of interface stress curves within the first 40 percent of stance phase. Two types of HFEs were found. Those early in stance, 'early HFEs' occurred within the first 12 percent of stance phase and matched up well with HFEs in shank force and moment waveforms, while those later in stance, 'late HFEs' usually occurred just before the shank resultant force shifted from being directed anterior of the midline to posterior of the midline. Thus, the source of early HFEs was HFEs in the prosthetic shank loads, while the source of late HFEs was a rotational shift in the sagittal plane of the residual limb within the prosthetic socket. In addition, the dynamic response of residual limb tissues could also have contributed to late HFEs.

Early HFEs were often present in analytical data when present in the corresponding clinical data waveforms, but they were usually not of the same magnitude (**Figure 7a, 7b**). In postero-proximal resultant shear stress, postero-distal resultant shear stress, antero-lateral distal resultant shear stress, and antero-lateral distal normal stress, timings of early HFEs usually corresponded to timings of early HFEs in prosthetic shank axial force and shear force waveforms.

Late HFEs were present in analytical results at some sites, but they were often shifted in time with respect to clinical data. For example, in **Figure 7a** clinical late HFEs occurred later than those in analytical data. **Figure 7b**, however, shows a case where late HFEs occurred simultaneously.

First Peaks. The timing of interface stress maxima occurred at or near the time of the prosthetic shank axial force and sagittal shear force

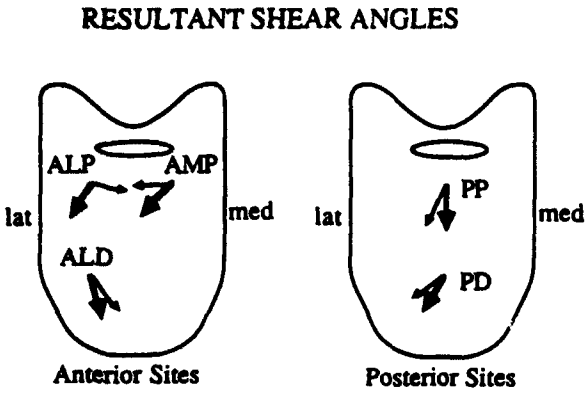

Figure 4.
Resultant shear direction on socket surfaces for clinical (thin arrows) and analytical results (thick arrows) during mid-stance. lat = lateral; med = medial.

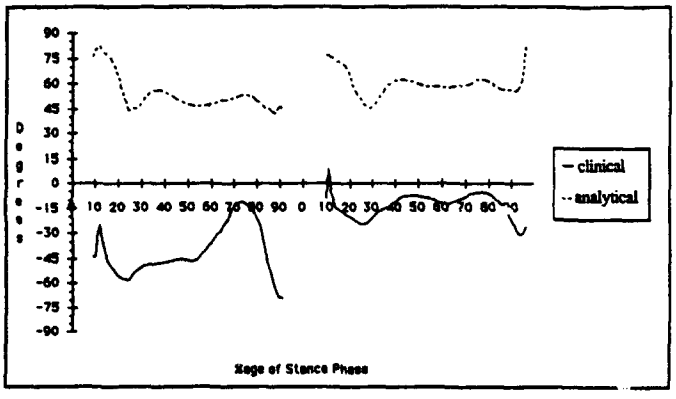

Figure 5.
Resultant shear angles at an antero-medial proximal site for clinical and analytical data during stance phase are shown from two consecutive steps with a zero alignment setting. Swing phase between the two steps, the first 8% of stance, and the last 8% of stance have been removed for clarity.

peaks, approximately the same as in clinical data. Exceptions were postero-proximal normal stress, antero-lateral distal normal stress, and antero-lateral distal resultant shear stress which, in model results, had negative slopes or were at minima at axial force and sagittal shear force peaks.

Unlike clinical data, peak magnitudes in the first half of stance phase in analytical results changed for different alignment settings. The following were significantly ($p<0.05$) lower for the dorsiflexion alignment setting compared with the plantarflexion setting: antero-lateral distal normal stress and resultant shear stress, and antero-lateral

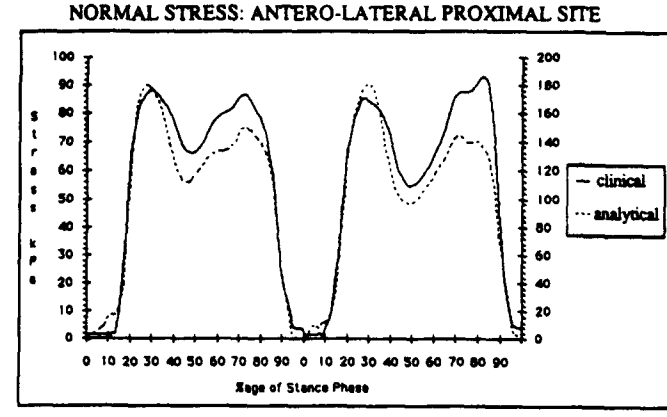

Figure 6.
Normal stress at an antero-lateral proximal site during stance phase of two consecutive steps at a plantarflexion alignment setting are shown. Stance phase between the steps has been removed for clarity. The left scale is for clinical data (solid line) and the right scale is for analytical data (dashed line).

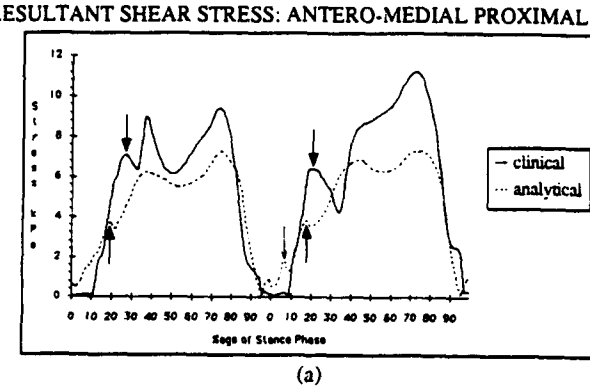

(a)

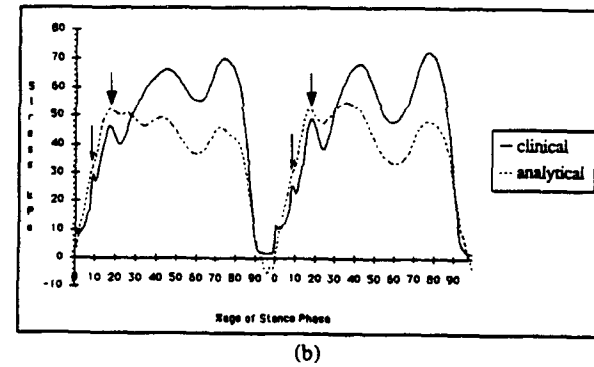

(b)

Figure 7.
Early HFEs are indicated with thin arrows while late HFEs are indicated with thick arrows. *(a)* Resultant shear stress at an antero-medial proximal site at a plantarflexion alignment setting. *(b)* Normal stress at a postero-distal site at a dorsiflexion alignment setting.

proximal normal stress. Antero-medial proximal resultant shear stress was significantly higher for dorsiflexion vs. plantarflexion alignments.

Central Stance. Model results were usually more underestimated during central stance (i.e., the time between the first and second peaks), compared with the rest of stance phase.

Toe-Off. In analytical data at anterior sites, interface stress waveforms at the antero-lateral distal site showed a maximum or a minimum right before toe-off that was not present in clinical data. This was because in the model, slip was not allowed between the residual limb and socket. Tension was induced during toe-off in skin elements that bordered the interface.

Analytical Model: Sensitivity Analyses

Prosthetic Shank Loading Directions. Analyses were conducted to evaluate sensitivity to prosthetic shank loading directions. **Table 3** shows model interface stress results for maximal magnitude shank loads for each of the six force and moment directions. Thus, the table provides an assessment of which shank loading directions most significantly contributed to horizontal shear, vertical shear, normal, and resultant shear stresses, given the assumption that only maximal magnitude shank forces and moments were considered.

There were several trends apparent (**Table 3**):

1. For all normal and resultant shear stresses, except antero-lateral distally, frontal shear force and frontal bending moment values were low compared to other directions;
2. For all vertical shear stresses, except at the antero-lateral distal site, interface stresses for axial force were at least twice that of any other shank force and moment direction;

Table 3.
Model interface stresses (in kPa) for maximal stance phase loads for each prosthetic shank force and moment direction.

		SHANK LOAD DIRECTION						
TRANS-DUCER SITE	STRESS DIRECTION	Frontal Shear Force	Sagittal Shear Force	Frontal Bending Moment	Sagittal Bending Moment	Axial Force	Torsion Moment	Total
antero-lateral proximal	horiz shear	0.02	−1.27	0.33	1.41	2.11	2.34	4.94
	vert shear	−1.04	−1.44	−0.59	1.88	6.94	−0.72	5.03
	normal	14.83	36.39	8.58	−37.24	119.24	27.06	168.85
	result shear	−1.04	−1.93	0.68	2.35	7.25	2.45	9.77
antero-lateral distal	horiz shear	1.31	−1.63	0.73	2.89	−3.07	1.14	1.36
	vert shear	1.12	1.90	1.36	−8.42	6.22	−0.21	1.97
	normal	107.19	198.35	71.96	−410.45	97.80	13.29	78.14
	result shear	−1.72	−2.51	1.54	8.90	6.94	1.16	14.30
postero-proximal	horiz shear	−0.30	−0.03	0.07	−0.02	−0.79	1.27	0.20
	vert shear	−0.28	1.08	−0.12	−1.83	5.05	0.09	4.00
	normal	−2.03	−12.68	1.05	5.07	11.62	4.84	7.88
	result shear	−0.41	−1.08	0.14	1.83	5.11	1.27	6.86
postero-distal	horiz shear	0.13	0.43	0.17	−0.91	2.11	0.87	2.79
	vert shear	−0.42	0.52	−0.15	−0.37	3.04	0.18	2.79
	normal	−0.55	−22.58	−0.68	17.17	62.19	−2.44	53.11
	result shear	−0.44	−0.67	0.23	0.99	3.70	0.89	4.69
antero-medial proximal	horiz shear	0.41	−0.16	0.42	0.22	2.18	1.72	4.78
	vert shear	−0.40	−2.32	−0.28	3.01	6.15	−0.72	5.43
	normal	−17.78	55.51	−10.44	−63.90	61.09	−20.39	4.10
	result shear	−0.57	−2.33	0.51	3.02	6.52	1.86	9.01

3. Except at the antero-lateral distal site, normal stresses were most sensitive to axial force, sagittal bending moment, and sagittal shear force. Resultant shear stresses were most sensitive to axial force, sagittal bending moment, and sagittal shear force at antero-lateral distal and antero-medial proximal sites, but were most sensitive to axial force, sagittal bending moment, and torsional moment at antero-lateral proximal, postero-proximal, and postero-distal sites.

It is important to note that the relative proportions of shank force and moment components changed over the course of stance phase. The results in **Table 3** are only an assessment at maximal shank force and moment magnitudes; thus, they were not necessarily reflective of the entire gait cycle.

Tissue Material Properties. Changes in skin material property specifications in the model affected quantitative results, but had minimal effect on shape. When E_{skin} was increased from 3.5 kPa to 6.9 kPa, peak stance phase interface stresses decreased at all but the postero-distal normal stress site. For antero-medial proximal and antero-lateral proximal normal and resultant shear stresses, the average decrease was 7.4 percent ($\pm$1.9 percent), while for postero-proximal and antero-lateral distal stresses, the decrease was 28 percent ($\pm$12.8 percent). Shapes of interface stress waveforms changed more during early stance phase than later in stance phase (**Figure 8**). It is important to reemphasize that linear material properties were specified in the model. To more thoroughly evaluate effects of material properties, a biphasic or multiphasic load-deformation curve would need to be considered and tested using a sensitivity analysis.

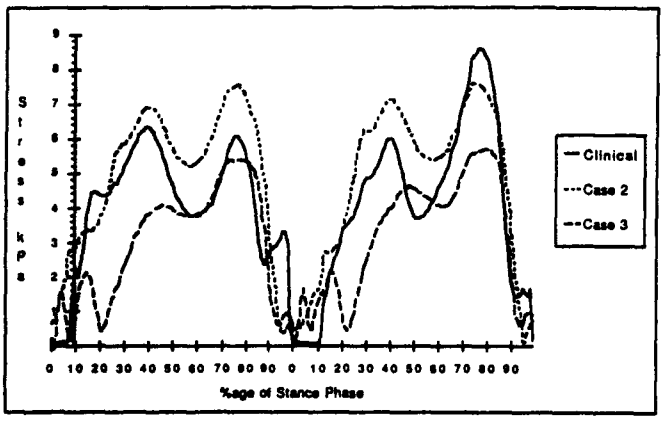

Figure 8.
Analytical results for material property Cases 2 and 3 from **Table 1** are compared with clinical data.

DISCUSSION

In the field of lower-limb prosthetics, analytical finite element modeling offers strong potential to make significant contributions to improvement in the treatment and quality of life of individuals who require prosthetic limbs. Stresses at the interface of the residual limb and the prosthetic socket, as well as stresses within the residual limb tissues themselves could, in concept, be predicted by FE models, adding powerful new tools to current clinical techniques of prosthetic design and fitting as well as prosthetics research. Clinicians and researchers would be provided with more information than ever before previously possible about the manifestations of a particular prosthetic design on amputee interface mechanics.

This paper contributes toward this goal by addressing three hypotheses concerning a FE model. The model is quasi-static and linear, and soft tissues are assumed homogeneous and isotropic. Thus, the model is a tremendously simplified representation of the actual residual limb and prosthetic socket and the very fundamental nature of this model should be emphasized. However, it is useful because assessment of the three hypotheses provides insight into aspects of the model that need further development and indicates where further attention should be concentrated.

(i) Hypothesis #1 is false. The model does not accurately predict magnitudes and shapes within the instrumentation error. The four features described below, if added to the model, would improve the match between experimental and analytical data. The basis and justification for selection of the four features is described.

Slip/Loss of Contact. A lack of accounting for slip or loss of contact was a principal cause of several described errors in model fit to experimental data. Because elements were permitted to carry tension across the interface, resultant shear stresses on the skin surface as a whole were underestimated. Strong evidence is provided during the loading delay

phase of stance phase at the antero-medial proximal site which experienced negative normal stress which, from shank sensitivity analyses, was clearly a result of contributions from sagittal bending and sagittal shear forces. Further evidence of the importance of not allowing loss of contact was provided later in the central part of stance phase. Postero-distal and antero-proximal sites matched the best of all transducer sites because the positive sagittal plane bending moment caused them to experience compressive normal stress, unlike the postero-proximal and antero-lateral distal sites which were in much greater error because they experienced tension when under a positive sagittal bending moment. Postero-proximal normal stress, antero-lateral distal normal stress, and antero-lateral distal resultant shear stress in analytical data had negative slopes or were at a minimum at the time of the first peak in experimental data.

Silver-Thorn (10) has described a technique to account for loss of contact across the interface during standing with weight-bearing. An iterative procedure is used whereby tissue interface elements are searched after an analysis run and 'released' if they are in tension in a direction normal to the interface. The analysis is then repeated with the new boundary conditions. Such a procedure could be used to study interface stresses during ambulation, though each datapoint in a stance phase waveform would need to be analyzed independently because unit load results could no longer be superposed, adding considerable computation time to the analysis. Another alternative would be to specify springs at the interface with different properties in tension and compression.

Material Nonlinearities. The assumption that soft tissues and Pelite behaved mechanically as linear materials was another source of error in the model. An approximately biphasic stress-strain curve would be a more accurate description of skin mechanical response. In the model presented in this paper, only the first slope portion of the curve was modeled and interface stress sensitivity to the modulus investigated. Further modeling efforts with a nonlinear load-deformation curve should investigate interface stress sensitivity to the second slope and to the location of the 'elbow' at the intersection of the first and second linear portions. The location of the 'elbow' has been shown to be highly sensitive to age (18) which is related to elastin content, thus for modeling of residual limbs tissues the location of the 'elbow' would be expected to be sensitive to body location and orientation and the presence of scar tissue. In addition, attachments between tissue layers must be considered. On the anterior residual limb surface, skin is adherent to underlying fascia, thus under moderate shear loading on the skin surface, stress concentrations within the skin would be expected to be induced. On the posterior surface, however, skin slides over underlying fascia. In addition, the deep fascial layer beneath the skin is characterized by a high in-plane stiffness (19), but a low in-plane bending stiffness. In posterior tissues, the fascia layer would be expected to redistribute concentrated normal stress so that muscle and connective tissue within the compartments surrounded by fascia experience a uniform stress distribution. Skin has also been shown to be sensitive to stress history, though after a few repeated cycles, load-deformation curves become repeatable (12). Anisotropic characteristics have been demonstrated in animal skin (20), though the degree of anisotropy depends on the location. Thus, appropriate further directions in model development are to evaluate interface stress sensitivity to the shape of material property curves, anisotropy, connections between tissue layers, and interface properties.

Pre-Stresses. A modeling error related to material nonlinearities is the assumption of initial total contact and zero pre-stress between the residual limb and the prosthetic socket. Slight geometry differences between the actual and modeled residual limbs are not important as demonstrated by Silver-Thorn (3). Instead, it is the manifestations of geometry mismatching between the residual limb surface and the socket surface on skin pre-stresses that is important. Slight pre-stress will cause a shift in the 'elbow' region of the biphasic load-deformation curve for skin toward the origin which would be expected to drastically alter subsequent interface stress distributions generated during gait. Thus, nonlinear tissue and interface material property specifications as described above would allow this hypothesis to be tested. The initial total contact specified in the model is an explanation for error between analytical and experimental resultant shear directions on anterior surfaces. There was no socket relief for the tibial crest in the model; thus there was a high interface normal stress on the tibial crest.

Measurement of All Shank Components Simultaneously. The effects of adding two shank loads that were not measured during the steps being modeled was to effect the shapes of model interface stress results. Mismatches in the timings of high-frequency content events (i.e., loading delays and HFEs) were apparent. As shown in **Figure 2b**, the low-frequency content of prosthetic shank waveforms changed minimally for different steps; however, the high-frequency content changed appreciably. To overcome these problems, a modified prosthetic force and moment measurement system is being constructed at the University of Washington to measure all six shank components simultaneously.

(ii) Hypothesis #2 is false. Model interface stresses were significantly different for a skin modulus of 3.5 kPa compared with a skin modulus of 6.9 kPa. It should be noted however, that changes at postero-proximal and antero-lateral distal sites were greater than those at antero-proximal locations. Skin modulus in the antero-proximal area was not as highly sensitive a parameter as at postero-proximal and antero-lateral distal sites. It is important to note that linear material properties were assumed. Further investigation using nonlinear tissue material specifications as described above are needed to verify the finding of low sensitivity.

(iii) Hypothesis #3 is false. While it is true that all normal stresses and some resultant shear stresses were most sensitive to prosthetic shank axial force, sagittal bending moment, and sagittal shear force, it was demonstrated that resultant shear stresses at postero-distal, postero-proximal, and antero-lateral proximal sites were more sensitive to torsion than to sagittal shear force. Low posterior site sensitivity is expected because the peak stance phase sagittal shear force is directed posteriorly, which unloads posterior sites. Because the antero-lateral proximal site was oriented such that the normal direction was parallel with the sagittal plane, resultant shear stresses at the antero-lateral proximal site were minimally sensitive to sagittal shear force.

Both normal stresses and resultant shear stresses were minimally sensitive to frontal shear force and frontal bending moment, suggesting that those directions have minimal influence on interface stress magnitudes. Further investigation using the nonlinear tissue and interface properties described above need to be conducted to verify this finding. In addition, it should be noted that possibly other parameters important to fit (such as stability and comfort) are affected by the frontal shear and frontal bending values.

In addition to evaluation of the three hypotheses presented in this paper and identification of necessary parameters to consider in future modeling efforts, analytical model results also provide insight into an understanding of interface mechanics, adding useful knowledge applicable to clinical treatment. Effects on interface mechanics of loading delays, alignment, and material property sensitivity are described below.

Two sources of the loading delays were hypothesized previously (17): 1) slip at the interface; and, 2) a manifestation of the antero-proximally directed shank resultant force vector. Because data from the analytical model, which did not allow for slip at the interface, demonstrated loading delays, it is concluded that direction of the anterior resultant force vector played a significant role in generating loading delays. Loading delays are important because if they end at uneven times on the residual limb, skin will be put in tension (14), a potentially detrimental stress configuration.

As supported by the results presented here (**Table 2**), the lack of a change in interface stress magnitudes for different alignment settings is not necessarily exclusively a result of differences in shank loading combinations. Instead, a factor not accounted for in the model, such as the residual limb being aligned differently with respect to the socket surface, a change in the amount of slip at the interface, or a change in residual limb muscle activation, was responsible.

Sensitivity analyses to tissue material properties showed that interface stresses were lower if material properties on both sides of the interface were more closely matched. Skin/liner interface stresses were reduced if the modulus difference between the skin and liner was reduced. It should be noted, however, and it is certainly recognized clinically, that amputee gait stability will also be affected by material properties. Thus, they should also be considered when selecting properties for liner materials.

ACKNOWLEDGMENTS

We gratefully acknowledge support for this research from the Department of Veterans Affairs Rehabilitation

Research and Development Service, the Whitaker Foundation, and the University of Washington Center for Bioengineering, Department of Rehabilitation Medicine, and Graduate School Research Fund. Artwork by Lori Mathews and Bob Borchers is appreciated.

REFERENCES

1. Pearson JR, Grevsten S, Almby B, Marsh L. Pressure variation in the below-knee patellar tendon bearing suction socket prosthesis. J Biomech 1974:7:487-96.
2. Nissan M. A simplified model for the short-below-knee stump. J Biomech 1977:10:651-8.
3. Silver-Thorn MB, Childress DS. Use of a generic, geometric finite element model of the below-knee residual limb and prosthetic socket to predict interface pressures. In: Proceedings of the Seventh World Congress of the International Society of Prosthetics and Orthotics. Chicago: 1992:272.
4. Mak AFT, Hong ML, Chan C. Finite element models for analyses of stresses within above-knee stumps. In: Proceedings of the Seventh World Congress of the International Society of Prosthetics and Orthotics. Chicago: 1992:147.
5. Quesada P, Skinner HB. Analysis of a below-knee patellar tendon-bearing prosthesis: a finite element study. J Rehabil Res Dev 1991:28(3):1-12.
6. Winarski DJ, Pearson JR. Least-squares matrix correlations between stump stresses and prosthesis loads for below-knee amputees. J Biomech Eng 1987:109:238-46.
7. Krouskop TA, Muilenberg AL, Doughtery DR, Winningham DJ. Computer-aided design of a prosthetic socket for an above-knee amputee. J Rehabil Res Dev 1987:24(1):1-8.
8. Steege JW, Silver-Thorn MB, Childress DS. Design of prosthetic sockets using finite element analysis. In: Proceedings of the Seventh World Congress of the International Society of Prosthetics and Orthotics. Chicago: 1992:273.
9. Torres-Moreno R, Solominidis SE, Jones D. Load transfer characteristics at the socket interface of above-knee amputees. In: Proceedings of the Seventh World Congress of the International Society of Prosthetics and Orthotics. Washington, DC: 1992:274.
10. Silver-Thorn MB. Prediction and experimental verification of residual limb/prosthetic socket interface pressures for below-knee amputees. (Dissertation). Evanston, IL: Northwestern University, 1991.
11. Sanders JE. Ambulation with a prosthetic limb: mechanical stresses in amputated limb tissues. (Dissertation). Seattle, WA: University of Washington, 1991.
12. Daly CH. The biomechanical characteristics of human skin. (Dissertation). Glasgow, Scotland: University of Strathclyde, 1966.
13. Shock RB, Brunski JB, Cochran GVB. In vivo experiments on pressure sore biomechanics: stresses and strains in indented tissues. 1982 Advances in Bioengineering. Thibault L, ed. 1982:88-91.
14. Sanders JE, Daly CH, Burgess EM. Interface shear stresses during ambulation with a prosthetic limb. J Rehabil Res Dev 1992:29(4):1-8.
15. Sanders JE, Daly CH. Measurement of stresses in three orthogonal directions at the residual limb/prosthetic socket interface. IEEE Trans Rehabil Eng 1993:1(2). In press.
16. Sanders JE, Daly CH, Burgess EM, Boone DA. Interface mechanics: effects of alignment change. In: Proceedings of the Seventh World Congress of the International Society of Prosthetics and Orthotics. Chicago: 1992:370.
17. Sanders JE, Daly CH, Burgess EM. Clinical measurement of normal and shear stresses on a transtibial residual limb. characteristics of waveform shape during walking. Prosthet Orthot Int 1993:17:38-48.
18. Daly CH, Odland GF. Age-related changes in the mechanical properties of human skin. J Invest Dermatol 1979:73:84-7.
19. Gratz CM. Tensile strength and elasticity tests on human fascia lata. J Bone Joint Surg 1931:13:334-40.
20. Lanir Y, Fung YC. Two-dimensional mechanical properties of rabbit skin—II. Experimental results. J Biomech 1974:7:171-82.

Department of Veterans Affairs

Journal of Rehabilitation Research and Development Vol. 30 No. 2, 1993
Pages 205-209

A Technical Brief

Modelling the mechanics of narrowly contained soft tissues: The effects of specification of Poisson's Ratio

William M. Vannah, PhD and Dudley S. Childress, PhD
Rehabilitation Engineering Program, Northwestern University, Chicago, IL 60625

Abstract—Many soft tissues are considered to be virtually incompressible. A number of recent analyses of the mechanics of these tissues have used Poisson's ratios in the range of 0.45 to 0.49 with little or no documentation, the apparent assumption being that a small change in Poisson's ratio will not significantly affect the results. We demonstrate here that the mechanics of a narrowly contained soft tissue are, instead, strongly sensitive to small changes in compressibility about the incompressible limit. Relevant practical examples include analysis of the mechanics of soft tissues within the sockets of artificial legs, pressure sore problems, and the calculation of strains within the soft tissues of a fracture gap.

Key words: *above-knee prosthetic sockets, Poisson's ratio, pressure relief, soft tissue mechanics, tissue compressibility.*

INTRODUCTION

Soft tissues support the body's weight whenever that weight is rested on a surface. The resulting deformations within the soft tissues, if excessive, can damage the tissues. As a result, the study of these deformations has clinical relevance in a number of areas: socket design for lower-extremity prostheses, prevention of decubitus ulcers (bedsores), design of orthopaedic footwear, molding techniques for prosthodontics, etc. In each of these examples, there exists a "soft tissue support system," consisting of a load being transmitted between two hard objects by the intermediate soft tissue.

For all the examples listed above, we shape the external surfaces on which the body's weight is rested, in order to relieve pressures in and about bony prominences. We also attempt to shape these external surfaces so that the internal strains do not damage the soft tissue. A common design feature of these surfaces is that they wrap around and partially contain the soft tissue and internal bony structure. To improve the design of these surfaces, a number of investigations into the mechanics of the soft tissues within these systems have been conducted. In particular, the design of sockets has recently received attention (1,2,3,4).

Consider a typical example: a residual limb after an above-knee (AK) amputation, inserted into a prosthetic socket, as shown in **Figure 1**. As the limb is loaded in stance, the bony structure moves downward into the socket of the prosthesis, displacing soft tissue. If the tissue is incompressible, a volume of tissue equal to that volume displaced by the bony structure must be extruded from the socket. The socket forces the volume displacement to "travel" a great distance before it can be "released" at a free boundary, and so a great deal

Address all correspondence and requests for reprints to: William M. Vannah, PhD, Director, Orthopaedic Biomechanics, Tufts University, 750 Washington Street, Boston, MA 02119.

Journal of Rehabilitation Research and Development Vol. 30 No. 2 1993

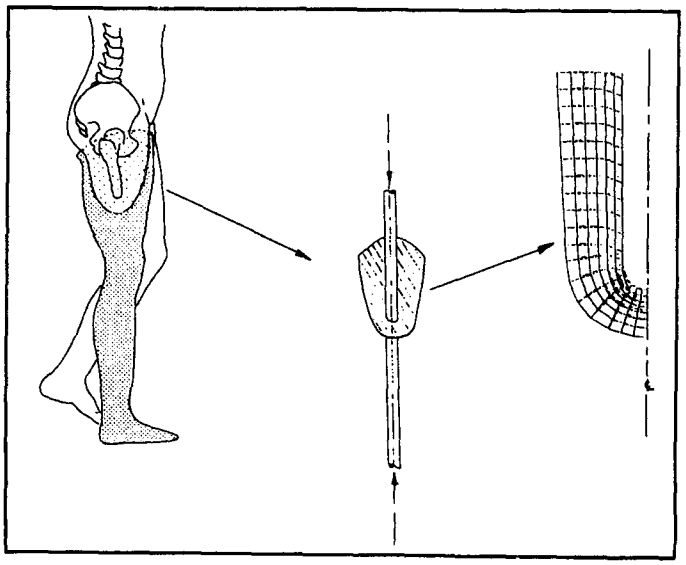

Figure 1.
The Above-Knee (AK) socket model: anatomic structure, idealized model, finite element model.

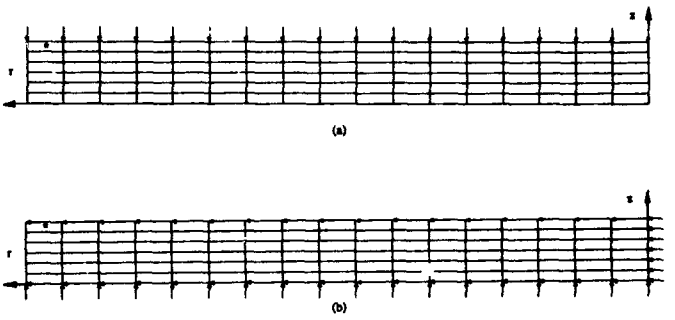

Figures 2a&b.
Axisymmetric layer model. The axis of symmetry is vertical (z-direction). The model is 1.0 cm high and 10.0 cm in radius. Figure 2a shows the displacements imposed on the model; the top surface is pressed down, as if by a flat plate, by imposing a 0.5 mm vertical displacement on each of the nodes labelled with an arrow. Figure 2b shows the nodes where displacements in one or more directions are fixed. Nodes along the axis of symmetry and along the top and bottom are constrained against radial displacement. Nodes along the bottom are constrained against vertical displacement; again, as if supported by a flat surface.

of the tissue within the socket is deformed slightly. This deformation is resisted by the tissue, resulting in a reaction force on the bony structure. The magnitude of this deformation, and the resulting reaction force, depend upon (among other things) the narrowness and length of the path that the volume displacement must travel before it is released. The stiffness of the residual limb/socket coupling is the amount of reaction force generated due to a given motion of the bony structure. In this note, we will show that the predictions of the distortions and the reaction forces for this type of mechanical system are strongly dependent on the specification of compressibility used.

METHODS

Layer Model

Consider a model consisting of an axisymmetric flat disk of tissue, 1.0 cm high and 10.0 cm in radius, compressed as if between two flat, rigid plates (**Figure 2a** and **2b**; note that the "plates" are imaginary and are, therefore, not shown). The upper surface is displaced downward 0.5 mm, and the lower surface is fixed. The tissue is bonded to the "plates."

This model is solved using the finite element method. Conventional finite element formulations become poor approximations—behaving too stiffly—as Poisson's ratio approaches 0.5 (5,6). To avoid this artificial stiffening, we used an unconventional formulation which does allow use of Poisson's ratios closely approaching the incompressible limit. A number of formulations have been described for modelling incompressible behavior (6), and these are becoming available in a number of commercial packages; the method used here uses selectively reduced integration rules and is part of the MARC finite element analysis software (MARC Analysis, Palo Alto, CA). The model is discretized using elements with linear shape functions. A Young's modulus of 0.0207 MPa (3.00 psi) is specified. [Note that this value is a rough estimation of the stiffness of bulk muscular tissue at low strains (7). A number of estimations of the "average" stiffness of residual lower limbs have been made: Young's modulus of 0.0062 to 0.109 (2); Young's modulus of 0.050 to 0.145 (3). The stiffness of a given residuum is presumably as varied from the "average" as residual limbs themselves are, and further consists of a number of tissue types—skeletal muscle, skin, fat layers and pads, fascia and loose connective tissue—making assigning an "average" stiffness questionable, semantically. However, for the purposes of this demonstration, the exact value is not a sensitive parameter.] A range of

Poisson's ratios is used, and the resulting shear stresses and reaction forces are compared (**Table 1**).

The reaction force is profoundly sensitive to the Poisson's ratio chosen, showing a 15-fold increase over the range studied. Figures of the deformed mesh (**Figure 3**) clearly show the migration of the volume displacement toward the free boundary and the resulting shear distortion of the tissue. The effect of Poisson's ratio on the distortion can be qualitatively evaluated by visually comparing the level of distortion in the deformed meshes. Von Mises stresses presented are for the center of the outer corner elements; this position is marked with an asterisk in each of the deformed plots.

Table 1.
Effect of Poisson's ratio for the layer model (displacement = 0.5 mm).

Poisson's Ratio	Reaction Force (N)	von Mises Stress (MPa)
0.4500	109	0.16
0.4900	370	0.35
0.4990	1220	0.74
0.4999	1630	0.91
0.5000	1630	0.91

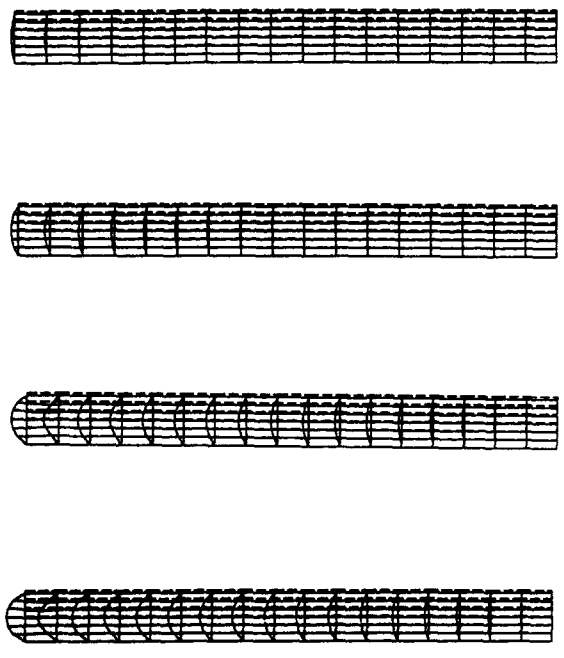

Figure 3.
Deformed shapes of layer model. This group of figures shows the effect of specification of Poisson's ratio on the layer model. In descending order from the top, the Poisson's ratios are 0.450, 0.490, 0.499 and 0.500. The upper surface is displaced downwards 0.5 mm; distortions are to scale. Note the migration of the volume displacement towards the free boundary, and the resulting distortion in the material.

The type of boundary conditions existing at the interface between the tissue disk and the imaginary rigid plates is significant. If we switched to a zero shear stress boundary condition at the interface, we would simply have uniaxial compression between the plates. In this case, the distortions would be much lower. However, the configuration used in the model—a thin layer of an approximately incompressible material with zero-slip boundary conditions—occurred often in our study of soft tissue support systems within rehabilitation engineering, and we have described it using the term "narrow containment."

In general, the effect also increases as the stiffness of the tissue decreases. Using the terminology of engineering mechanics, a more precise statement is that the effect increases as the ratio of the shear stiffness (resistance to shape change) to the bulk stiffness (resistance to volume change) decreases. Solids with this type of very high ratio of bulk stiffness to shear stiffness (typically of the order 10 or lower) are called "virtually incompressible" (8,9). Soft tissues fall into this category based on their exceedingly low shear stiffness. Rubber-like solids generally also fall into this category. It is important to note that the term "virtually incompressible" does not mean that the material is completely incompressible, only that the volume changes occurring during deformation are negligible in comparison to shape changes. The fact that the deformations are "virtually incompressible" is relevant because it means that different analytical methods must be used.

Above-Knee Prosthetic Socket Model

Consider now a model representing an above-knee (AK) residual limb and socket (**Figure 1; Figure 4a** and **4b**). This model is also axisymmetric—and therefore misses significant asymmetric features of the typical AK socket system—but it will serve to illustrate the effect of specification of compressibility in a case relevant to the biomechanics of prosthetic sockets. This model also uses linear elements with selectively reduced integration rules and a Young's modulus of 0.0207 MPa (3.00 psi).

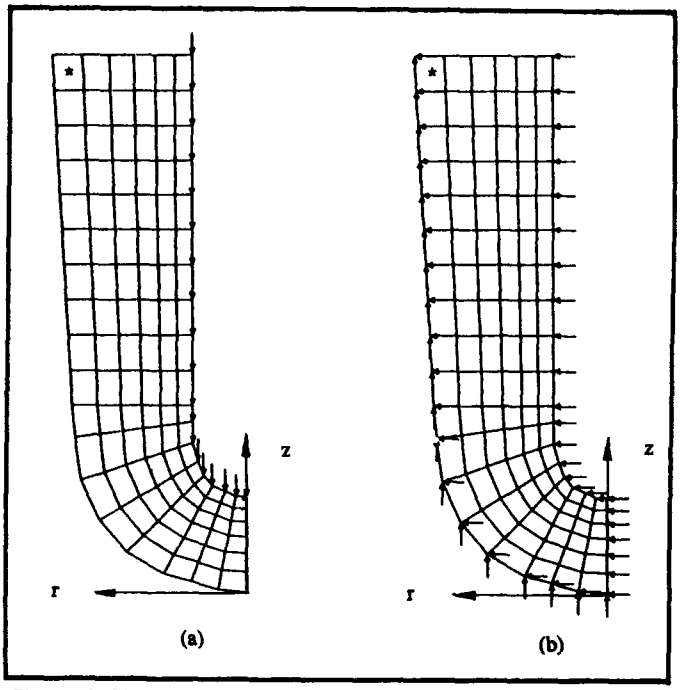

Figure 4a&b.
Axisymmetric AK residual limb/socket model. The axis of symmetry is vertical. The model is 200.0 mm high and 72.0 mm in radius. Figure 4a shows the displacements imposed on the model; the downward motion of the femur is modelled by imposing 5.0 mm vertical displacement on each of the nodes labelled with an arrow. Figure 4b shows the nodes where displacements are fixed. Nodes along the axis of symmetry and along the femur are constrained against vertical displacement. The socket is modelled by constraining all nodes along the outer surface of the model against all displacements.

The femur is displaced downward 5.0 mm. Again, a range of Poisson's ratios is used; the resulting shear stresses and reaction forces are compared (**Table 2**, and **Figure 5**).

The AK model shows a sensitivity to Poisson's ratio that is similar in nature to that of the layer model, but less in magnitude. The reaction forces roughly double as the Poisson's ratio is increased from 0.4500 to 0.5000.

Table 2.
Effect of Poisson's ratio for the AK model (displacement = 5.0 mm).

Poisson's Ratio	Reaction Force (N)	von Mises Stress (MPa)
0.4500	44.7	0.12
0.4900	64.5	0.15
0.4990	91.4	0.66
0.4999	91.4	0.66
0.5000	91.4	0.66

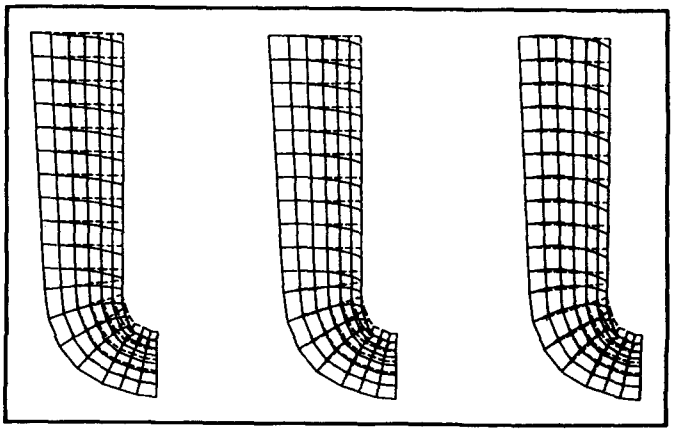

Figure 5.
Deformed shapes of the AK residual limb/socket model. This group of figures shows the effect of specification of Poisson's ratio on a typical AK residual limb/socket system. From left, the Poisson's ratios are 0.450, 0.490 and 0.500. Vertical displacement of the femur is 5.0 mm downward, and distortions are to scale. Note the displacement of material out the top end of the socket in the incompressible case (figure on right).

DISCUSSION

Variations in compressibility approaching the incompressible limit have a strong effect on the reaction forces and distortions in the models presented here. Many similar analyses of narrowly contained soft tissues have used Poisson ratios in the range 0.45 to 0.49 with little or no documentation (perhaps in recognition of the artificially high stiffness that conventional finite element formulations exhibit near the incompressible limit). Examples are analyses of the bulk muscular tissues within the socket of a prosthetic limb (2,3), and in wheelchair seating systems (10,11). The apparent assumption is that a small change in Poisson's ratio will not significantly affect the results. The preceding analyses show that this assumption can, instead, have substantial, if not overriding, effects. The observation may also apply to studies of the soft repair tissues of a healing fracture (12,13), albeit to a lesser extent, because the stiffness of the tissues may be higher.

The sensitivity of narrowly contained soft solids to compressibility places more weight on the assumption that soft tissues are incompressible. The argument commonly made for this assumption is that the shear stiffness of soft tissue is so low that any plausible value for the bulk modulus renders the tissue virtually incompressible. Calculations will show that this is true in many cases; however, careful assessment seems warranted.

The following three technical points on the analysis may be of interest. First, it should be noted that the sensitivity of the mechanics of a narrowly contained solid to compressibility has no relation to the artificially high stiffness that conventional finite element formulations exhibit at Poisson's ratios approaching 0.5 (5,6); the results of the layer model match an analytical solution from linear elasticity (14). Secondly, this is not a "large-strain" effect, i.e., the observation is different from that of Vawter (15). Thirdly, in reference to the (large) strain levels used, we would note that large-strain, geometrically and materially nonlinear solutions of both models presented here give results which are essentially identical to the linear solutions (7).

Narrow containment is probably not the primary support mechanism in a prosthetic socket. It is commonly thought (though it has yet to be quantitatively shown) that the majority of the support given by a typical AK socket is due to the gluteal-ischial seat. However, it has been suggested that additional support may be given by the narrow containment mechanism (16,17). The percentage of support the typical lower-extremity socket derives from trapping soft tissues has not been determined, or at least has not been reported. The purpose of this report is not to determine what this percentage is, or describe how to increase it. Instead, the intent is to suggest that this may be an important factor in the design of soft tissue support systems, and leading from this, to show the sensitivity to Poisson's ratio in modeling this effect.

REFERENCES

1. Steege JW, Schnur DS, Childress DS. Finite element prediction of pressure at the below-knee socket interface. In: Biomechanics of normal and prosthetic gait (ASME), BED-Vol. 4, 1987:39-44.
2. Krouskop TA, Muilenberg AL, Dougherty DR, Winningham DJ. Computer-aided design of a prosthetic socket for an above-knee amputee. J Rehabil Res Dev 1987:24(2):31-8.
3. Reynolds D. Shape design and interface load analysis for below-knee prosthetic sockets [thesis]. London: University of London, 1988.
4. Sanders JE, Boone DA, Daly CH. The residual limb/prosthetic socket interface: normal stress and shear stress. In: Proceedings of the 13th Annual RESNA Conference. Washington (DC): Resna Press, 1990:234-5.
5. Knauss WG. Displacements in an axially accelerated solid propellant grain. In: 20th Meeting Bulletin JANAF-ARPA-NASA Panel on Physical Properties of Solid Propellants I. 1961:175-86.
6. Hughes TJR. The finite element method (Chapter 4). Englewood Cliffs (NJ): Prentice-Hall, 1987.
7. Vannah WM. Indentor tests and finite element modelling of bulk muscular tissue in vivo [dissertation]. Evanston (IL): Northwestern University, 1990.
8. Ogden RW. Elastic deformations of rubberlike solids. In: Hopkins HG, Sewall MJ, editors. Mechanics of solids: the Rodney Hill 60th anniversary volume. Oxford: Pergamon Press, 1982:499-537.
9. Treloar LRG. The physics of rubber elasticity. 3rd ed. Oxford: Clarendon Press, 1975.
10. Chow WW, Odell EI. Deformations and stresses in soft body tissues of a sitting person. J Biomech Eng 1978:100:79-87.
11. Todd BA, Thacker JG, Chung KC. Finite element model of the human buttocks. In: Proceedings of the 13th Annual RESNA Conference. Washington (DC): Resna Press, 1990:417-18.
12. Blenman PR, Carter DR, Beaupre GS. Role of mechanical loading in the progressive ossification of a fracture callus. J Orthop Res 1989:7:398-407.
13. Cheal EJ, Mansmann KA, DiGioia AM III, Hayes WC, Perren SM. Role of interfragmentary strain in fracture healing: ovine model of a healing osteotomy. J Orthop Res 1991:9:131-42.
14. Robert M, Keer LM. Stiffness of an elastic circular cylinder of finite length. J Appl Mech 1988:55:560-5.
15. Vawter DL. Poisson's ratio and compressibility. J Biomech Eng 1983:105:194-5.
16. Murphy EF. Sockets, linings, interfaces. Clin Prosthet Orthot 1984:8:4-10.
17. Pritham CH. Biomechanics and shape of the above-knee socket considered in the light of the ischial containment concept. Prosthet Orthot Int 1990:14:9-21.

Department of Veterans Affairs

Journal of Rehabilitation Research and Development Vol. 30 No. 2 1993
Pages 210–223

A Technical Note

Basic gait parameters: Reference data for normal subjects, 10–79 years of age

Tommy Öberg, MD, PhD; Alek Karsznia, PT, PhD; Kurt Öberg, PhD
Department of Biomechanics and Orthopaedic Technology, University College of Health Sciences, S-551 11 Jönköping, Sweden; Department of Agricultural Engineering, Swedish University of Agricultural Sciences, S-750 07 Uppsala, Sweden

Abstract—Basic gait parameters were extracted from 233 healthy subjects—116 men and 117 women, 10 to 79 years of age. The measurements were made in a gait laboratory on a 5.5 m walkway. The results are presented in a series of reference tables for slow, normal, and fast gait. Mean, standard deviation, coefficient of variation, 95% confidence intervals, and 95% prediction intervals were calculated. Significant sex differences exist in all gait parameters. In a two-way analysis of variance (ANOVA) model, there was a statistically significant age-variability for gait speed and step length at normal and fast gait, but not for step frequency. In the step length parameter there was a significant interaction effect of age and sex at normal and fast gait. The reference data are considered valid in an indoor laboratory situation.

Key words: *gait, gait parameters, stride characteristics.*

INTRODUCTION

The basic gait parameters most frequently used are velocity, step length, and step frequency. Many reports are concerned with pathological gait, but such data must be compared with valid normal reference data to be interpretable. Published data are generally limited to specific groups, for example, normal men (1), normal women (2), and elderly women (3,4). These reports are often based on relatively small numbers of subjects, spread over many age groups. Different investigators use varying units of measurement, further hampering comparisons. Reference data for outdoor walking, based on measurements from 260 subjects, men and women divided into four age groups, have been published (5). The aim of this study was to present reference data on basic gait parameters for normal subjects.

Address all correspondence and requests for reprints to: Tommy Öberg, MD, PhD, Director, Associate Professor, Department of Biomechanics and Orthopaedic Technology, University College of Health Sciences, S-551 11 Jönköping, Sweden.

MATERIAL AND METHODS

Subjects

Two hundred and forty healthy subjects were examined. However, seven subjects were excluded from the original material, 3 girls and 3 boys aged 0–9 years, and one subject aged 80, because they were too few to represent an age group. Age and sex characteristics are shown in **Table 1**.

Gait Analysis

We have used the gait analysis method that was developed at the Biomechanics Laboratory, University of California, Berkeley, California, and the

Table 1.
Age and sex characteristics of the subjects.

	Number		
Age group, years	**Men**	**Women**	**Total**
10-19	27	27	54
20-29	15	15	30
30-39	15	15	30
40-49	15	15	30
50-59	15	15	30
60-69	15	15	30
70-79	14	15	29
Total	116	117	233

Department of Orthopaedic Surgery at the University of Uppsala, Sweden (6). The method was later further developed at the Department of Biomechanics and Orthopaedic Technology, Jönköping, Sweden. The gait laboratory has a walkway about 10 m long, including acceleration and deceleration distances. Two photocells with 5.5 m intervals, self-aligning electrogoniometers, a computer, and a plotter constitute the equipment used (**Figure 1**). The measurement was performed between the two photocells. Goniometry was not used in the present study. Heel strike was indicated by means of a manual switch.

Basic temporal gait parameters (gait speed, step length, and step frequency) were collected during slow, normal, and fast gait. The subject had to walk between the photocells 13 times—10 times without goniometers, and 3 times with goniometers. The mean of the 10 measurements without goniometers was calculated for each gait parameter.

Statistical Methods

Analysis of variance (ANOVA) and regression analysis were performed according to standard methods (7,8). All computations were made with a commercial statistics package for a personal computer, SYSTAT 5.0/SYGRAPH 1.0.

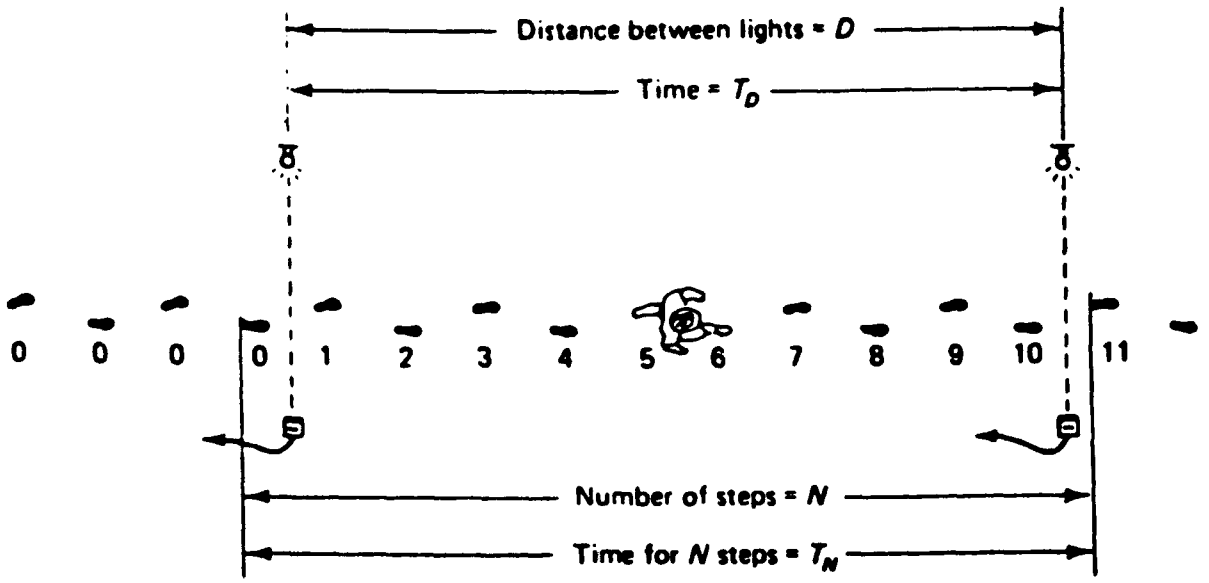

Figure 1.
Schematic top view of the walkway showing the measured variables desired for analysis (after Öberg and Lamoreaux, 1979).

RESULTS

Reference tables for slow, normal, and fast gait for different age groups and sexes are shown in the **Appendix** (*see p. 215*), and include mean, standard deviation, coefficient of variation, 95 percent confidence interval, and 95 percent prediction interval.

The results of one- and two-way ANOVA are presented in **Table 2** and **Table 3**. The results of regression analysis are presented in **Table 4**.

Table 2.
Gait parameters. One-way analysis of variance.

		p-value	
		Age group	Sex
Gait speed	Slow gait	N.S.	<0.001
	Normal gait	<0.01	<0.001
	Fast gait	<0.001	<0.001
Step length	Slow gait	N.S.	<0.001
	Normal gait	N.S.	<0.001
	Fast gait	<0.05	<0.001
Step frequency	Slow gait	N.S.	N.S.
	Normal gait	N.S.	<0.001
	Fast gait	N.S.	<0.001

N.S. = Not significant (p>0.05)

Table 3.
Gait parameters. Two-way analysis of variance.

		p-value		
		Age group	Sex	Age * Sex
Gait speed	Slow gait	N.S.	<0.001	N.S.
	Normal gait	<0.001	<0.001	N.S.
	Fast gait	<0.01	<0.001	N.S.
Step length	Slow gait	N.S.	<0.001	<0.05
	Normal gait	<0.01	<0.001	<0.05
	Fast gait	<0.001	<0.001	N.S.
Step frequency	Slow gait	N.S.	N.S.	N.S.
	Normal gait	N.S.	<0.001	N.S.
	Fast gait	N.S.	<0.001	N.S.

N.S. = Not significant (p>0.05)

Table 4.
Gait parameters and age. Regression analysis. Test for significant slope of regression line.

		p-value	
		Men	Women
Gait speed	Slow gait	N.S.	<0.05
	Normal gait	<0.05	N.S.
	Fast gait	<0.05	<0.01
Step length	Slow gait	N.S.	<0.01
	Normal gait	N.S.	<0.01
	Fast gait	N.S.	<0.001
Step frequency	Slow gait	N.S.	N.S.
	Normal gait	<0.001	N.S.
	Fast gait	<0.05	N.S.

N.S. = Not significant (p>0.05)

DISCUSSION

Methodological Considerations

The results of all measurements, including gait analysis, are dependent on the test conditions. Consequently, reference data are only valid for a test situation similar to the conditions of the original reference test situation. Gait analysis data should always be interpreted with regard to a thoroughly defined test situation. Dahlstedt (9) reviewed 15 articles with respect to walking speed. He found values of 1.3–1.6 m/s for men and 1.3–1.5 m/s for women for normal self-selected gait. The mean speed in shopping centers was 1.17 m/s for women, and 1.33 m/s for men (10). However, laboratory gait data cannot be considered valid for such practical walking situations. We have a general impression that gait velocity data reported from long walkways tend to be higher than data obtained from a short walkway.*

These observations are supported by the results of a study by Waters et al. (5), who examined 260 healthy subjects aged 6 to 80 years along a level outdoor track of 60.5 m. In the present study, using a 5.5 m walkway with a 2.5 acceleration distance, and a 2.5 m retardation distance, we found mean normal self-selected gait speed to be 118–134 cm/s

*Healthy subjects tested in a long basement corridor, 65 m walking distance (Öberg U, Öberg T, unpublished observations).

for men and 110–129 cm/s for women. Thus, our values were slightly lower than those reported in the review of Dahlstedt. Murray et al. found the self-selected gait speed to be 151 cm/s for men (1), and 130 cm/s for women (2). Compared with the results of Waters et al., gait speed was lower in slow and normal gait in our study, but at fast gait the results were equivalent in the two studies. We also found higher step frequencies and lower step lengths at all gait speeds in our study. These results indicate that the gait pattern is different in indoor and outdoor gait. Most gait analysis is performed on relatively short indoor walkways. Thus, the results of our study together with the Waters et al. study seem to indicate that there is a need for separate reference data for free gait outdoors or on a long walk-way, and for short walkways in laboratory situations.

Sex Differences

Gait velocity and step length were lower, and step frequency was higher for women than for men. In the ANOVA, the influence of sex was highly statistically significant except for step frequency at slow gait. These results are in accordance with the results reported in the literature (1,2).

Age Effects

The changes of the basic gait parameters most frequently seen with advancing age are a reduction of gait speed and step length, but only small changes of the step frequency (11). In our study we found statistically significant age-related changes in gait speed at normal and fast gait and of step length at fast gait in the one-way ANOVA, and almost the same results were found in the two-way ANOVA (where also interaction effects were evaluated). In the two-way ANOVA there were no age variations with respect to step frequency. These findings are in general agreement with the findings reviewed by Winter (11). The magnitude of age-related reduction of gait velocity reported in the literature varies between 0.1 percent/year and 0.7 percent/year (3,12,13,14). Such differences between different studies may be due to differences between the examined groups and differences in technique as well. In the two-way ANOVA model, we also found significant interaction effects of age and sex in the step length parameter.

In old age groups (over 70 years), Dahlstedt (9) found slow pedestrians with a normal gait speed of only 0.9 m/s, a high speed of 1.1 m/s, and very high speed of 1.3 m/s. However, in our study, we had only few people of these old ages, and none over the age of 80.

Practical Use of the Reference Data

Our data may be used for the interpretation of gait analysis data, collected in a laboratory situation comparable with that of ours, for both healthy adults and those with neuromuscular or other pathology.

CONCLUSION

We have presented reference data for basic gait parameters in slow, normal, and fast gait for healthy subjects aged 10–79 years to be applied on gait measurements on short walkways under laboratory conditions.

REFERENCES

1. Murray MP, Kory RC, Clarkson BH, Sepic SB. Comparison of free and fast speed walking patterns of normal men. Am J Phys Med 1966:45:8-24.
2. Murray MP, Kory RC, Sepic SB. Walking patterns of normal women. Arch Phys Med Rehabil 1970:51:637-50.
3. Finley FR, Cody KA, Finizie RV. Locomotion patterns in elderly women. Arch Phys Med Rehabil 1969:50:140-7.
4. Leiper CI, Craik RL. Relationships between physical activity and temporal-distance characteristics of walking in elderly women. Phys Ther 1991:71:791-803.
5. Waters RL, Lunsford BR, Perry J, Byrd R. Energy-speed relationship of walking: standard tables. J Orthop Res 1988:5:215-22.
6. Öberg K, Lamoreux LW. Gait assessment of total joint replacement patients by means of step parameters and hip-knee angle diagrams. In: Kenedi R, Paul J, Hughes J, eds. Disabilities. London: McMillan, 1950.
7. Armitage P, Berry G. Statistical methods in medical research. 2d ed. Oxford: Blackwell Scientific Publications, 1987.
8. Altman DG. Practical statistics for medical research. London: Chapman and Hall, 1991.
9. Dahlstedt S. Slow pedestrians: walking speeds and walking habits of old-aged people. Stockholm: The Swedish Council for Building Research, Report R2:1978, 1977.
10. Braun WI. The pedestrian. In: Evans HK, ed. Traffic engineering handbook, 2d ed. New Haven: ITE, 1950.
11. Winter D. The biomechanics and motor control of human gait: normal, elderly and pathological. 2d ed. Waterloo: University of Waterloo Press, 1991.

12. Cunningham DA, Rechnitzer PA, Pearce ME, Donner AP. Determinants of self-selected walking pace across ages 19 to 66. J Gerontol 1982:37:560-4.
13. Blanke D, Hageman P. Comparison of gait of young and elderly men. Phys Ther 1989:69:144-8.
14. Bendall MJ, Bassey EJ, Pearson MB. Factors affecting walking speed of elderly people. Age Aging 1989:18:327-32.

Appendix

Basic Gait Parameters

Tables

Table 1a.
Gait speed. Slow gait. Men.

Age years	N	Mean cm/s	S.D. cm/s	C.V.	95% C.I. cm/s	95% P.I. cm/s
10-14	12	88.7	12.0	0.14	81.1-96.3	62.3-115.1
15-19	15	85.7	21.4	0.25	73.5-97.9	38.6-132.8
20-29	15	83.1	9.1	0.11	78.2-88.0	64.0-102.2
30-39	15	88.3	18.9	0.21	78.1-98.5	48.6-128.0
40-49	15	93.5	10.4	0.11	87.7-99.1	71.7-115.3
50-59	15	85.8	16.1	0.19	77.1-94.5	52.0-119.6
60-69	15	87.9	13.3	0.15	80.7-95.1	60.0-115.8
70-79	14	79.5	13.7	0.17	71.8-87.2	50.7-108.3

Table 1b.
Gait speed. Slow gait. Women.

Age years	N	Mean cm/s	S.D. cm/s	C.V.	95% C.I. cm/s	95% P.I. cm/s
10-14	12	70.1	12.8	0.18	62.0-78.2	41.9-98.3
15-19	15	91.3	21.4	0.23	79.1-103.5	44.2-138.4
20-29	15	83.7	19.7	0.24	73.0-94.4	42.3-125.1
30-39	15	86.7	15.7	0.18	78.2-95.2	53.7-119.7
40-49	15	79.2	18.2	0.23	69.3-89.1	41.0-117.4
50-59	15	72.9	15.7	0.22	64.4-81.4	39.9-105.9
60-69	15	73.9	18.3	0.25	64.0-83.8	35.5-112.3
70-79	15	73.5	10.1	0.14	68.0-79.0	52.3-94.7

N = number of subjects
S.D. = standard deviation
C.V. = coefficient of variation
C.I. = confidence interval
P.I. = prediction interval

Table 2a.
Gait speed. Normal gait. Men.

Age years	N	Mean cm/s	S.D. cm/s	C.V.	95% C.I. cm/s	95% P.I. cm/s
10-14	12	132.3	19.6	0.15	119.9-144.7	89.2-175.4
15-19	15	135.1	13.3	0.10	127.5-142.7	105.8-164.4
20-29	15	122.7	11.1	0.09	116.7-128.7	99.4-146.0
30-39	15	131.6	15.0	0.11	123.5-139.7	100.1-163.1
40-49	15	132.8	9.8	0.07	127.5-138.1	112.2-153.4
50-59	15	125.2	17.7	0.14	115.6-134.8	88.0-162.4
60-69	15	127.7	12.4	0.10	121.0-134.4	101.7-153.7
70-79	14	118.2	15.4	0.13	109.8-126.6	85.9-150.5

Table 2b.
Gait speed. Normal gait. Women.

Age years	N	Mean cm/s	S.D. cm/s	C.V.	95% C.I. cm/s	95% P.I. cm/s
10-14	12	108.6	11.2	0.10	101.5-115.7	84.0-133.2
15-19	15	123.9	17.5	0.14	114.0-133.8	85.4-162.4
20-29	15	124.1	17.1	0.14	114.8-133.4	88.2-160.0
30-39	15	128.5	19.1	0.15	118.1-138.9	88.4-168.6
40-49	15	124.7	14.4	0.12	116.9-132.5	94.5-154.9
50-59	15	110.5	9.7	0.09	105.2-115.8	90.1-130.9
60-69	15	115.7	16.7	0.14	106.6-124.8	80.6-150.8
70-79	15	111.3	12.5	0.11	104.5-118.1	85.1-137.6

N = number of subjects
S.D. = standard deviation
C.V. = coefficient of variation
C.I. = confidence interval
P.I. = prediction interval

Table 3a.
Gait speed. Fast gait. Men.

Age years	N	Mean cm/s	S.D. cm/s	C.V.	95% C.I. cm/s	95% P.I. cm/s
10-14	12	167.9	32.1	0.19	147.5-188.3	97.3-238.5
15-19	15	184.3	17.0	0.09	174.6-194.0	146.9-221.7
20-29	15	162.6	20.1	0.12	151.7-173.5	120.4-204.8
30-39	15	176.8	28.5	0.16	161.3-192.3	117.0-236.7
40-49	15	171.7	17.6	0.10	162.2-181.2	134.7-208.7
50-59	15	164.0	24.6	0.15	150.7-177.3	112.3-215.7
60-69	15	163.9	20.2	0.12	152.9-174.9	121.5-206.3
70-79	14	158.6	24.9	0.16	144.6-172.6	106.3-210.9

Table 3b.
Gait speed. Fast gait. Women.

Age years	N	Mean cm/s	S.D. cm/s	C.V.	95% C.I. cm/s	95% P.I. cm/s
10-14	12	146.7	17.6	0.12	135.5-157.9	108.0-185.4
15-19	15	163.1	21.5	0.13	150.9-175.3	115.8-210.4
20-29	15	169.3	23.0	0.14	156.8-181.8	121.0-217.6
30-39	15	172.1	28.0	0.16	156.9-187.3	113.3-230.9
40-49	15	166.7	17.9	0.11	157.0-176.4	129.1-204.3
50-59	15	147.1	18.1	0.12	137.3-156.9	109.1-185.1
60-69	15	155.5	23.2	0.15	142.9-168.1	106.8-204.2
70-79	15	141.8	17.3	0.12	132.1-151.5	105.5-178.1

N = number of subjects
S.D. = standard deviation
C.V. = coefficient of variation
C.I. = confidence interval
P.I. = prediction interval

Table 4a.
Step frequency. Slow gait. Men

Age years	N	Mean steps/s	S.D. steps/s	C.V.	95% C.I. steps/s	95% P.I. steps/s
10-14	12	1.68	0.19	0.11	1.56-1.80	1.26-2.10
15-19	15	1.55	0.29	0.19	1.39-1.71	0.91-2.19
20-29	15	1.55	0.13	0.08	1.53-1.57	1.28-1.82
30-39	15	1.55	0.25	0.16	1.41-1.69	1.03-2.08
40-49	15	1.63	0.12	0.07	1.56-1.70	1.38-1.88
50-59	15	1.53	0.15	0.10	1.45-1.61	1.22-1.85
60-69	15	1.55	0.19	0.12	1.45-1.65	1.15-1.95
70-79	14	1.49	0.14	0.09	1.41-1.57	1.20-1.78

Table 4b.
Step frequency. Slow gait. Women.

Age years	N	Mean steps/s	S.D. steps/s	C.V.	95% C.I. steps/s	95% P.I. steps/s
10-14	12	1.48	0.21	0.14	1.35-1.61	1.02-1.94
15-19	15	1.68	0.21	0.13	1.56-1.80	1.22-2.14
20-29	15	1.59	0.20	0.13	1.48-1.70	1.17-2.01
30-39	15	1.632	0.18	0.11	1.53-1.73	1.25-2.01
40-49	15	1.61	0.24	0.15	1.48-1.74	1.11-2.11
50-59	15	1.54	0.29	0.19	1.38-1.70	0.93-2.15
60-69	15	1.50	0.28	0.19	1.35-1.65	0.91-2.09
70-79	15	1.53	0.12	0.08	1.46-1.60	1.28-1.78

N = number of subjects
S.D. = standard deviation
C.V. = coefficient of variation
C.I. = confidence interval
P.I. = prediction interval

Table 5a.
Step frequency. Normal gait. Men.

Age years	N	Mean steps/s	S.D. steps/s	C.V.	95% C.I. steps/s	95% P.I. steps/s
10-14	12	2.14	0.19	0.09	2.02-2.26	1.72-2.56
15-19	15	2.02	0.20	0.10	1.91-2.13	1.58-2.46
20-29	15	1.98	0.13	0.07	1.91-2.05	1.71-2.25
30-39	15	2.00	0.14	0.07	1.92-2.08	1.71-2.29
40-49	15	2.01	0.11	0.05	1.95-2.07	1.78-2.24
50-59	15	1.96	0.18	0.09	1.86-2.06	1.58-2.34
60-69	15	1.95	0.14	0.07	1.87-2.03	1.66-2.24
70-79	14	1.91	0.14	0.07	1.83-1.99	1.62-2.20

Table 5b.
Step frequency. Normal gait. Women.

Age years	N	Mean steps/s	S.D. steps/s	C.V.	95% C.I. steps/s	95% P.I. steps/s
10-14	12	1.97	0.17	0.09	1.86-2.08	1.60-2.34
15-19	15	2.09	0.18	0.09	1.99-2.19	1.69-2.49
20-29	15	2.08	0.15	0.07	2.00-2.16	1.77-2.40
30-39	15	2.13	0.17	0.08	2.04-2.22	1.77-2.49
40-49	15	2.16	0.16	0.07	2.07-2.25	1.82-2.50
50-59	15	2.03	0.13	0.06	1.96-2.10	1.76-2.30
60-69	15	2.06	0.18	0.09	1.96-2.16	1.68-2.44
70-79	15	2.03	0.14	0.07	1.95-2.11	1.74-2.32

N = number of subjects
S.D. = standard deviation
C.V. = coefficient of variation
C.I. = confidence interval
P.I. = prediction interval

Table 6a.
Step frequency. Fast gait. Men.

Age years	N	Mean steps/s	S.D. steps/s	C.V.	95% C.I. steps/s	95% P.I. steps/s
10-14	12	2.51	0.29	0.12	2.33-2.69	1.87-3.15
15-19	15	2.41	0.24	0.10	2.27-2.55	1.88-2.94
20-29	15	2.34	0.17	0.07	2.25-2.43	1.98-2.70
30-39	15	2.39	0.24	0.10	2.26-2.52	1.87-2.89
40-49	15	2.39	0.21	0.09	2.28-2.50	1.95-2.83
50-59	15	2.33	0.31	0.13	2.16-2.50	1.68-2.98
60-69	15	2.32	0.19	0.08	2.22-2.42	1.92-2.72
70-79	14	2.27	0.23	0.10	2.14-2.40	1.79-2.7.

Table 6b.
Step frequency. Fast gait. Women.

Age years	N	Mean steps/s	S.D. steps/s	C.V.	95% C.I. steps/s	95% P.I. steps/s
10-14	12	2.42	0.18	0.07	2.31-2.53	2.02-2.82
15-19	15	2.52	0.27	0.11	2.37-2.67	1.93-3.11
20-29	15	2.56	0.25	0.10	2.42-2.70	2.04-3.09
30-39	15	2.59	0.24	0.09	2.46-2.72	2.09-3.09
40-49	15	2.61	0.25	0.10	2.47-2.75	2.09-3.14
50-59	15	2.49	0.23	0.09	2.37-2.61	2.01-2.97
60-69	15	2.53	0.24	0.09	2.40-2.66	2.03-3.03
70-79	15	2.40	0.21	0.09	2.29-2.51	1.96-2.84

N = number of subjects
S.D. = standard deviation
C.V. = coefficient of variation
C.I. = confidence interval
P.I. = prediction interval

Table 7a.
Step length. Slow gait. Men.

Age years	N	Mean cm	S.D. cm	C.V.	95% C.I. cm	95% P.I. cm
10-14	12	51.7	3.0	0.06	49.8-53.6	45.1-58.3
15-19	15	53.8	6.8	0.13	49.9-57.7	38.8-68.8
20-29	15	52.7	3.1	0.06	51.0-54.4	46.2-59.2
30-39	15	55.1	5.1	0.09	52.3-57.9	44.4-65.8
40-49	15	56.2	3.3	0.06	54.4-58.0	49.3-63.1
50-59	15	55.4	7.4	0.13	51.4-59.4	39.9-70.9
60-69	15	56.0	3.5	0.06	54.1-57.9	48.7-63.4
70-79	14	52.7	5.2	0.10	49.8-55.6	41.8-63.6

Table 7b.
Step length. Slow gait. Women.

Age years	N	Mean cm	S.D. cm	C.V.	95% C.I. cm	95% P.I. cm
10-14	12	46.6	3.2	0.07	44.6-48.6	39.6-53.6
15-19	15	51.8	4.4	0.08	42.1-61.5	49.3-54.3
20-29	15	51.8	7.2	0.14	47.9-55.7	36.7-66.9
30-39	15	51.5	5.2	0.10	48.7-54.3	40.6-62.4
40-49	15	48.5	5.2	0.11	45.7-51.3	37.6-59.4
50-59	15	46.8	2.8	0.06	45.3-48.3	40.9-52.7
60-69	15	47.5	4.5	0.09	45.1-49.9	38.1-57.0
70-79	15	47.1	4.1	0.09	44.9-49.3	38.5-55.7

N = number of subjects
S.D. = standard deviation
C.V. = coefficient of variation
C.I. = confidence interval
P.I. = prediction interval

Table 8a.
Step length. Normal gait. Men.

Age years	N	Mean cm	S.D. cm	C.V.	95% C.I. cm	95% P.I. cm
10-14	12	61.5	3.9	0.06	59.0-64.0	52.9-70.1
15-19	15	66.0	4.8	0.07	63.3-68.7	55.4-76.6
20-29	15	61.6	3.5	0.06	59.7-63.5	54.3-69.0
30-39	15	64.9	4.6	0.07	62.4-67.4	55.2-74.6
40-49	15	64.7	3.7	0.06	62.7-66.7	56.9-72.5
50-59	15	63.5	6.0	0.09	60.2-66.8	50.9-76.1
60-69	15	65.0	3.6	0.06	63.0-67.0	57.4-72.6
70-79	14	61.5	5.1	0.08	58.6-64.4	50.8-72.2

Table 8b.
Step length. Normal gait. Women.

Age years	N	Mean cm	S.D. cm	C.V.	95% C.I. cm	95% P.I. cm
10-14	12	54.2	2.9	0.05	52.4-56.0	47.8-60.6
15-19	15	59.3	4.3	0.07	56.9-61.7	49.8-68.8
20-29	15	59.1	6.3	0.11	55.7-62.5	45.9-72.3
30-39	15	59.7	5.3	0.09	56.8-62.6	48.6-70.8
40-49	15	57.1	3.7	0.06	55.1-59.1	49.3-64.9
50-59	15	53.5	2.6	0.05	52.1-54.9	48.0-59.0
60-69	15	55.3	4.2	0.08	53.0-57.6	46.5-64.1
70-79	15	54.2	3.7	0.07	52.2-56.2	46.4-62.0

N = number of subjects
S.D. = standard deviation
C.V. = coefficient of variation
C.I. = confidence interval
P.I. = prediction interval

Table 9a.
Step length. Fast gait. Men.

Age years	N	Mean cm	S.D. cm	C.V.	95% C.I. cm	95% P.I. cm
10-14	12	68.7	7.9	0.11	63.7-73.7	51.3-86.1
15-19	15	78.7	6.0	0.08	75.3-82.1	65.5-91.9
20-29	15	71.2	5.7	0.08	68.1-74.3	59.2-83.2
30-39	15	76.0	8.2	0.11	71.6-80.4	58.8-93.2
40-49	15	73.7	4.4	0.06	71.3-76.1	64.5-82.9
50-59	15	72.2	5.7	0.08	69.1-75.3	60.2-84.2
60-69	15	73.6	5.3	0.07	70.7-76.5	62.5-84.7
70-79	14	71.5	7.4	0.10	67.3-75.7	56.0-87.0

Table 9b.
Step length. Fast gait. Women.

Age years	N	Mean cm	S.D. cm	C.V.	95% C.I. cm	95% P.I. cm
10-14	12	62.6	5.3	0.08	59.2-66.0	50.9-74.3
15-19	15	67.8	4.4	0.06	65.3-70.3	58.1-77.5
20-29	15	66.7	6.1	0.09	63.4-70.0	53.9-79.5
30-39	15	68.6	6.9	0.10	64.9-72.3	54.1-83.1
40-49	15	65.4	3.5	0.05	63.5-67.3	58.1-72.8
50-59	15	60.3	4.5	0.07	57.9-62.7	50.8-69.8
60-69	15	62.5	5.6	0.09	59.5-65.5	50.7-74.3
70-79	15	60.4	3.9	0.06	58.3-62.5	52.2-68.6

N = number of subjects
S.D. = standard deviation
C.V. = coefficient of variation
C.I. = confidence interval
P.I. = prediction interval

Department of Veterans Affairs

Journal of Rehabilitation Research and Development Vol. 30 No. 2 1993
Pages 224-232

A Technical Note

Characterization of the dynamic stress response of manual and powered wheelchair frames

J. David Baldwin, MS and John G. Thacker, PhD
Rehabilitation Engineering Center, University of Virginia, Charlottesville, VA 22903

Abstract—Two wheelchairs, one manual, one electrically powered, were instrumented with strain gages and operated over various laboratory terrains. Both wheelchairs were folding models with cross tubes pinned together at the center. The wheelchairs were operated on a constant speed treadmill with no bump, and with 0.953 cm (0.375 in) and 1.6 cm (0.625 in) dowels simulating bumps. The wheelchairs were also rolled off a 10.8 cm (4.25 in) platform to simulate a curb drop. The von Mises stresses were computed from the recorded strains, and statistical hypothesis tests were performed to determine whether the stresses were consistent with a stationary, narrow-band Gaussian random process. Such a stress history has been used in random fatigue analyses. Summary data for two strain gage locations on each wheelchair, for the four different test terrains, suggest that the von Mises stress can be considered stationary, but neither narrow-banded, nor Gaussian distributed.

Key words: *dynamic response, manual wheelchair, metal fatigue, power wheelchair, random process, strain gage, treadmill testing.*

INTRODUCTION

Active wheelchair users operate their wheelchairs over many different terrains in the course of their day. The roughness of the terrain and the response of a particular wheelchair structure to that terrain are the controlling factors in several aspects of wheelchair performance, including ride comfort and the long-term survivability of the structure. Long-term survivability of the wheelchair frame is basically an issue of the susceptibility of that frame to metal fatigue, and the accumulation of fatigue damage over the lifetime of the wheelchair. One measure of structural longevity that accounts for the inherent variability in loading, structural response, and material properties, is the probability of failure of the structure.

It was shown by Rice (1) that the peaks of a stationary, narrow-band Gaussian (SNG) random process follow the Rayleigh distribution. Miles (2) first used this result in studying the fatigue of aerospace structures excited by acoustic emissions. If the stresses in a solid are assumed to be adequately modeled by a SNG process, then it follows that the stress peaks are Rayleigh distributed. By coupling a probability distribution of stress peaks with a fatigue model (S-N curve), and cumulative damage rule (generally Miner's hypothesis), random fatigue models have been derived from which various statements of the probability of fatigue failure are given (2,3,4,5,6). None of these investigators, however, addressed the task of substantiating the validity of the stress random process assumption for their analyses.

Address all correspondence and requests for reprints to: J.D. Baldwin, PhD, School of Aerospace and Mechanical Engineering, Room 212, Felgar Hall, University of Oklahoma, Norman, OK 73019-0601.

The probability of fatigue failure of a tubular wheelchair frame has been addressed (7,8,9), but purely from the perspective of assumed structural loading. Structural loading and response data for the wheelchair frame under consideration were presumed known. The primary assumption made by Baldwin, et al. (7,8,9) was that the dynamic stresses acting in a wheelchair structural element could be adequately modeled by a SNG random process (at the time no real data for the response of a wheelchair structure under load were available). Then, a probability density function for the number of stress cycles to failure in fatigue was derived following Lambert's method (4).

This study was undertaken to investigate the accuracy of the SNG stress random process model as it applies to specific locations on two wheelchair frames. Dynamic strain gage data were recorded and analyzed for a manual and power wheelchair with a human occupant riding over bumps on a treadmill and performing a simulated curb drop. Statistical hypothesis testing was performed to provide an objective measure of the agreement of the computed von Mises stress data with the SNG assumption. Testing was carried out so that data collection occurred only for one pass of the wheelchair over a given bump, or for one drop from the platform; therefore, the validity of the SNG assumption is addressed only for that event. Summary test data and findings from this testing are presented.

The collection of dynamic strain gage data serves two purposes. First, the data will be used to form an objective assessment of the validity of the SNG assumption for the stresses occurring at specific locations in the wheelchairs under test. Second, the body of strain data will provide the basis for future fatigue life estimates of the wheelchair frame locations investigated. It should be stressed that the results presented here are valid only for the wheelchairs tested, for the specific locations instrumented, and for the test terrain under consideration.

Test Equipment and Procedure

Two wheelchairs, an Invacare Rolls IV (manual), and an Invacare Rolls Arrow (power), were used in this investigation. Both wheelchairs were of the folding type with two steel cross tubes pinned together at the center; the steel alloy was unknown in both cases. The manual wheelchair had solid front and rear tires and chrome-plated frame tubes. The front tires of the manual wheelchair had an outside diameter of about 20 cm (7.9 in), and a radial thickness of about 1.9 cm (0.75 in). The power wheelchair had solid front tires, pneumatic rear tires, and painted frame tubes. The front tires of the power wheelchair had an outside diameter of about 19 cm (7.5 in), and a radial thickness of about 3.8 cm (1.5 in).

The major components of the data acquisition system were an AT&T 6300 personal computer containing a MetraByte DAS16 data acquisition board, Measurements Group model 2120 strain gage conditioners, and low pass filters. The data acquisition system was configured to record three channels of data simultaneously. The data acquisition system is illustrated schematically in **Figure 1**; the strain gage terminal blocks are shown at the left side of the figure. A BASIC language computer program initialized and controlled the data collection and a FORTRAN program performed the data reduction and analysis.

The wheelchairs were instrumented with 3-element rectangular strain gage rosettes (WA-06-060WR-120, Micro Measurements Division, Measurements Group, Inc.). The three elements of the rosette have been designated Gage 1, Gage 2, and Gage 3, as shown in **Figure 2**. Each element of the rosette has a gage length and grid width of 1.5 mm (0.060 in), a nominal resistance of 120 ohms, a gage factor of 2.09, and a transverse sensitivity of +0.5 percent. Rosettes such as these allow full determination of the two-dimensional strain state existing at their point of attachment (10).

Two strain gage rosettes were attached to a cross tube, one on the side of the tube directly adjacent to the center pin, the other on the bottom of the tube lying along the pin. The strain gage wiring terminal blocks are shown schematically to

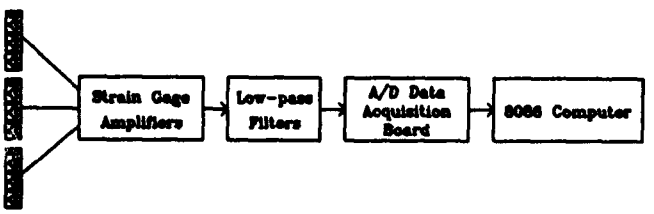

Figure 1.
Schematic representation of data acquisition system.

indicate the orientation of the gage elements (**Figure 3**). The cross tube was chosen for this initial investigation because several finite element analyses of this type of structure (7,11) have shown that large static stresses occur in this area. The strain gages were installed in the same locations on both the manual and power wheelchairs: they were attached directly to the chrome surface of the manual wheelchair tube. This is a potential source of error in that the strain gages were not attached directly to the base metal. On the power wheelchair, the paint was scraped from the tube at the points of application of the strain gages. The strain gage rosettes have been designated XG1 and XG2 (for "cross ›e Gage 1," etc.).

Strain gages measure the average strain over their gage length. If the strain gage is measuring a strain field with large gradients relative to the gage length of the strain gage, an error is introduced into the measurement. For this investigation, it was assumed that the strain gradients at the gage locations were not large with respect to the active length of the strain gages.

Strain gages respond to the deformation of the metal to which they are bonded by a change in their electrical resistance. The change in resistance is measured as a voltage, E, output by a Wheatstone bridge circuit in a "quarter-bridge" configuration (**Figure 4**). The three-wire circuit configuration shown has the advantage of minimizing any temperature variation effects from the data collection (12). The bridge excitation voltage V was nominally 6 volts dc. Each strain gage element had its own Wheatstone bridge circuit.

The strain gages were connected to a bank of strain gage conditioners/signal amplifiers which provided the excitation voltage, bridge calibration and balancing functions, and controlled the amplification of the voltage outputs from the bridge. The signal conditioners had a frequency response of 0–5,000 Hertz ±5 percent with a gain continuously adjustable from 100 to 2,100 Hz.

The amplified voltage output from each Wheatstone bridge passed through a fourth-order Butterworth active low-pass filter with a nominal signal cutoff at 30 Hz. The low-pass filter acted as a frequency limiter, eliminating elements of the dynamic strain signal that had frequencies larger than the cutoff. This effectively eliminated the electrical noise (typically found at 60 Hz) induced by the

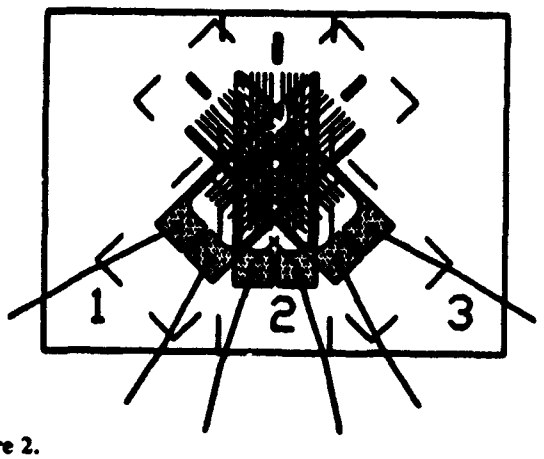

Figure 2.
Rectangular strain gage rosette.

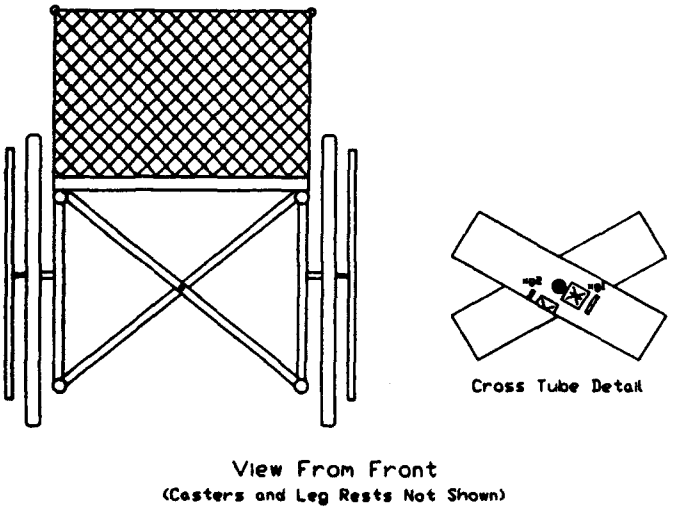

Figure 3.
Location of strain gage rosettes on cross tubes.

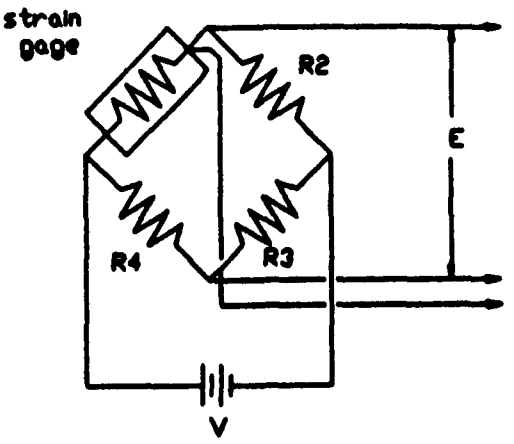

Figure 4.
Wheatstone Bridge circuit.

fluorescent room lighting, nearby power equipment, and miscellaneous atmospheric electrical disturbances. When filtering a signal, one must consider how much data is being thrown away by the filtering process. In this case, unfiltered dynamic strain signals were examined in the frequency domain, and it was found that no significant frequency content existed above about 15 Hz (except a contribution at 60 Hz attributable to lighting). Comparing unfiltered signals to filtered signals showed that more than 98 percent of the unfiltered RMS voltage existed in the filtered data streams; thus, no real data loss occurred due to filtering. It is conceivable, though, that an experimental testing program may excite strains in the wheelchair frame that have higher frequency content, in which case, a different filtering strategy must be used.

The sampling rate for this investigation was set at 512 samples per second from each strain gage channel. This rate was more than ten times the filtered signal bandwidth, allowing accurate detection of the strain wave forms (13) and minimizing the phenomenon of frequency aliasing. Samples were recorded for 4 seconds. This combination of sampling rate and duration produced data streams with an integer power of two number of points, suitable for use in Fourier transform frequency analysis.

The filtered strain signals were sampled by a MetraByte DAS16 analog-to-digital (A/D) data acquisition board mounted in a personal computer. The A/D board was programmed to sample the analog strain signals (voltages) and convert them to digital values suitable for computer storage and manipulation.

To date, both wheelchairs have been tested on both a constant speed treadmill fitted with wooden dowel bumps, and in simulated curb drops. The treadmill testing employed 0.953 cm (0.375 in) and 1.588 cm (0.625 in) diameter bumps, as well as no bump testing. The dowels extended across the width of the treadmill belt and were aligned so that they would be perpendicular to the direction of relative travel of the wheelchair under test. Both front casters impacted the dowels simultaneously. The data collection was initiated manually by the wheelchair occupant and was timed to have the wheelchair impact the bump near the middle of the 4-second data window.

The curb drop test platform simulated a 10.8 cm (4.25 in) drop. The occupied wheelchairs were held in a wheelie position and rolled off the platform. After rear wheel impact, the front casters were allowed to fall to the ground freely. Data collection was triggered manually prior to the wheelchair rolling off the platform.

The treadmill test with no bump was intended to simulate smooth surface operation. The treadmill bump testing was intended to provide data on the response of wheelchairs as they cross obstacles similar to those that might be encountered in everyday operation. The curb drop simulation was from a platform that was not as high as a standard curb, but would nonetheless provide useful data on the response of wheelchairs under rear wheel impact conditions.

A test series involved recording the output of one of the strain gage rosettes on one of the wheelchairs as it traversed one of the test terrains. Thus, for this test program, there were 16 test series; between 5 and 30 data sets were recorded for each test series. For all of the tests reported here, the wheelchair occupant was a nondisabled male with a mass of 80.3 k (177 lbs) and a height of 1.8 m (70 in).

Computational Models

The data processing stage of the investigation required that the recorded digital values be converted to voltages and then to strains. The strains were corrected for the transverse sensitivity of the strain gages (14), and then the mean and standard deviation of each strain gage output data stream were calculated.

The principal strains and stresses were computed from the output of the strain gage rosettes. The principal strains ϵ_1, ϵ_2, and γ_{max} were calculated using the relationships between the strains measured by the rosettes (10):

$$\epsilon_{1,2} = \frac{\epsilon_0+\epsilon_{90}}{2} \pm \frac{\sqrt{(\epsilon_0-\epsilon_{90})^2+[2\epsilon_{45}-(\epsilon_0+\epsilon_{90})]^2}}{2}$$

$$\gamma_{max} = \sqrt{(\epsilon_0-\epsilon_{90})^2+[2\epsilon_{45}-(\epsilon_0+\epsilon_{90})]^2} \quad [1]$$

$$\phi = \frac{1}{2}\tan^{-1}\left[\frac{2\epsilon_{45}-(\epsilon_0+\epsilon_{90})}{\epsilon_0-\epsilon_{90}}\right]$$

The quantities ϵ_0, ϵ_{45} and ϵ_{90} were the strains measured by Gage 1, Gage 2, and Gage 3 of the rosette, respectively. The angle ϕ measured the angle between the line of Gage 1 and the maximum

principal strain, ϵ_1. Once the principal strains had been calculated using **Equation 1**, the principal elastic stresses were computed using the plane stress constitutive relationships (15):

$$\sigma_1 = \frac{E}{1-\nu^2}(\epsilon_1 + \nu\epsilon_2)$$

$$\sigma_2 = \frac{E}{1-\nu^2}(\epsilon_2 + \nu\epsilon_1) \quad [2]$$

$$\tau_{max} = \frac{E}{2(1+\nu)}\gamma_{max}$$

where ν is the Poisson ratio and E is the elastic modulus. For the steel tube material considered here, these parameters were assumed to have the values $\nu = 0.285$ and $E = 29.5 \times 10^6$ psi. The quantities σ_1, σ_2 and τ_{max} are the maximum principal stress, minimum principal stress, and maximum shear stress, respectively, in the frame tube at the location of the strain gage. The von Mises stress was computed from the principal stresses using the relationship

$$\sigma_e = \sqrt{\sigma_1^2 + \sigma_2^2 - \sigma_1\sigma_2} \quad [3]$$

Several statistical hypothesis tests were performed on each data set to determine the agreement of the recorded data with the SNG assumption. The Reverse Arrangements Test for data independence addressed the stationary nature in time of the data stream; in this case, the stationary nature of the mean square value of the data was investigated. A parameter known as the *regularity factor* was computed to determine whether the data exhibited narrow-band behavior. Finally, the chi-square goodness of fit test provided an estimate of the agreement between the measured data and a Gaussian distribution. It was the time variation of the von Mises stress, σ_e, that was examined for consistency with the stationary, narrow-band Gaussian random process assumption.

In order to perform the Reverse Arrangements Test (16,17), the σ_e data stream was divided into 20 intervals. The mean square value was computed for each interval and reverse arrangements were then calculated. The 95 percent confidence interval for the Reverse Arrangements Test with 20 intervals is from 65 to 125 reversals. If the data sample produced less than 65 or more than 125 reverse arrangements, the assumption of stationary data was rejected.

The regularity factor α of the σ_e data stream was calculated to determine whether the data represented narrow-band response. For experimental data, the regularity factor is defined as the number of times a data stream has an upcrossing of its mean value divided by the number of peaks above the mean value (18). The regularity factor can have values in the interval $0 < \alpha < 1$. A regularity factor $\alpha \approx 1$ indicates narrow-band response where nearly every positive peak occurs above the mean value of the data. This situation arises when there is one dominant frequency in the data. When $\alpha \approx 0$, very few of the positive peaks occur above the mean value and wide-band response is indicated. Wide-band response refers to the fact that the frequency content of a signal is spread over a range of frequencies. It is the higher frequency cycles superimposed on the low frequency cycles that lead to peaks below the signal mean value.

Finally, a chi-square goodness of fit test (16) was performed on the σ_e data stream. Using the computed mean and standard deviation, the stresses were compared with a Gaussian distribution having the same mean and standard deviation. The data were grouped into 16 bins 0.4 standard deviations wide ranging from -2.8 to $+2.8$ standard deviations and compared with the expected number of observations assuming a Gaussian distribution. The 95 percent confidence limit for a chi-square test with 13 degrees of freedom is 22.4. If the data sample produced a chi-square statistic greater than 22.4, the assumption of conformance with the Gaussian distribution was rejected.

RESULTS AND DISCUSSION

Because of the volume of data on hand (370 data sets of 6,144 data points each), a complete data presentation will not be given in this paper. However, one data set from one of the manual wheelchair treadmill tests will be examined in detail, and the statistics of several other treadmill and curb drop data sets will be presented.

The data set designated TRD55 is from a 4-second treadmill test on the manual wheelchair, recording strain gage rosette XG1. The treadmill bump was 0.953 cm (0.375 in) in diameter, the

wheelchair occupant was a nondisabled male with a mass of 80.3 k (177 lbs), and the nominal treadmill speed was 1 m/sec. The strain versus time plot of this test is shown in **Figure 5**. The data are plotted in terms of microstrain (= strain * 10^6).

Notice that the strains recorded by Gage 1 were nearly always in compression, while Gage 3 was usually in tension. Gage 2 strains went through both tension and compression in a cyclic fashion. It is also interesting to note that the Gage 2 signal had a wider range between the maximum and minimum strains (~91 microstrain) than either Gage 1 (~39 microstrain) or Gage 3 (~46 microstrain). This was the result of the orientation of the Gage 2 element of the XG1 rosette along the tube axis, as shown in **Figure 3**, tending to measure the overall axial tension and compression of the tube, as well as any bending action out of the plane of the tubes. This observation was not surprising, given that the vertical motions of the wheelchair occupant (caused by the bump) would tend to be transmitted to the cross tube in a predominantly compressive manner. The orientations of Gages 1 and 3 were such that they tended to measure the twisting of the tube, which the data show to be a relatively constant state.

A very noticeable feature of this data set is the rapid variations shown by all three gages in the time interval from approximately 1.5 to 2.0 seconds. This is the time period where the measured strains varied most widely in response to the bump on the treadmill. It can be seen in **Figure 5**, that the Gage 2 strain had large compressive peaks near times 1.5 seconds and 2.0 seconds. These points are about 0.5 seconds apart and represent a spatial separation of approximately 50 cm (19.6 in) at the 1 m/sec treadmill speed. The points of contact of the front and back wheels of the manual wheelchair were about 35.6 cm (14 in) apart. It seems reasonable to assume that the large negative strain peaks seen in the Gage 2 signal at times 1.5 seconds and 2.0 seconds were the response of the wheelchair to the bump impacting the front and rear wheels, respectively. What appears to be another response increase occurred just prior to 3.0 seconds. It is felt that this response was due to the settling of the wheelchair occupant after passing over the bump. These three events are marked with arrows in **Figure 5**.

Given the rosette strain output, the principal stresses were calculated for this test. **Figure 6** shows the maximum principal stress, minimum principal stress, maximum shear stress, and the angle counterclockwise from Gage 1 to the maximum principal stress. All four of these quantities exhibit increased variation during the bump. The figure shows that the rotation angle is typically in the neighborhood of 90°, which is aligned with Gage 3.

It can be seen that the angle to the maximum principal stress ϕ is not constant, but varies with time (**Figure 6**). The implication of this observation is that a biaxial fatigue theory incorporating nonproportional loading (i.e., variable angle to maximum principal stresses) should be considered when designing such a connection for fatigue. Also, like the strains, the principal stresses exhibited larger than average variations in the time intervals near 1.5–2.0 seconds and 3.0 seconds.

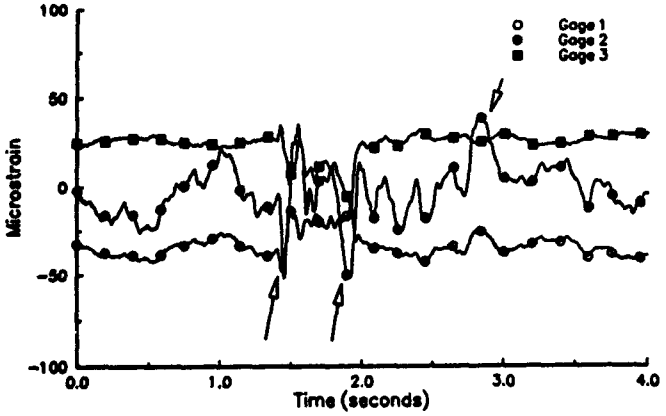

Figure 5.
Strain vs. time history for a treadmill test.

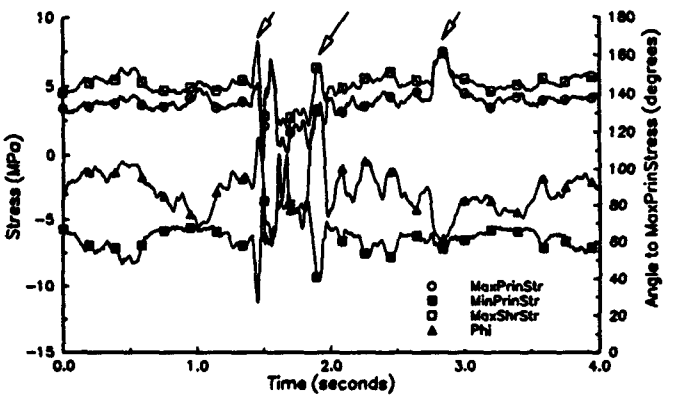

Figure 6.
Principal stresses and angle for a treadmill test.

The von Mises stress history was computed using **Equation 3** and is plotted in **Figure 7**. As with the strains and principal stresses, the von Mises stress exhibits increased variation in the time intervals near 1.5–2.0 seconds and 3.0 seconds.

The Reverse Arrangements Test for the TRD55 σ_e data stream yielded 81 reverse arrangements, indicating that the mean square von Mises stress was stationary in time. The σ_e regularity factor α was found to be 0.129, indicative of wide-band variations. Thus, the narrow-band assumption was rejected for this data set. The calculated chi-square measure was 1,082, which was large enough to cause rejection of the Gaussian distribution hypothesis.

The TRD55 chi-square, reverse arrangements, and regularity factor numbers were typical of the other data sets. Summary test data for both the manual and powered wheelchair treadmill tests is presented in **Table 1**. A similar summary of data from the curb drop simulations is presented in **Table 2**. The data sets chosen for analysis were considered to be representative of the body of test data. The data in **Table 1** and **Table 2** show that for most of the test data presented, the null hypothesis that the von Mises stresses are stationary could not be rejected. All of the tabulated data exhibit wide-band behavior (i.e., $\alpha \ll 1.0$). Finally, a most notable result is that none of the tests were even close to satisfying the Gaussian assumption. It is felt that this is due to the highly correlated (in time) nature of the deformations in a structure as it vibrates. The Gaussian distribution presumes independent data points. It appears that any sampling of structural

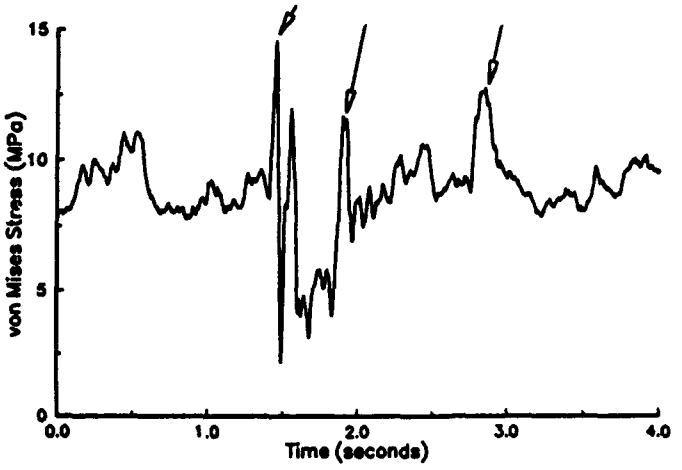

Figure 7.
Von Mises stress for a treadmill test.

Table 1.
Summary treadmill test data.

Test Index	Wheelchair	Gage	Bump Diam. (cm/in)	von Mises Stress		
				Rev. Arr.	α	χ^2
10	Manual	XG2	0.0/0.0	25	0.026	1466
30	"	XG1	0.0/0.0	69	0.126	171
55	"	XG1	0.953/0.375	81	0.129	1082
80	"	XG2	0.953/0.375	38	0.036	1110
115	"	XG2	1.59/0.625	107	0.070	4750
145	"	XG1	1.59/0.625	85	0.212	957
195	Power	XG1	0.0/0.0	86	0.143	136
215	"	XG2	0.0/0.0	54	0.182	178
250	"	XG2	0.953/0.375	47	0.214	796
270	"	XG1	0.953/0.375	100	0.377	655
305	"	XG1	1.59/0.625	92	0.168	655
330	"	XG2	1.59/0.625	107	0.192	1935

Table 2.
Summary curb drop test data.

Test Index	Wheelchair	Gage	von Mises Stress		
			Rev. Arr.	α	χ^2
3	Manual	XG1	119	0.343	2344
7	"	XG2	112	0.045	1524
12	Power	XG1	61	0.300	4111
18	"	XG2	145	0.024	4066

responses, such as strains, that occurs at a rate high enough to capture the peaks of the signal, will result in data points that are too strongly correlated to be accurately modeled by a Gaussian distribution.

The frequency content of the dynamic strains is displayed in **Figure 8**, which shows the magnitude of the Fourier transform of the strain data from each gage of the rosette. It was stated earlier that the frequency content of the strain data was confined to the lower frequencies; this is demonstrated in **Figure 8**. The low frequency content of the strains extended to the von Mises stresses also (**Figure 9**). It can be seen from **Figure 9** that the frequency content of the von Mises stress extends beyond the large component at 0 Hz. The band of frequency components above 0 Hz is graphical indication that the narrow-band assumption is not satisfied.

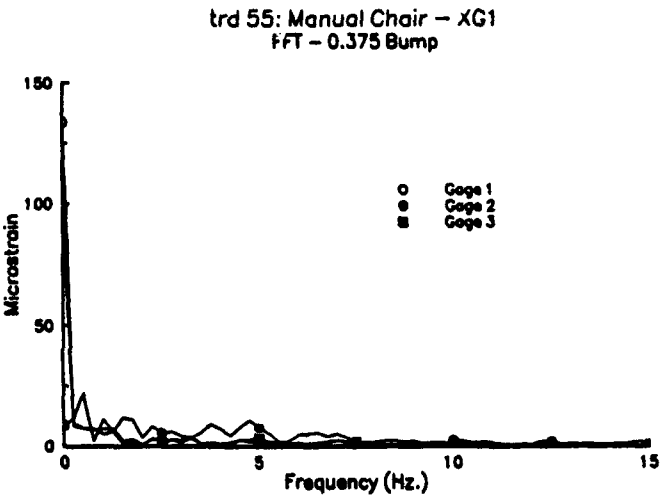

Figure 8.
Frequency content of strain data.

CONCLUSIONS

The test program described here has been useful in demonstrating the time-varying nature of the dynamic strains and stresses in a wheelchair cross tube. The implementation of a data collection and analysis system has allowed the examination of the dynamic response of wheelchair frames and the nature of the deformations that cause metal fatigue. Specifically, the assumption that the dynamic von Mises stresses developed in the manual wheelchair, impacting a 0.953 cm (0.375 in) treadmill bump, are narrow-band and Gaussian distributed at the cross tube location investigated, does not appear to be valid. The data did indicate, however, that the von Mises stress response could be taken to be stationary during the bump. Data have been presented for other wheelchair/strain gage location/terrain combi-

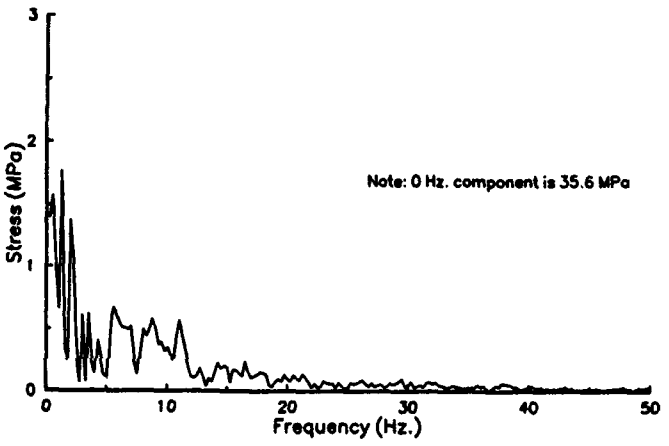

Figure 9.
Fourier transform magnitude of von Mises stress.

nations that lead to the same conclusions. One should remember, however, that other wheelchair/location/terrain combinations may exhibit the assumed narrow-band Gaussian response, although this outcome seems unlikely due to the correlation in time of the deformations of a vibrating structure

It has also been shown that the computed principal stresses tend to change directions during the traverse of a bump. Such behavior may indicate that a biaxial fatigue analysis is required when analyzing the probability of failure of joints such as those investigated here.

The data and findings presented here are for a very small fraction of the possible wheelchair frame locations and load conditions that may be examined. It is not to be inferred from these findings that the von Mises stress in a dynamically loaded wheelchair frame can generally be considered stationary, but neither narrow-band nor Gaussian distributed. Similarly, the frequency spectra presented can be considered valid only for the specific test configuration used here.

In the future, effort will be made to implement fatigue analysis procedures that take advantage of the recorded strain signals to develop estimates of the time-to-failure of dynamically loaded wheelchair frames. Also, testing could be expanded to explore the effect of different test terrains, investigate other high stress wheelchair frame locations, and other types of wheelchair structures.

ACKNOWLEDGMENTS

This work was carried out at the University of Virginia Rehabilitation Engineering Center. The authors are pleased to acknowledge the support provided under NIDRR Grant Number H133E80003.

REFERENCES

1. Rice SO. Mathematical analysis of random noise. Bell systems technical journal. 1944:23:282-322; 1945:24:46-156.
2. Miles JM. On structural fatigue under random loading. J Aeronaut Sc Nov 1954:753-62.
3. Crandall SH, Mark WD, Khabbaz GR. The variance in Palmgren-Miner damage due to random vibration. In: Proceedings of the fourth U.S. National Congress of Applied Mechanics, 1962:119-26.
4. Lambert RG. Analysis of fatigue under random vibration. Shock Vibration Bull Aug 1976:55-71.
5. Shin YS, Lukens RW. Probability based high cycle fatigue life predictions. In: Shin YS, Au-Yang MK, eds. Random fatigue life prediction, PVP-Vol 72. New York: American Society of Mechanical Engineers, 1983:73-87.
6. Wirsching PH, Haugen EB. Probabilistic design for random fatigue loads. J Eng Mech Div 99(EM6):Dec 1973:1165-79.
7. Baldwin JD. Structural reliability analysis of power wheelchair frames. (Thesis). Charlottesville, VA: University of Virginia, 1990.
8. Baldwin JD, Thacker JG. Structural reliability techniques applied to tubular wheelchair frames. In: Proceedings of the 14th annual RESNA conference. Washington, DC: RESNA Press, 1991:237-9.
9. Baldwin JD, Thacker JG, Baber TT. Estimation of structural reliability under random fatigue conditions. In: Service TH, ed. Reliability, stress analysis and failure prevention. New York: American Society of Mechanical Engineers, 1991:43-8.
10. Perry CC, Lissner HR. The strain gage primer. New York: McGraw-Hill, 1962.
11. Disher TD. Stress analysis of three wheelchair frames. (Thesis). Charlottesville, VA: University of Virginia, 1986.
12. Dally JW, Riley WF. Experimental stress analysis, 3rd ed. New York: McGraw-Hill, 1991.
13. Scott K, Owens A. Instrumentation. In: Window AL, Hollister GS, eds. Strain gage technology. London: Applied Science Publishers, 1982.
14. Errors due to transverse sensitivity in strain gages. (Bulletin TN-509). Raleigh, NC: Measurements Group, Inc., 1982.
15. Timoshenko SP, Goodier JN. Theory of elasticity. 3rd ed. New York: McGraw-Hill, 1970.
16. Bendat JS, Piersol AG. Random data: analysis and measurement procedures. 2nd ed. New York: John Wiley & Sons, 1986.
17. Kendall MG, Stuart A. The advanced theory of statistics. Volume II: inference and relationship. 3rd ed. New York: Hafner Publishing Company, 1973.
18. Thoft-Christensen P, Baker MJ. Structural reliability theory and its applications. New York: Springer-Verlag, 1982.

Department of Veterans Affairs

Journal of Rehabilitation Research and Development Vol. 30 No. 2, 1993
Pages 233-249

Design of a composite monocoque frame racing wheelchair

Michael S. MacLeish, MS; Rory A. Cooper, PhD; Joe Harralson, MS; James F. Ster III
Human Engineering Laboratory, Biomedical Engineering Program, School of Engineering and Computer Science, California State University, Sacramento, CA 95819-6019; Department of Rehabilitation Science and Technology, School of Health and Rehabilitation Sciences and Bioengineering Program, School of Engineering, University of Pittsburgh, Pittsburgh, PA 15261

Abstract—Design of present-day racing wheelchairs developed out of necessity and common sense. The chairs first used in racing were everyday chairs; through years of trial and modification the racing chairs of today evolved. Very little advanced engineering has been applied to the design of racing chairs. The Finite Element Analysis model executed on a computer provided insight into structural problem areas in the design of unibody frame racing chairs. Slight modifications to the model can be used to investigate new shapes, loads, or materials without investing large amounts of time and money. Wind tunnel testing with scale models provided perspectives on different improvements to reduce drag. Shape improvements may play an important role in reducing the racer's time during competition. Shape may help to decrease drag for the user in either the upright or down position. Considering that the frontal area increases around 30% in the up position with current strut and chassis frames, monocoque shapes should excel. Finite element analysis and air drag analysis are important to the design of a composite racing wheelchair. Composite materials may promote more efficient and ergonomic racing wheelchairs.

Key words: *aerodynamics, composite materials, ergonomics, finite element analysis, racing wheelchair, wheelchair design.*

Address all correspondence and requests for reprints to: Rory A. Cooper, PhD, Department of Rehabilitation Science and Technology, School of Health and Rehabilitation Sciences, University of Pittsburgh, Pittsburgh, PA 15261.

INTRODUCTION

Design for present-day racing wheelchairs developed out of necessity and common sense. The chairs first used in racing were everyday chairs; through years of trial and modification the race chairs of today evolved. It was hypothesized that their design could be greatly improved by applying modern engineering. A literature search was used to identify how engineering technology could best be applied. Using available engineering tools, a chair was designed and a monocoque prototype built. A monocoque vehicle is one in which the body is integral with the chassis. This paper presents a detailed design methodology and rationale for a composite monocoque frame racing wheelchair.

Importance of Designing Better Race Chairs

Approximately one spinal cord injury occurs every 45 minutes in the United States. Excluding all the cerebral palsy, muscular dystrophy, and other mobility-impairing diseases, that alone translates to about 10,000 new wheelchair users per year (1). Sports and competition are just as important to persons with disabilities as to "able-bodied" people, if not more so (1,2,3,4,5,6). Competition helps maintain an individual's fitness while improving feelings of self-worth. Lack of physical fitness can result in obesity and cardiorespiratory ailments to which chair users are particularly prone (1). Sports have proven to be an effective way to keep fit; improving the design of the equipment can help

Journal of Rehabilitation Research and Development Vol. 30 No. 2 1993

decrease the incidence of sports-related injuries. In turn, improved sports equipment will lead to improved everyday equipment (2,7,8,9). Technology developed to enhance the performance of racing chairs may someday become both realizable and affordable for use in everyday chairs. Increased mobility for persons with disabilities will help them overcome the stereotypes imposed upon them by society. The chair should not limit the individual.

History and Rules of Wheelchair Racing

Wheelchair racing was first introduced in 1948 (10). The first chairs were simply modified everyday chairs. Racing did not grow significantly in popularity until 1975, when Bobby Hall competed in his first marathon (7,10). Since then, wheelchair athletes have accomplished under 1-hour and 30-minute marathons and 4-minute miles (2). Some athletes support themselves with prize money from their racing (7).

The National Wheelchair Athletic Association (NWAA), which is the governing body regulating all wheelchair sports in the United States, has developed a set of rules governing allowable designs of racing chairs. In a wheelchair race, the object is to propel a wheelchair equipped with push-rings over a predesignated course in a minimum amount of time (11).

Chairs are required to have at least three wheels. The rear wheels are permitted a maximum diameter of 70 cm; the front wheel(s) are limited to a maximum diameter of 50 cm. Each rear wheel is allowed to have only one push-ring. The greatest width of the chair must be measured either at the wheels or the push-rings. The chair cannot rely on any chains, levers, or gears for propulsion; it must be propelled directly through the push-rings. Any structures for the sole purpose of gaining aerodynamic advantage are prohibited. All of the driver's limbs must be stable or securely fastened to avoid injury and the possibility of the driver falling out. The chair must be structurally sound to preclude catastrophic failure during a race (3).

Racing Wheelchair Design Parameters

Many factors influence the effectiveness of a racing wheelchair design: weight, materials, design, physical dimensions, fitness and ability of the user, interface compatibility between chair and user, as well as many external factors such as road surface and terrain (12). A description of some of the technologies in use or available for use to improve racing wheelchair design follows.

The Frame. The basic frame structure of the chair should provide good positioning of the pilot for better aerodynamics, propulsion ergonomics, and torso support. It must also be maneuverable and moderately stable, as well as stiff, to promote efficient transmission of energy to the wheels. Two main frame types have evolved so far, the cage seat and the bucket seat. Both incorporate a nonadjustable box design to help maintain the desired stiffness with light weight. The cage frame, being closed, can be made slightly stiffer. The bucket seat frame is open across the front allowing easier access; it is often preferred by quadriplegic persons (13). The frame struts should fit snugly to the sides of the user's chest and hips during propulsion. Side guards may be added to help protect the user from the wheels (3).

The chair's front end can be supported by either a cantilever or a fork wheel mount. Each requires "trail" (i.e., the distance between the contact point of the front wheel with the road surface to the extension of the pivot axis to the road surface) to keep the steering mechanism stable (13). A light front end permits the user to make minor steering adjustments easily (3). If the front becomes too light, the chair may easily tip into a "wheelie" during acceleration.

Frame size is determined by the user's body dimensions and stability requirements. The width must allow easy access to the push-rings for propulsion, while providing a stable wheelbase (14). Cambering the wheels can help increase the effective wheelbase track and improve pushing ergonomics. The wheelbase is also dependent on chair length. Long chairs are dynamically more stable, while short chairs have been found to have superior performance in short races and can also "draft" behind other chairs more effectively (15,16).

Seat Position. The pilot's position substantially affects the handling characteristics of the chair. Positioning the center of gravity is an important factor in race chair design. Presently, positioning decisions are made using a few rules of thumb and trial and error (7). Most seats consist of a nylon or cloth sling with straps, which positions the user ergonomically and aerodynamically while helping to remove unwanted motions. A knees-up position

helps gain more driving force while giving some upper-torso support (3). This support should not be so much that it restricts the motions required for propulsion. Other important seat dimensions include the seat-to-back angle and back height; these control the degree of support that the user has during propulsion. Some attempts to make an adjustable seat include a "hill climber" position (13).

The fore and aft position of the seat determines where the center of gravity falls relative to the wheelbase. A forward position helps to distribute the load over all the wheels. Positioning the seat too far forward can result in poor stroke kinematics, increased resistance in the steering, and a large downhill turning tendency. A good rule of thumb puts the center of gravity somewhere over the back third of the wheelbase (17). Downhill turning tendency occurs when the center of gravity is forward of the main wheels and the chair is on a side slope or crowned road. Its magnitude depends on wheelbase, steering mechanism, total mass of the chair and user, and their center of gravity. This creates a moment arm which causes the chair to turn downhill. Moving the center of gravity over the main wheels removes the moment arm but causes the chair to lose its directional stability (18,19). To correct these problems, chairs now include a compensator connected to the steering mechanism. There are three major types of compensators defined by the function of the springs: push-push, push-pull, and pull-pull. Pull-pull is the least effective; the other two are equally acceptable (12). Probably the most important seating consideration is body position relative to the push-rings. The user's shoulders should be slightly forward of the push-rings in order to employ the correct muscles. This enables efficient propulsion and minimizes the possibility of injury. This position depends on the user's skill and anthropometric measures, push-ring size, and the type of competition being raced (2,4,16,20).

The Wheels. Depending on the user's reach, strength, and experience, a 65–70 cm rear wheel is usually used. Smaller wheels, though easier to propel (e.g., they require less torque), can result in lower top speed. Two tire types are available: clinchers and sew-ups; the latter are slightly lighter and more expensive (13).

Spokes play an important role in the aerodynamics of the wheel. As they spin, the spokes mix up the air, creating turbulence. Reducing the number of spokes can reduce turbulence. However, using fewer spokes also decreases the wheel's strength and stiffness. This can be compensated for by lacing spokes radially instead of crossed (14). Spoke cross-sections can be flat or elliptical to increase their ability to cut through air. Some modern designs use a three-spoke or a monospoke wheel. The monospoke resembles a solid disk; more expensive and heavier, it is also faster, stiffer, and may possibly reduce injuries (15). Specialized Corporation presently markets a tri-spoke carbon fiber, Kevlar Aramid and glass composite rim which was aerodynamically designed using a super computer (21).

Rims can also be made aerodynamic by utilizing a high flange and a narrow profile. Care must be taken to ensure that the tire and the rim interface smoothly to decrease turbulence due to discontinuity. High flange rims help to improve wheel stiffness (7,13). The true aerodynamics of wheel design are not well understood; wind tunnel testing is needed at speeds and conditions similar to those encountered during racing (15).

Push-rings, attached directly to the spokes via stand-offs, are usually between 12 and 18 inches in diameter. Larger diameter rings allow faster acceleration but may decrease peak speeds (3).

The rear wheels can be mounted rigidly or with quick-release axles. Rigid threaded mounts provide a stiffer fit (7,13). Mounting the wheels with camber gives the chair a larger footprint, increasing its stability. Camber also permits a more natural push motion straight down from the shoulders (20). Too much camber often stresses the spokes and decreases wheel rigidity (3). A camber of about 10° is preferred by most users but varies between individuals from around 2° to as much as 12° (4). Alignment of the wheels is also critical. Tires that toe-in or out increase road friction (13,14,20). Misalignment due to repeated rim removal, frame settling, or abuse during a race is common. For these reasons, procedures to correct alignment should be as simple as possible. One method uses spacers to torque the frame into alignment (11). Kushall developed a method in sports chairs which uses a rotating shaft for alignment. Other manufacturers use a mounting plate that can be shimmed to the desired camber and alignment.

Using only one front wheel helps reduce rolling resistance and chair weight, but makes the chair less

Journal of Rehabilitation Research and Development Vol. 30 No. 2 1993

stable (13,17). Using larger tires (35–50 cm) in place of small casters helps avoid front wheel flutter, spreads the weight out more evenly, and allows for easier steering methods (7,19). However, a small front wheel can reduce the chair's aerodynamic drag (15). Front wheels can be mounted using a fork or a cantilever-type design.

Steering mechanisms require some trail. Trail helps eliminate flutter and makes the steering system stable (13). Steering mechanisms and compensators are used to allow propulsion through corners and adjust for road crown (22), allowing the user to concentrate on propulsion.

Aerodynamics. Wind resistance "drag" is caused by both normal and tangential (skin friction) forces whenever a body moves through the air. The flow of air over each individual part of the system is influenced by the flow over the rest of the system.

Aerodynamic drag is expressed by:

$$\text{Drag Force} = \frac{C_d \rho_{air} v^2 A}{2g}$$

where C_d = drag coefficient
ρ_{air} = density of air
v = air velocity
A = frontal area
g = gravitational constant

The power consumed in overcoming this force during motion is:

$$\text{Power} = \text{Drag force} \times v$$

Therefore, the power to overcome wind drag is proportional to the cube of the velocity of the vehicle (23). Obviously, this can become a determining factor in racing competition. As an example: over 80 percent of the energy to propel a bicycle at 20 miles an hour goes toward moving 1,000 pounds of air out of the way every minute (24). Since air density and gravity are uncontrollable, there are two ways to maximize velocity by minimizing the drag force: 1) by reducing the frontal area, or 2) by reducing the drag coefficient. The drag is a function of the shape and surface finish of the human/vehicle system. The shape and surface finish control how the air passes over the system. Three possible types of air flow are associated with drag: laminar flow, which governs when the vehicle shape makes gradual transitions, and the surface is smooth so that the air can flow smoothly with low drag; turbulent flow, caused by sharp transitions or rough surfaces, which makes the air eddy over the surface, producing much higher drag; and separated flow, caused by sharp transitions that eddy the air in large swirls, which causes less drag than turbulent flow. Separation is more likely to occur from laminar upstream flow than from turbulent flow (23). With this in mind, the shape of the human/chair system should be designed with smooth transitions, a smooth finish, and the smallest frontal area possible.

Smooth transitions and finish should be part of the design criteria for the frame, keeping in mind how the user fits into the flow path. Frontal area is best minimized by altering the position of the pilot, taking careful note of how the frame fits around him/her. Other considerations, such as helmet shape and material, water bottle position, and frame material can also be used to help reduce drag (24).

Ergonomics. Ergonomics is the science of optimizing human work conditions with respect to human capabilities. Some major areas addressed by ergonomics include health, safety, comfort, and efficiency (20).

The interface between chair and user needs more research. Quantification of variables and performance parameters for this biomechanical system can provide the most useful results (7,8,25). Though some quantifying work has been done, much more is needed (5,6,8,11,12,16,18,19,20,22, 25,26). Some quantified test results have shown how efficiency and speed are related to stroke length and race length, elbow position, and optimal push-ring diameter.

The major problem so far is that each chair must be custom-fitted to each user. Many race chairs are individually hand-crafted (7,13). No interpretable data has been collected that can relate the importance of anthropometric and other physical body measurements to chair dimensions and performance. Because of this lack of data, it is uncertain which parameters are important. Relationships between chair dimensions, chair controller locations, body dimensions, range of motion, physiological efficiency, and system performance all need to be researched. Quantitative results are not only much more readily interpretable, but also permit mathematical modeling, simulation, and computer analysis of the human/chair system.

Materials. Most current racing chairs are made of high-strength, low-density metals, such as chromium molybdenum alloy steel (chromoly), titanium,

or aluminum alloy. These provide the needed strength, stiffness, and low weight desired for racing chairs. For small-scale projects, chromoly has the advantage of low material and manufacturing costs. Though composite materials have the desired properties for racing chair design, there have been few attempts to use them. Composites have seen extensive use in many other sports and for high-performance equipment such as fishing poles, golf clubs, tennis rackets, skis, bikes, boats, planes, and race cars (27,28,29). For several reasons, the entry of composites into the field of racing chair design has been slow. High-tech composites are fairly new, being developed only about 20 years ago (29). A widespread understanding of their uses and limitations is just now becoming a reality. Also, composite materials are still more expensive for manufacturing purposes than are metals, though they are becoming more competitive (30).

There are many advantages to using composites. Composite structures can be stronger and stiffer than steel and aluminum at a fraction of the weight. They show superior impact resistance and dissipate less energy into vibration. They can be contoured to almost any desired shape, using fewer joints and with less wasted material (28).

There are many different types of composites. Three general categories are particulate, laminar, and fiber. Laminated fiber composites provide the necessary physical attributes for racing chair design. Laminated composites consist of layers of fibers in predesignated orientations imbedded in a resin matrix. The matrix provides ductility and toughness. The fibers add strength and stiffness while keeping the weight down. A strong bond between the matrix and the fibers must exist to preserve the beneficial qualities of each component (31).

Many different materials can be used for the fibers. The strength of the fiber depends on its material and diameter (31). Carbon or graphite offer the best characteristics for race chair design. Their high stiffness with low density provide the best mix of properties, though the cost is higher. Cost, strength, and stiffness trade-offs must be dealt with (30). Also, graphite can be laid-up (i.e., placing resin-impregnated cloth made of composite fibers on the mold and/or over preceding layers) by hand, unlike many other composites (27). Often a foam core is used with the composite lay-up on the outer surfaces. This "sandwich" construction increases the cross-sectional inertia of the lay-up, reducing the bending stresses while maintaining the weight and tensile strength properties of the material (30,31).

The amount of fiber to be used and its direction of lay must be determined. Many weights and weaves of fiber are possible, each with different working properties. The term "tow" is used to describe the direction which has the most strands of filaments running parallel. Warp is the direction of the fibers used to hold the tow strands in place. The different types of weave determine the drapability, cost, wetability, and stiffness of the cloth (30). Two major categories of tow and warp combinations are commonly used for hand lay-ups: unidirectional and bidirectional. Unidirectional composites consist mostly of tow fibers with just enough warp to hold them in place. Bidirectional composites have an even mix of tow and warp fibers, creating more cloth-like material. A proper understanding of composite lay-up technique can allow passive tailoring to create an end material with the desired bending and torsion coupling, taking full advantage of the material's anisotropic behavior (28).

Determining how much material and what directional strength is required is not an easy task. Careful planning of the lay-up order and direction can result in a superior strength-to-weight ratio material. Simple isotropic material theories cannot be used with composites. Thermal stresses, residual stresses, hydrothermal factors, and load stresses and strains must all be considered.

This increased number of variables requires special attention. Some work has been done to fit nonlinear composite data to statistical curves. Other theories show some correlation between properties such as density, conductivity, and Young's modulus to a mixture ratio (31). Many times, the increased difficulty in analyzing anisotropic materials has lead designers to default to using quasi-isotropic lay-ups that can be analyzed and laid-up more easily. The drawback is over-engineering the material strength required in some directions, resulting in a slightly heavier design.

The most effective analytical methods require the use of computers. Computers can be used to do both micro- and macro-mechanical analysis of the design to determine the required ply strength and stacking order. Stiffness characteristics can be estimated using laminated plate theory, and strengths using modified quadratic failure criteria. These

techniques must be judiciously applied in areas such as joints or near holes. Use of finite element analysis (FEA) and simulation softwares can determine the load needed to create "first ply failure," for complex-shaped designs (29).

When the analysis has been completed, construction may begin. Hand lay-up techniques are good for working on prototypes. Many publications offer guidance on these techniques, giving suggestions on the order in which plies should be laid, how to get superior wetting (i.e., impregnating the composite cloth/yarn with resin) without getting air bubbles, how to avoid irritation from the epoxy, and much more. One point, unanimously stressed, was that the most importantant step in doing a composite lay-up is preparation (27,28,30,32).

METHODS

Creating the Shape of the Frame

The importance of a favorable aerodynamic shape was discussed during the literature review. Air drag is reduced by decreasing frontal area and streamlining the contours of the chair pilot system. NWAA rules state that no items may be added to a chair strictly for the purpose of creating aerodynamic advantage. This has been interpreted in several cases to mean that nonstructural components which serve primarily to reduce wind resistance are unacceptable. A common test used is: if the chair still functions with the aerodynamic components removed, those components are disallowed. Some racers currently use strapping and seat buckets which serve to reduce aerodynamic drag as well as provide support. For this reason, design features must demonstrate primary structural and/or safety benefits; any accrued aerodynamic improvement must be secondary. Thus, a space frame being completely structural might incidentally provide much better contouring aerodynamically than a strut-chassis-type frame.

Determining the Best Shape. Not only should the shape be streamlined, it must also be fit to the pilot's position. To accomplish a prototype design, profile photos were superimposed, in both the up and down positions, with the pilot in his current racing chair. The rear wheel axle was designed to be in the same position with respect to the seat, to allow the stroke motions to be the same. The front and rear wheel diameters were chosen by the pilot to be 16 and 26 inches, respectively. These sizes were chosen to create the desired power gear ratio, while simultaneously decreasing rolling resistance. The aim was to have the frame profile provide minimal aerodynamic drag for the rider in either the up or down position. Using results from the profile layout, clay models of potential chair designs were made. Width dimensions in the cockpit were determined using dimensions of the pilot. The nose width was designed to accommodate the front wheel while allowing for approximately 15° of steering angle with a 6 cm cantilever trail arm.

The frame was molded to partially shroud the rear wheels with 10.75° of camber. The shrouding primarily serves to protect the pilot's arms during propulsion and is common practice for racing wheelchairs. Models varied in attack angle of the contoured nose and rear wheel shrouds. Wheel guards can improve the streamlining of the frame while improving safety by helping to keep the pilot's arms from contacting the spinning tires.

Wind Tunnel Testing. Two scale models were made of plaster of paris. These models were smoothed, painted, and fitted with wheels and a rider model. Model A had a narrow nose, guards over the wheels, and a steep front-end attack angle. Model B had a slightly wider, round nose, no wheel guards, and a more gradual front-end angle of attack. The model rider, made of soft clay, was mounted in race position. Soft clay was used to simulate the skin and clothing of a real racer. These models were wind tunnel tested with a stationary ground surface. Drag force was measured in the direction opposite the wind flow. Drag forces for each model were recorded at wind speeds from 3,000 to 9,000 feet per minute at 1,000 foot per minute intervals. Because similitude requires the model and the actual system to have the same Reynolds number, and these wind speeds are slightly low for a one-ninth scale model to exactly simulate the behavior of a full-size chair under normal conditions, the results proved to be worthwhile (**Table 1** and **Figure 1**). The results showed the drag force to be proportional to the square of the velocity, as expected. The models with a rider in place showed almost twice as much drag as their pilotless counterparts. Interestingly, model B with its wider nose and no wheel hubs showed slightly less overall drag than the narrow-nosed model. A 2×2 analysis of variance

Table 1.
Wind tunnel model results.

Air Speed (m/s)	Drag Force (grams)			
	Model A w/Pilot	Model B w/Pilot	Model A w/o Pilot	Model B w/o Pilot
15.24	46	43	27	26
20.32	78	75	46	44
25.40	110	112	65	65
30.48	155	161	82	88
35.56	205	215	112	120
40.64	260	275	132	137
45.21	340	360	192	188

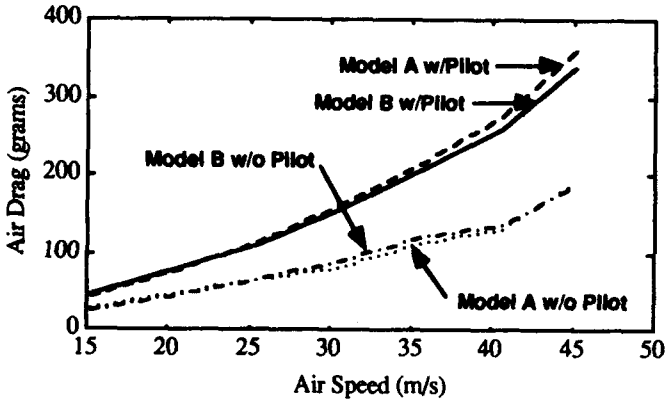

Figure 1.
Wind tunnel results for composite racing wheelchair models.

(ANOVA) showed the effect of the pilot on air drag to be significant ($p=0.024$), and the difference between the aerodynamic drag of models A and B not to be significant ($p>0.05$). The interaction was also not significant ($p>0.05$). Also of importance but not apparent from the data in **Table 1** was the stability of the shapes. Even though model B showed less overall drag, it experienced more lateral oscillation during testing than model A. Reaching a definitive, conclusive decision from this observation is difficult. The increased oscillation of the first model may be attributed to the sharp transition over the unhubbed rear wheels. Even a slight misalignment of one of the rear wheels could excite oscillations. The lower drag was probably due to the rounder nose and smoother attack angle of the front end. From these observations, the final chair shape was designed to incorporate a slightly rounder nose, a gradual attack angle, and guards over the rear wheels (**Figure 2**).

Determining the Frame Structure

There is always a trade-off between strength and weight in any structural design. Carbon graphite fibers can increase the strength-to-weight ratio. Correctly identifying high stress areas allows the strength-to-weight ratio to be optimized. FEA was used to determine the frame contour. FEA uses a computer model in which the frame is represented by many small elementary units or "elements." Each element is defined by a shape function: an equation that models the shape of the element. Stresses and displacements across elements can be estimated by minimizing the potential energy equation for all elements simultaneously. Because of computational complexity, software packages must be used to determine an optimal solution. The FEA package ALGOR was chosen to solve this project's finite element model. Like most FEA software packages, ALGOR optimizes the order of solution using complex analysis methods that account for shear, tensile, and compressive loads. It can display the results in many different ways. The solution's accuracy depends on the placement, size, and shape of the modeling elements. Areas with a high stress gradient require more elements to give the same degree of accuracy as regions where the stresses vary more gradually. Some initial assumptions about where the high stress areas might be located must be

Figure 2.
Clay model of the aerodynamic composite racing wheelchair space frame.

made before the FEA model is created. More elements are then placed in anticipated high stress areas. It was assumed that stress would be higher near points where loads were to be applied. Therefore, more elements were placed near wheel, seat, and steering mounts. The results of FEA are sensitive to element shape. The frame, much wider and longer than it is thick, can readily be modeled as a (curved) two-dimensional thin plate. Either three- (triangular) or four- (quadrilateral) sided elements can be used. Triangular elements appear stiffer under FEA than do quadrilateral elements; thus, mixing element types should be avoided.

Developing the Model. A computer model was based on the more aerodynamically shaped clay model (**Figure 3a, b, c**). A reference line was scored down the length of the clay model; a similar line was placed on the profile drawing. The line on the profile drawing was used to determine the angular orientation of the frame in space and relative to wheel positions. Cross-sections were sliced perpendicular to the scored line from the tip to the tail of the model. The width of each cross-section was 7.5 mm to preserve the shape of the model and create sufficient elements. These cross-sections were traced onto grid paper. For each cross-sectional slice, points chosen along its contour defined the curve. Extra points were placed in areas where high stresses were expected. Horizontal and vertical positions of all points were recorded along with slice depth to create x, y, and z coordinates for each point. The y and z coordinates were then plotted back onto grid paper. This insured that the model shape had been preserved and allowed for lines to be drawn in to connect the points. These lines created the edges of the elements of the FEA model. The elements were configured as quadrilaterals whenever the frame geometry allowed; otherwise, triangular elements were created. Once a satisfactory shape was determined, all three coordinates were multiplied by nine to return the dimensions to the full-scale coordinates used to develop the model on ALGOR. The points were connected with lines as had been done before by hand. The model was rotated back to its world position as calculated by the profile drawing and the score line. The resulting FEA model consisted of 411 points, 844 lines, for a total of 435 elements. Before any FEA results can be attained, material properties must be specified for the elements, and the loads must be assigned to the model. Additional nodes

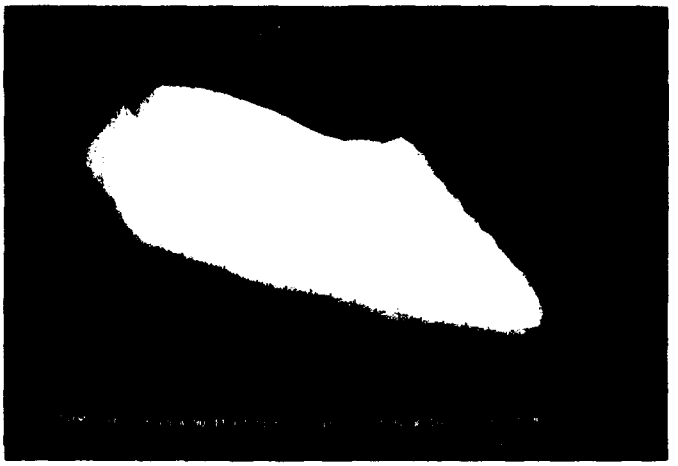

(a)

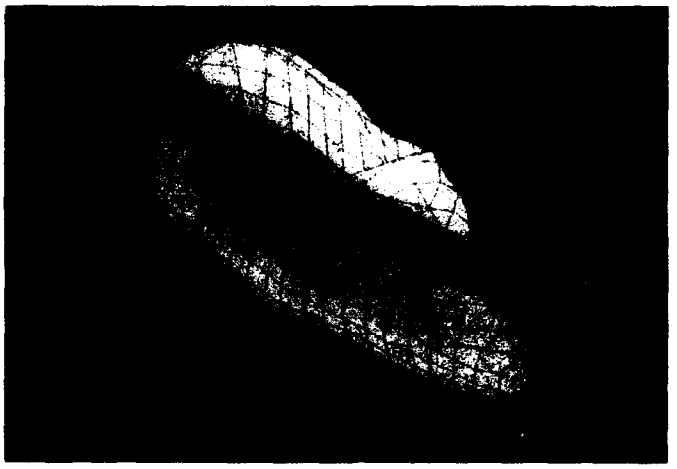

(b)

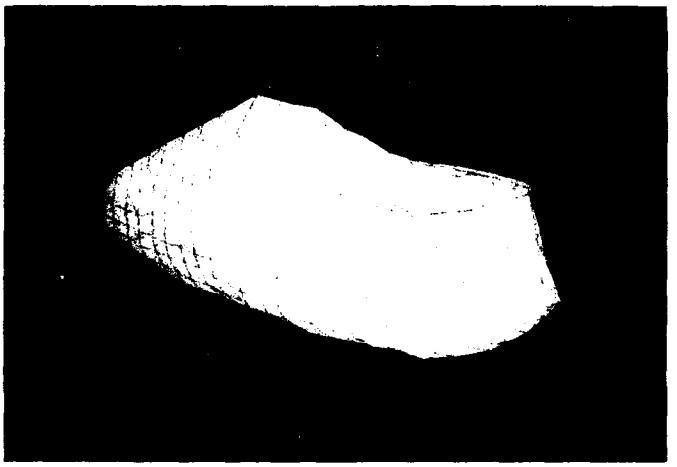

(c)

Figures 3a,b,c.
Computer finite element model of aerodynamic composite racing wheelchair space frame.

were added to areas which showed high levels of strain. The analysis was then repeated with the modified mesh.

Modeling Material Properties. Material properties were determined by testing specimens made of quasi-isotropic carbon fiber and of a quasi-isotropic carbon fiber and glass mix. These materials were chosen because of their good drapability and wetability (18,27). Load and strain data collected for these specimens led to the results shown in **Figure 4a** and **Figure 4b**. The glass did not add any strength to the material, only bulk, but it did give a better finish which would be less abrasive to the pilot, being less susceptible to environmental wear. Peculiar units of measurement are required to allow ALGOR, which was designed to use English units, to process the FEA model, which was formulated in metric units.

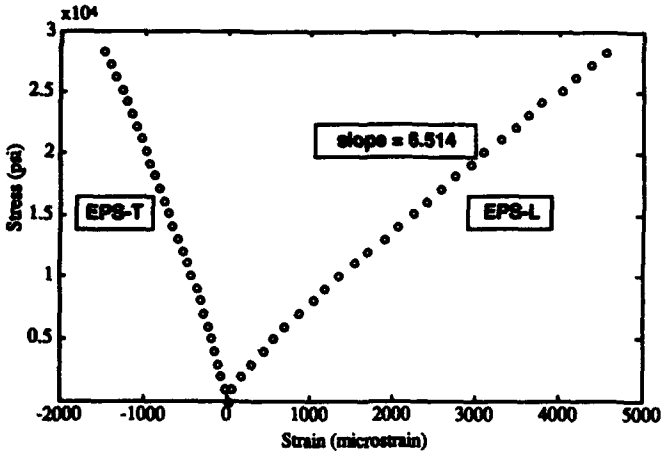

Figure 4a.
Stress and strain data for carbon fiber test specimens.

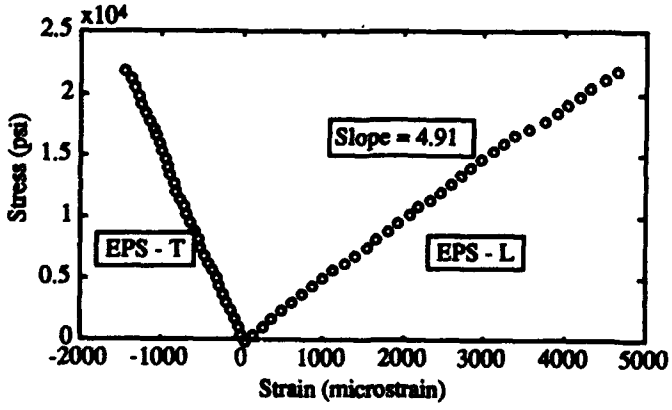

Figure 4b.
Stress and strain data for carbon fiber-glass test specimens.

Ultimate strength = 2,000 kg/cm^2 (28 ksi), Young's modulus = 458,000 kg/cm^2 (6,5000 ksi), Poisson's ratio = 0.325. These results concur sufficiently with those published. Similar materials such as T300, AS, and IM6 composites have Young's moduli of 10.10, 7.95, and 11.36 msi, and Poisson's ratios of 0.30, 0.28, and 0.30, respectively (29). Our first FEA models employed elements with the properties of one layer of quasi-isotropic carbon fiber. From the results of the one-layer models, areas that required strengthening were located. These areas were strengthened by multiplying the thickness of the elements by some multiple of a single layer or by adding core material to the center of the quasi-isotropic lay-up. Since the tensile strength was already adequate for the in-plane loads, foam provided a good core material to improve the bending stiffness without adding weight. For cored areas, the properties can be estimated by noting that Poisson's ratio does not change when a core is added. Young's modulus can be estimated using the primary flexural modulus of the composite lay-up.

The primary flexural modulus is determined by first integrating over the thickness of the composite defined by its ply stiffness matrix Q.

$$[Q] = \begin{bmatrix} \frac{E}{1-\upsilon^2} & \frac{\upsilon E}{1-\upsilon^2} & 0 \\ \frac{\upsilon E}{1-\upsilon^2} & \frac{E}{1-\upsilon^2} & 0 \\ 0 & 0 & \frac{E}{2(1+\upsilon)} \end{bmatrix}$$

Where E = Young's Modulus
υ = Poisson's Ratio

The flexural stiffness, D, becomes

$$[D] = 2\int_{z_c}^{\frac{h}{2}} [Q]\, z^2 dz$$

Where h = the laminate thickness
z_c = the top face of the core

$$D_{ij} = (\tfrac{2}{3})Q_{ij}[(h/2)^3 - (c/2)^3]$$

Where c = the core thickness

The primary flexural modulus, E_{flex}, can be determined by first normalizing the moment of inertia matrix:

$$[D^*] = \frac{12[D]}{h^3}$$

and then finding its inverse matrix

$$[d^*] = [D^*]^{-1}$$

whose major element is d_{11}^*.

$$E_{flex} = \frac{1}{d^*_{11}}$$

Loading the Model. A number of cases of frame loading were chosen to mimic loads that a race chair might experience in a race. Loading points were determined from the grid drawings. Six points were used to mount the seating system; four points were used to mount the three wheels and a compensator (**Figure 5**). The position of the compensator mount was determined geometrically. A 22-cm lightweight stainless steel push-pull compensator was manufactured. On a top view of the front of the frame, drawn using the coordinates of the FEA model, the position of the front wheel was drawn with a 6 cm cantilever trail arm. The size of the moment arm created by this mounting scheme can be determined from the drawing. Three load cases were designed to model possible pilot positions, and four load cases were used to model possible road shocks.

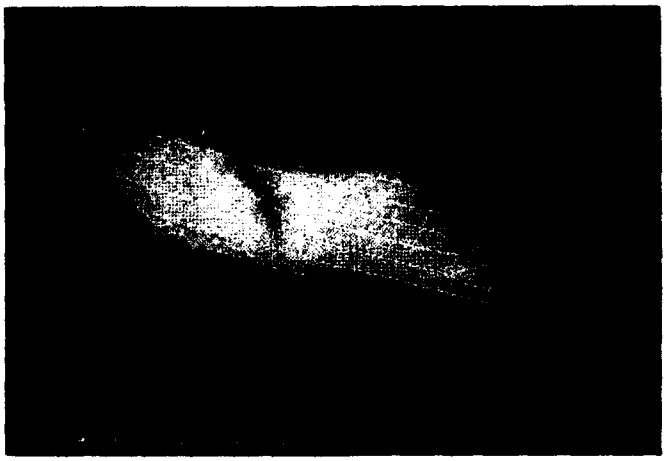

Figure 5.
Loading points for finite element analysis. 'A' and 'B' are the right and left rear seat mounts; 'C' and 'D' are the right and left center seat mounts; 'E' and 'F' are the right and left front seat mounts; 'G' and 'H' are the right and left rear wheel mounts; 'I' is the compensator mount; and 'J' is the front wheel mount.

In **Figure 5**, 'A' and 'B' are the right and left rear seat mounts; 'C' and 'D' are the right and left center seat mounts; 'E' and 'F' are the right and left front seat mounts; 'G' and 'H' are the right and left rear wheel mounts; 'I' is the compensator mount; and 'J' is the front wheel mount. Pilot loads were estimated using a 70 kg pilot distributed over six seat mounts while holding the wheel mounts fixed. The seat mounts protrude inward with an estimated moment length of 1 cm. Three load cases were used: loads distributed toward the rear seat mount, loads equally distributed over the seat mounts, and loads distributed toward the front seat mount. The pilot loads were all in the back third of the wheelbase. Road loads, applied while fixing seat mounts, were determined using the forces resulting from the worst-case pilot position during seating loads. Front wheel impact loads were determined for the pilot in the forwardmost position; rear wheel loads were those for the pilot in the rearmost position. Loads were also applied to the compensator mount to mimic jarring of the front wheel in either direction. The compensator spring constant was determined to be 80 lbs/in. Moments for the front wheel were determined using the frame geometry, and moments for the rear wheels were determined knowing the camber, wheel radius, and an estimated typical mounting distance. For all load cases, these static forces were multiplied by three to allow for the effects of dynamic loading (31).

Initial Model Findings and Improvements. Each FEA solution for the loaded model required simultaneous reduction of 2,443 equations. Areas requiring strengthening were identified by using the results from the single thickness model. Areas with deflections exceeding one-hundredth mm, or with stresses exceeding one-third the ultimate strength of the material were strengthened. A safety factor of three was applied to account for the effects of fatigue and possible unexpected loadings (**Figure 6a** and **Figure 6b**). With only a single quasi-isotropic carbon fiber layer, stresses at some points on the frame exceeded four times the ultimate strength of the material. The high stress areas were divided into those that exceeded the ultimate strength and those that exceeded one-third of the ultimate strength. The small areas with the highest stresses, such as wheel mounting sites, were enhanced with a 1-inch core. High stresses near the cockpit were enhanced with a half-inch core. Other high stress areas were strength-

Figure 6a.
Areas exceeding safety factor of three for single isotropic layer with pilot loads.

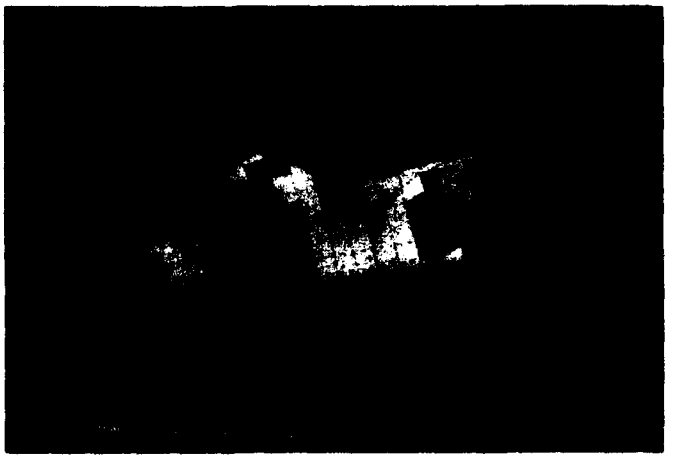

Figure 7a.
Material layout for quasi-isotropic cored body (left side).

Figure 6b.
Areas exceeding safety factor of three for single isotropic layer with road loads.

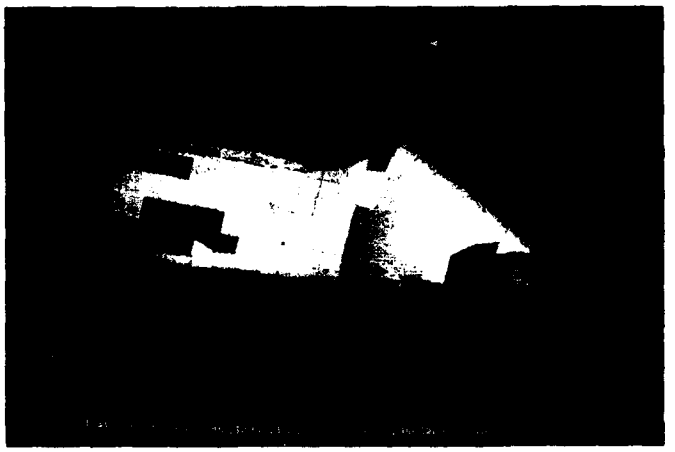

Figure 7b.
Material layout for quasi-isotropic cored body (right side).

ened with quarter-inch core material. Double thickness quasi-isotropic carbon fiber was used in transition to the lower stress areas. The final material lay-out may be seen in **Figure 7a** and **Figure 7b**. The properties for the cored areas were estimated using the flexural modulus as previously described. This combination of decreased modulus with an increased thickness resulted in improved strength; a result typical of flexural estimation.

Improved Model Results. **Figures 8a, 8b,** and **8c** and **Figures 9a** and **9b** show stress contours of the reinforced model in the pilot and road load cases, respectively. Results from the modified model met the stress and deflection requirements. The stress scale on the improved material model was different from that used with the single thickness layer of material. The cored FEA models are shown on a scale of 0–400 kg/cm^2, while the single-layer models were displayed on a scale of 0–1,000 kg/cm^2. The highest stress level found for the improved model in any of the loadings was only 635 kg/cm (almost 15 times less stress than in the original model). Locations of high stress areas from road loads are almost opposite the position of high stress areas from the pilot loads. This could help avert any failure due to combinations of loading.

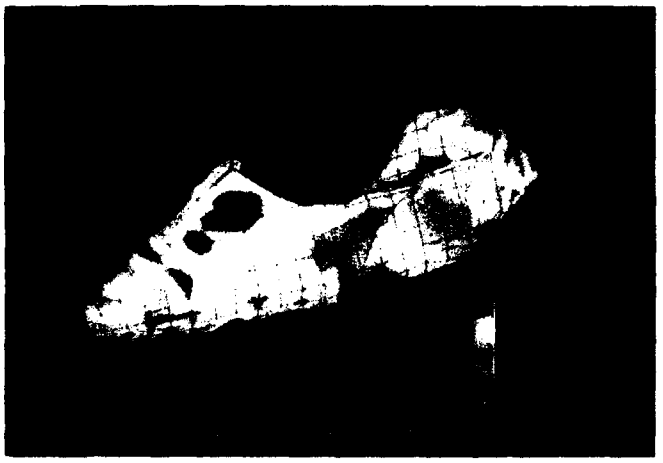

Figure 8a.
Stress contours for quasi-isotropic cored body: pilot load aft.

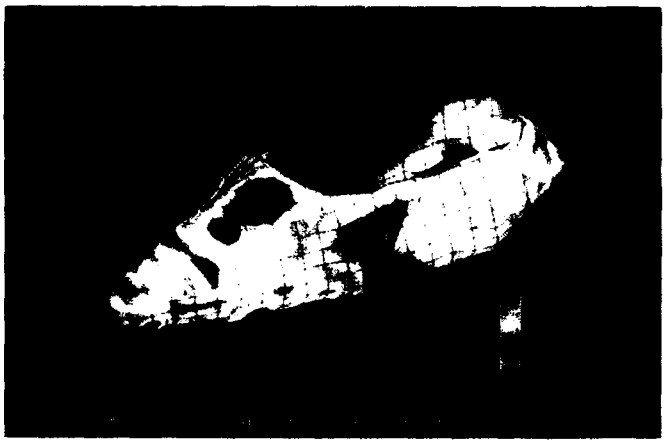

Figure 8c.
Stress contours for quasi-isotropic cored body: pilot load forward.

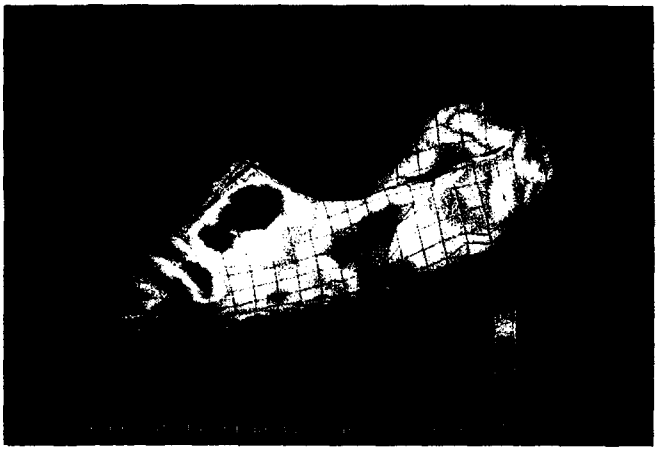

Figure 8b.
Stress contours for quasi-isotropic cored body: pilot load centered.

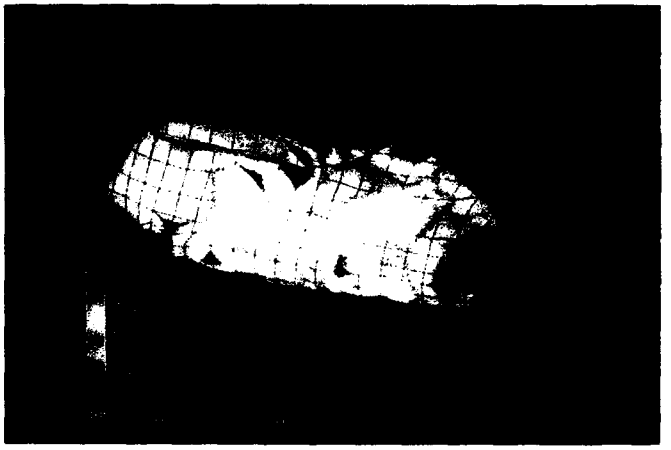

Figure 9a.
Stress contours for quasi-isotropic cored body: road load right rear wheel.

RESULTS

Building a Prototype

Building the prototype required creating a mold. When the lay-up was completed, the frame was seamed and trimmed. Next, the wheel and steering mounts and seat were attached to the frame. Finally, the wheels were aligned.

Building the Frame. Full-size patterns of the right and left halves of the chair were cut using cross-sectional data. These patterns were traced onto Styrofoam™ and cut using a hot wire. Cross-sectional widths, cut with a band saw, were glued together to form right and left halves of the chair. The two halves were sanded to smooth the surface contour. Sanding was also used to recess core material. The molds were covered with plastic wrap using double-stick tape to prepare them for lay-up. (The plastic wrap protects the foam from the resin and makes the finished shell easier to release.) A large aluminum sheet sprayed with mold-release was used as a work table. The carbon fiber was cut directionally to allow enough pieces to create a quasi-isotropic lay-up for each mold half. Some pieces required seams to cover the entire mold. No

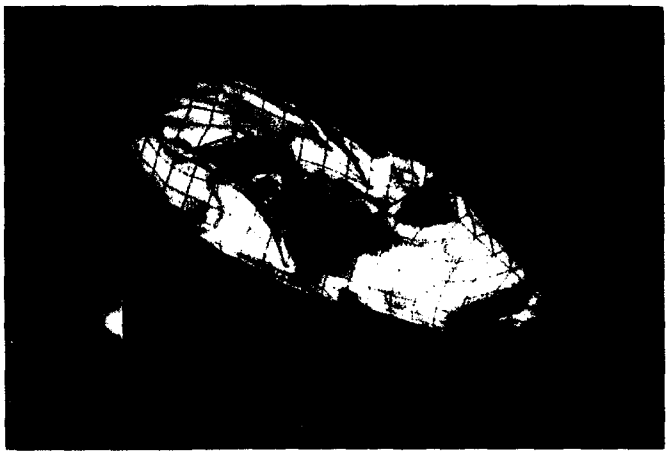

Figure 9b.
Stress contours for quasi-isotropic cored body: road load left rear wheel.

seams were placed directly over other seams to eliminate stress risers created by increased thickness at the seam (30). The two frame halves were molded by using standard hand lay-up procedures. The foam cores were puttied in the center of the lay-up using a microbubble slurry. A flange, left at the edge of the mold on the aluminum, helped to insure the lay-up's integrity at the edges and to create an easy way to match molded halves. Fiberglass was used for the outermost layer. After 2 days the molds were released and trimmed. The two halves were matched and bolted together along the flange. Seat and front wheel holes were cut, and the inside seam was sanded rough. Using long strips of carbon fiber, the inner half of a quasi-isotropic seam was created. When the seam dried, the outer flange was removed. The outer seam area was then sanded rough to create a bonding surface and the second half of the quasi-isotropic seam laid. Some extra material was laid-up around wheel and cockpit openings to increase their strength, and fiberglass was placed in areas that might contact the pilot. The rough frame and seat are shown in **Figure 10.**

Attaching Wheel and Steering Mounts. Click Studs (Click Studs, Bergdahl Associates, Inc., Reno, NV), were used to mount the wheels and steering mechanisms because they do not require drilling holes that may degrade the integrity of the frame material. The studs are surface-mounted using an epoxy cement. When properly adhered to a graphite substrate, each 1.25-inch mounting base can support 550 lb in tension of 1300 lb in shear. Used in the fashion proposed in the models, most of the load is expected to be in shear. The front and rear wheels mount to faceplates, which attach to the Click Studs. The compensator mounts directly to a stainless steel stud, slightly larger than a Click Stud, which had a face better suited for tightening. The wheel mounting plates were machined from aluminum 7075, T6 because of its high strength-to-weight ratio.

The front wheel was mounted first and adjusted with spacers until it was vertical. The rear wheels were mounted and aligned using an alignment tool (11).

The Seating System. The pilot of the chair must be securely seated in the proper position in order to get the best foundation from which to drive the chair. Using a Pin Dot seat molding frame (Pin Dot Products, Niles, IL), a plaster mold was made of the pilot's back and seat in his racing position. The seat was laid-up by using the same technique as with the chair mold in **Figure 10.** Fiberglass was chosen for the lay-up material because it would be less irritating to the pilot. The seat was mounted to the chair frame using Click Studs. Two rails, also fastened onto Click Studs, allow adjustment of seat position.

Finishing. A smooth finish was needed in order to decrease aerodynamic drag and skin irritation. The body was sanded to remove any major discontinuities. The texture was then smoothed, as much as possible, using primer paint. Finally, a

Figure 10.
Rough lay-up of composite space frame and seat.

Journal of Rehabilitation Research and Development Vol. 30 No. 2 1993

gloss paint coat was applied. **Figure 11** shows the finished chair.

Expenses. **Table 2** gives a rough estimate of material costs required to build this prototype. These costs alone make this racing wheelchair expensive compared to contemporary tubular chassis designs. Labor costs would also be relatively high; however, costs could be reduced if the chair went into commercial production and materials were purchased in larger quantities. If performance was improved, there would still be interest by elite athletes, despite the high cost, since racing wheelchairs are special purpose vehicles.

Figure 11.
Completed composite space frame racing wheelchair.

Table 2.
Prototype budget.

Bidirectional Woven Graphite 42" x .013", 8HS Weave, 32 yds. @ $70.00 = $2,240.00	
Unidirectional Graphite 5" x .006", Plain Weave, 20 yds. @ $1.35 = $27.00	
Safe-T-Poxy Resin, 2 Gallons, $100.00	
Foam Cores and Microbubble Filler, $50.00	
Foam for Mold Shape, Styrofoam, $50.00 Molding	
Supplies:	
Paint Brushes, Rollers, Rubber Gloves, Wrap, Saw Blades, Contact Cement, Cleaners, $100.00	
Modeling Supplies: Clay, Plaster, Mold®It, Epoxy Glue, Paint, Sandpaper, Graph Paper, $40.00	
Photography Supplies: Film and Developing, $75.00	
Mounting Studs, Click Studs, $25.00	
Wheel Mounts, Steering Mount, and Compensator Material and Machining, $140.00	
TOTAL	$2847.00

Testing the Prototype

The new design was tested to measure its improvement over existing designs. The pilot has used the chair several times. The best testing, through repeated usage in a competitive situation, is yet to come. Several simple performance checks were possible, however.

At 32 pounds, the complete composite chair is nearly twice the weight of a typical race chair. The pilot noted that although the chair accelerated slowly, it handled well at road speeds. It is difficult to determine, without performing destructive testing, whether the unibody frame is actually stiffer than its strut-chassis counterparts. The chair has a very stiff ride. The pilot felt as if he had a firm base to transmit force to the push-rings. He reported that the rear wheel positions were slightly too wide for his preference and the seat was too far forward. The seat position was moved all the way back on the adjustable rails. The unibody design prevents moving the seat any farther back without altering structural integrity. The width, however, can be corrected with a simple modification of the wheel mounts. The unibody frame allowed the pilot to tuck in his arms when coasting, which improved the aerodynamics.

FUTURE IMPROVEMENTS

Positioning Improvements

In future designs, care should be taken to allow ample adjustment of seat position. With a unibody design this is critical. In this design, trying to contour the back of the frame too close to the pilot resulted in limitations on the seat movement.

Aerodynamic Improvements

The preliminary aerodynamic studies with the wind tunnel and plaster models could also have been improved. The wind tunnel did not account for ground motion and air viscosity effects. Only forces in the axial direction could be measured; lift and twist forces were not accessible. The models themselves were not exact. Spoked wheels were difficult to model, and the surface finish could only simulate that of the final chair. Increasing the number of

shapes and possible pilot positions would be useful. A better wind tunnel and improved modeling techniques might be able to determine the best helmet design and clothing material. Besides using an improved wind tunnel and models, better results might have been attained through FEA on a computer. Simulation may possibly offer a more accurate and cost-effective alternative.

Apart from possible modeling refinements, the manufacturing process could be improved to produce a more aerodynamic frame. The final surface of our frame was lumpy because of the imperfect fit of the core pieces. The easiest "fix" for this is to use a female mold instead of a male one. Then the smooth, aerodynamic shape would be preserved on the outside, and the lumpiness from the core would be on the inside. Measuring the frontal area using photos and a planimeter could, in the future, be a useful way to compare the aerodynamics of the prototype with more traditional chairs, giving frontal area values for quick comparison. This could be useful to future designs.

Structural Improvements

Though the FEA results helped optimize the structural strength, thus keeping the weight at a minimum, the final chair was still much heavier than desired. Perhaps this occurred because the shape of the chair and its strength were optimized separately. Optimizing them together might give a weight and drag compromise which would result in the best overall chair, one that would be better than either the best-shaped or lightest-structured chair. The weight problem could also be addressed by removing material. The initial structure was designed using a single layer of material. High stress areas were beefed up, but low stress areas were left alone. By using a finer weave material or leaving lightening holes, weight in the low stress areas could have been significantly reduced. Taking advantage of the nonhomogeneous properties of composites could greatly reduce the weight of the chair. Not every element requires the same strength in every direction (the back region of the frame is a possible candidate for redesign).

Because of the churning of the wheels and the nonaerodynamic shape of the pilot, the air flow in the back region is not laminar. Turbulent flow creates the largest drag. A sharp disturbance upstream in the structure can cause full-scale separation, lowering the overall drag force: material in the rear structure of the frame might be reduced so that only as much material remained as was needed to maintain the stiffness. This would be clarified during a more complete aerodynamic and structural optimization.

Integrating a seat base into the unibody frame would remove the need for any extra hardware that increases the system's weight. It is important to allow for full adjustability of seat position.

Frame weight might be further decreased by improving the lay-up technique. Because the core pieces did not fit perfectly, a slurry of resin and microbubble was used as filler. This filler was much heavier than the core material. The core reinforcement was 1 inch, 0.5 inch, and 0.25-inch-thick material. It is important that the transitions from one core thickness to another are continuous. Although the layout process would be more difficult, an exterior mold would make the exterior transitions smoother. Also, during hand lay-up, special care must be taken to insure that the material is completely impregnated with resin. This may have led to using excess resin in the material. Using a technique known as vacuum bagging, excess resin can be sucked out, leaving only the resin that is required.

Several Click Studs had to be replaced. Although the studs were strong, the epoxy adhesive had difficulty standing up to impact loads. Roughing up the bonding surfaces and increasing the mounting area might help to improve their strength.

More tests should be run on this chair to determine its strengths and limitations. The safety factor of three may be more conservative than was necessary. Some of the weight increase may turn out to be acceptable due to the decreased drag and increased frame stiffness. A kinematic analysis of the pilot may permit interface improvement.

DISCUSSION

The FEA model executed on a computer provided insight into structural problem areas in the design of unibody frame racing chairs. Slight modifications to the model can be used to investigate new shapes, loads, or materials without investing large amounts of time and money. With aerodynamic FEA software, the model could provide perspectives

on different improvements to reduce drag. Shape improvements may play an important role in reducing the racer's time during competition by helping to decrease drag for the user in either the upright or down position. Considering how much the air flow is deflected by current strut frames and that the frontal area increases around 30 percent in the up position, monocoque shapes should excel. Future work on unibody race chairs could start from this design and attempt to improve upon it by reducing the weight of the chair, to bring it in line with that of current strut-chassis chairs, or could try to show that the drag of the unibody chair compensates for its extra weight.

Although this composite chair weighs more than its competitors, the extra weight is compensated for in other ways (e.g., the lack of joints and other high stress areas in the unibody style might make the chair stiffer and safer).

It is important to remember that the race chair is only part of the system. The racer's weight, which varies significantly between individuals, also affects the ease with which the system can be propelled.

Other ways to improve the chair were discovered during construction: using a female, instead of a male, mold could improve the outer surface shape and texture; vacuum bagging excess resin could reduce the weight of the frame; and adhesive Click Studs provided an easy way to mount things to the frame without deteriorating the integrity of the frames structure (but stronger bonds should be sought out).

The molded seat made with the Pin Dot molding system turned out well. The seat provides the support and positioning needed to effectively propel the chair. These findings clearly indicate that the application of engineering technology can improve the design of the racing wheelchairs.

ACKNOWLEDGMENTS

Carbon fiber material was donated by Hexcel Corporation, Click Studs were donated by Bergdahl Associates, and wheelchair components were supplied by Eagle Sports Chairs. Additional support was provided by the Rehabilitation Services Administration, U.S. Department of Education (#H129E00005), and California State University, Sacramento, CA. The authors thank Tom Andersen, Dave VanSickle, Ken Stewart, Dr. Chuck Washburn, and Dr. Leo Dabaghian for their assistance.

REFERENCES

1. Ryan AJ. Competition needed for disabled athletes. Phys Sports Med 1984:12(5):49.
2. Duda M. Wheelers make strides, all disabled people win. Phys Sports Med 1985:13(10):156-9.
3. Hedrick BN, Morse MI, Hedrick S. A guide for wheelchair sports training. Colorado Springs: National Wheelchair Athletic Association, 1988.
4. Higgs C. An analysis of racing wheelchairs used at the 1980 Olympic Games for the Disabled. Res Q Exerc Sport 1983:54(3):229-33.
5. Ridgway M, Pope C, Wilkerson J. A kinematic analysis of 800-meter wheelchair racing techniques. Adapt Phys Act Q 1988:5(2):96-107.
6. Sanderson DJ, Sommer HJ. Kinematic features of wheelchair propulsion. Biomechanics 1985:18(6):423-9.
7. Cooper RA. The racing wheelchair. SOMA Eng Hum Body 1990:4:28-34.
8. Depauw KP. Sp[illegible] for individuals with disabilities: research opportunities. Adapt Phys Act Q 1988:5(2):80-9.
9. McFarland SR, Scadden LA. Marketing rehabilitation engineering. SOMA Eng Hum Body 1986:1:19-23.
10. Cooper RA. Wheelchair racing sports science: a review. J Rehabil Res Dev 1990:27(3):295-312.
11. Cooper RA. Racing wheelchair rear wheel alignment. J Rehabil Res Dev 1989:26(1):47-50.
12. Cooper RA. Racing Wheelchair crown compensation. J Rehabil Res Dev 1989:26(1):25-32.
13. Cooper RA. Racing chair lingo... or how to order a racing wheelchair. Sports 'N Spokes 1988:13(6):29-32.
14. Quickie Designs Inc. The perfect fit, an adjustment guide to your manual wheelchair. Fresno, CA: Quickie Designs Inc., 1990.
15. Kyle CR. Aerodynamic wheels. Bicycling. Dec:1985:121-4.
16. York SL, Kimura IF. An analysis of basic construction variables of racing wheelchairs used in the 1984 International Games for the Disabled. Res Q Exerc Sport 1987:58(1):16-20.
17. Cooper RA. Racing wheelchair roll stability while turning. In: Proceedings of the 13th Annual RESNA Conference, 1990 June; Washington, DC: RESNA Press, 1990:65-6.
18. Brubaker EC. Wheelchair prescription: an analysis of factors that affect mobility and performance. J Rehabil Res Dev 1986:23(4):19-26.
19. Brubaker CE, McLaurin CA, McClay IS. Effects of side slope on wheelchair performance. J Rehabil Res Dev 1986:23(2):55-7.
20. Van der Woude LHV, Veeger HEJ, Rozendal RH. Ergonomics of wheelchair design: a prerequisite for optimum wheeling conditions. Adapt Phys Act Q 1989:6:106-32.
21. Soviero MM. Reinventing the wheel. Pop Sci 1990:Oct:76.
22. Cooper, RA. An international track wheelchair with a center of gravity directional controller. J Rehabil Res Dev 1989:26(2):63-70.

23. Whit FR, Wilson DG. Bicycling science. Cambridge: MIT Press, 1982.
24. Roosa D. Rider position: get yourself down. Bicycle Guide 1989:Aug:49.
25. Cooper RA. Simulating wheelchair racing. In: Proceedings of the 12th Annual RESNA Conference, 1989 June; New Orleans, LA, Washington, DC: RESNA Press, 1989:450-1.
26. Cooper RA, Bedi JF. Gross mechanical efficiency of trained wheelchair racers. In: Proceedings of the 11th Annual IEEE-EMBS Conference, Philadelphia, PA: IEEE-Press, 1990:12(5):2311-2.
27. Aircraft Spruce & Specialty Company. Composite materials. Fullerton, CA: The Company, 1990.
28. La Grace P. Introduction to composites. Cambridge: MIT Press, 1990.
29. Tsai SW. Composites design. Dayton, OH: Think Composites Publishers, 1988.
30. Walbridge C. Boat builders manual, building fiberglass canoes and kayaks for whitewater, 5th ed. Menasha Ridge, NC: Menasha Ridge Press, 1982.
31. Askeland D. The science of engineering and materials. Chicago: PWS Engineering, 1985.
32. Reinhart TJ. Composites engineering materials handbook. Vol. 1. Metals Park, OH: ASM International, 1990.

Department of Veterans Affairs

Journal of Rehabilitation Research and Development Vol. 30 No. 2, 1993
Pages 250-259

Analysis of sweat during soft tissue breakdown following pressure ischemia

Adrian Polliack, BS; Richard Taylor, PhD, MRCPath; Dan Bader, PhD
Oxford Orthopaedic Engineering Centre, University of Oxford, Oxford, OX3 7LD UK; Department Of Clinical Biochemistry, John Radcliffe Hospital, Oxford, OX3 9DU UK; I.R.C. Biomedical Materials, Queen Mary and Westfield College, University of London, London E1 4NS UK

Abstract—This paper examines the nature of tissue metabolites collected in thermally induced sweat following the application of different loading regimes on the soft tissues of able-bodied subjects. Loading was produced by 1) external application on the forearm via both a tourniquet and a uniaxial indenter system, and 2) ischial support on a wheelchair and sacral support on an examination bed. In each case sweat pads were attached to the tissue areas of a group of able-bodied subjects and interface pressures were recorded. After a prescribed period, the pads were removed and a quantitative analysis of a range of metabolites was performed. Results indicated that tissues subjected to pressure ischemia produced a general increase in concentrations of lactate, chloride, urea, and urate associated with a decreased sweat rate. In the reperfusion phase, some of these metabolites returned to unloaded levels. It is proposed that specific metabolites may be used as an indicator of soft tissue damage.

Key words: *pressure ischemia, pressure sores, soft tissue breakdown, sweat metabolism, thermal sweating.*

INTRODUCTION

There are a host of external factors, generally physical and biochemical in nature, that contribute to the development of tissue breakdown and the formation of pressure sores. However, the presence of pressures applied normally at the interface between the soft tissues and the patient support must be considered as an initiating cause. When prolonged pressure is applied to the skin, the underlying blood vessels are partially or totally occluded, and oxygen and other nutrients are not delivered at a rate sufficient to satisfy the metabolic demands of the tissue. To survive, the cells must draw upon their stores of energy. The lymphatic drainage will also be impaired; thus, the breakdown products of metabolism accumulate within both the interstitial spaces and the cells. As energy stores diminish, the cellular processes begin to fail, ionic gradients across cellular membranes begin to dissipate and cell necrosis can occur.

The nature of the loading of the soft tissues is also an important determinant. It is well-known that body tissues can support high levels of hydrostatic pressure, with equal components in all directions, with no resulting tissue damage. This is well illustrated by deep sea divers, who are regularly exposed to hydrostatic pressures in excess of 100 kPa (750 mmHg) for prolonged periods with no ill effects on the soft tissues. This is because the external pressures that develop as the depth of the dive increases are balanced by the increasing pressures of the gases breathed, resulting in no pressure differential between the tissues and the applied external pressure (1). However, if the external pressures are applied nonuniformly, tissue distortion leading to localized tissue damage can result. This occurs in many

Address all correspondence and requests for reprints to: Dr. D.L. Bader, I.R.C. in Biomedical Materials, Queen Mary and Westfield College, Mile End Road, London E1 4NS UK.

situations in which the body interfaces externally with load-supporting devices.

The soft tissues exhibit viscoelastic behavior; thus, the effects of loading will depend upon the rate and period of application as well as the magnitude of the load. The nature of the tissue recovery is determined by the resilience of the specific tissues and the tissue structures, including the blood and lymph vessels (2). Short-term loading generally produces elastic recovery on removal of the applied load, while long-term loading produces creep and requires a longer time for complete tissue recovery. It has been well established that tissue damage is often apparent following prolonged loading even at relatively low pressure intensities (3). Any significant period of loading will result in vascular and arterial occlusion. On load removal, there will be a period of increased blood flow through the tissues which had been ischemic. This phenomenon, termed reactive hyperemia, is a consequence of a local regulatory mechanism whereby the arterioles are dilated and the resistance to blood flow is reduced.

The microenvironment of the subject/support interface greatly affects the likelihood of tissue breakdown leading to the formation of a pressure sore. High moisture levels at the interface can be produced by incontinence or perspiration on impermeable cushion covers. This excess moisture can lead to maceration of the epidermis, a precursor of tissue breakdown which is accelerated by an alkaline environment.

There has been considerable speculation about the possible role of certain metabolites in tissue necrosis following insult of the soft tissues. The identity of the vasodilator agents remains unclear, although there are many possible candidates, such as histamine, adenosine, and prostaglandin-like substances, for the role. It has been shown that the nature of their release will be affected by the duration of ischemia (4). The role of oxygen-free radicals during reperfusion of ischemic tissues has also recently been discussed (5). The generation of these radicals is associated with the production of a series of metabolites, including urate and hypoxanthine.

Related Studies

The Oxford Pressure Monitor provides an accurate measure of the pressure distribution at the patient support interface (6). However, the measurement of interface pressure alone is not sufficient to alert the clinician to potential areas of tissue breakdown. For this, some measure of tissue damage is required which reflects an inadequate supply of nutrients or removal of metabolic products.

Transcutaneous gas monitoring has proved an accurate and repeatable method for investigating the effects of prolonged loading on the viability of tissues overlying bony prominences on a mixed group of debilitated subjects, who were considered to be particularly prone to the development of pressure sores (7). Results indicated a wide range of integrated pressure and time which the soft tissues will tolerate. The applied pressures to produce, for example, a 50 percent reduction in unloaded resting value of transcutaneous oxygen tension (T_cPO_2) ranged from 3.0 kPa (22 mmHg) to 12.2 kPa (92 mmHg). This emphasized the individual nature of the tissue response, which should be determined before clinical guidelines of safe pressure levels can be established. The level of T_cPO_2 gives some idea of tissue viability, but there is still no absolute evidence that prolonged periods below a specific threshold level of T_cPO_2 will inevitably lead to tissue damage.

Very little work has been reported on the analysis of sweat under ischemic conditions. Of the few reported studies, Van Heyningen and Weiner (8) examined the effects of ischemia on sweat composition and demonstrated a decreased sweat rate following tourniquet ischemia of the arm. They also indicated that prolonged arterial occlusion resulted in an increase in the lactate and urea concentrations. It is worthy of note that the absolute levels of these metabolites measured in sweat were an order of magnitude greater than the comparative levels generally observed in blood. In an important comparative study, Ferguson-Pell and Hagisawa (9) demonstrated the feasibility of measuring lactate and sodium concentrations in sweat collected locally from the volar aspect of the forearm, using electrochemical stimulation techniques. Elevated levels of sweat lactate were recorded during local tissue indentation which returned to basal levels following load removal in a group of able-bodied subjects. However, the system employed, the Macroduct sweat collector, uses an artificial means of inducing localized sweat via the introduction of pilocarpine nitrate using iontophoresis and its bulk size pre-

cludes its use at the loaded body support interface. Also, the volume of sweat collected in this study was relatively low with mean values not exceeding 40 μl.

The sweat glands are simple tubular glands, whose major functions are to control temperature and conductivity by secretion of water and electrolytes (10). Sweat is a hypotonic solution of sodium and chloride ions in water, together with other constituents including lactate, urea, and potassium. The presence of these metabolites accounts for about 95 percent of the osmotically active substances in sweat (8). Sweat is a true secretion and not simply a filtrate. It is controlled by mechanisms that are present in almost all levels of the nervous system. The hypothalamus is the primary center for temperature regulation of the body (11). However, there is evidence that local cutaneous thermoreceptors are the initial reflex response to exercise and may trigger the hypothalamus to act on the pituitary gland which, in turn, stimulates the sweat glands.

Objectives

This study describes two separate investigations to assess the sweat collected at the soft tissues of able-bodied subjects both during and after periods of pressure ischemia. In the first, the effects of two different loading regimes on forearm tissues were determined. The second study involved monitoring subjects who were supported either sitting in a wheelchair or lying supine on an examination bed, which provided loading at the ischial tuberosity and the sacral tissues, respectively. Sweat was analyzed for potential biochemical markers of compromised tissue viability in the loaded tissues.

METHODS AND MATERIALS

Sweat collection was achieved with cellulose chromatography paper (Whatman Paper Ltd., Maidstone, UK), which is known to be inert in contact with moist skin. For each test, a sweat pad of 5,000mm^2 was used, an area which could retain a maximum sweat volume of 1 ml. Skin preparation of the test site involved washing the skin with soap and rinsing with distilled water. Once the site was completely dry, the sweat pad was placed over the test site and folded over several times to achieve a localized collection area of typically 1,600mm^2. In order to minimize evaporation from the sweat pad, a 50 μm-thick transparent polypropylene sheet (455 SCB 50 Shorko, Cortaulds Films, Swindon, UK) of larger dimensions than the sweat pad was placed over it. The polypropylene sheet was hydrophobic in nature and thus, neither reacted with nor retained any of the collected sweat. The sheet was sealed to the skin with surgical tape (Blenderm Surgical Tape, 3M Health Care Ltd., Loughborough, UK). This tape is transparent, occlusive to moisture vapor transmission and hypoallergenic to skin.

Before the tests, each subject was acclimatized in an assessment room heated to a controlled temperature of 30°C for a 15-minute period; then the sweat collection pads were attached. This temperature was maintained for the duration of the test to facilitate thermal sweating of each subject.

Effects of Different Loading Regimes on Tissues of the Forearm

This series of tests required the subject to remain seated for the duration of the trial with both arms supported on a bead-filled support cushion, resting on a table at the same approximate level as the heart. A sweat pad was attached to the volar aspect of each forearm when the subject began sweating. Two distinct loading regimes were applied to the soft tissues:

1. Ischemic loading was achieved by applying a sphygmomanometer cuff around the biceps of the left arm, which was then inflated to a pressure of 20 kPa (150 mmHg). Sweat collection pads were applied to the volar aspect of both forearms with the right arm as control. Sweat was collected from control arms for 30 minutes, but on the experimental arm, the pain and discomfort in the forearm caused by the cuff could be tolerated for only 10 minutes, at which time the cuff and sweat pad were removed. Upon removal, the sweat pads were inserted immediately into separate airtight containers.

2. Uniaxial loading was applied via a rigid indenter positioned immediately beneath a loading pan which was incorporated in a balanced beam counterbalanced at the other end by a moveable weight (**Figure 1**). The 33 mm indenter was curved at its edges to minimize the effects of high stresses at the periphery of the indenter/soft tissue contact area (2). Careful alignment of the experimental system ensured that the loading was perpendicular to the skin surface, thereby avoiding significant shear forces, directly above the experimental sweat pad.

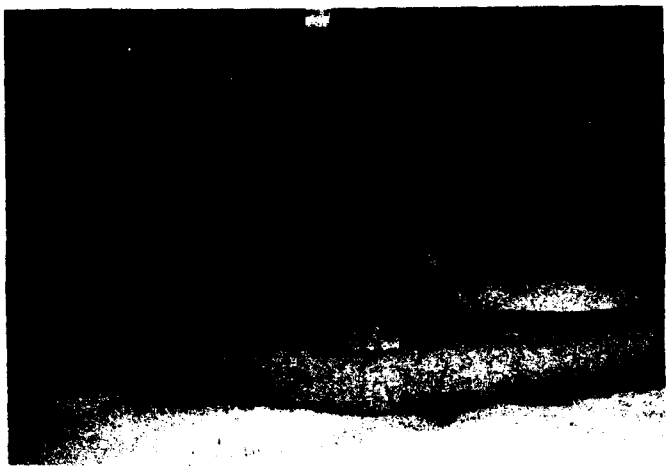

Figure 1.
Uniaxial loading of tissues by using an indenter on the subject's forearm.

The pressure at the interface between indenter and sweat pad was measured for each applied load using one cell of the Oxford Pressure Monitor (Talley Medical Equipment Ltd., Romsey, UK). Weights of 1 kg each were incrementally placed in the loading pan, until the interface pressure reached a value of approximately 20 kPa (150 mmHg). An applied pressure of this magnitude for a [illegible] test period of 30 minutes was considered to be sufficient to establish localized tissue ischemia (9). None of the subjects complained of any discomfort during the test. After 30 minutes, the indenter on the experimental arm was removed and both sweat pads were immediately removed and inserted into separate containers.

A subsequent test involved the collection of sweat during the postischemic or reperfusion period. On removal of the indenter, the existing sweat pad on the experimental arm was replaced by a fresh pad located over the test site. After a further 10 minutes, the second pad was removed to obtain sweat secreted during this reperfusion phase.

Analysis was restricted to the measurement of lactate and chloride levels in the collected sweat. Both sets of measurements were performed on six able-bodied subjects (5 males and 1 female), aged 22 to 26 years, with no underlying medical problems.

Effects of Wheelchair Sitting and Supine Lying on Soft Tissues

Initially, subjects lay prone on a standard examination bed with a sweat pad attached either over the sacral or ischial tissues. After approximately 40 minutes, sufficient sweat had been collected at the test sites. The pad was then removed and inserted into a separate container and a fresh pad was attached. The subjects then underwent one of two separate experimental test procedures as described below.

1. The subject was seated directly on the canvas of a standard wheelchair with sweat pads attached to the ischium, as shown in **Figure 2**. The interface pressure distribution across the ischium was continuously measured by the Oxford Pressure Monitor. This support was maintained for a period of 55 minutes—sufficient time to create minimal ischemia. Upon completion of this stage, the sweat pad was removed and replaced by a fresh pad, and the subject reassumed the prone position. After approximately 25 minutes, sufficient sweat had been collected at the test site during this reperfusion stage. The pad was then removed and placed in a container and the test was terminated.

2. The subject attained a supine position on the examination bed (**Figure 3**) with a sweat pad attached to the loaded sacrum. The interface pressure distribution across the sacral area was continu-

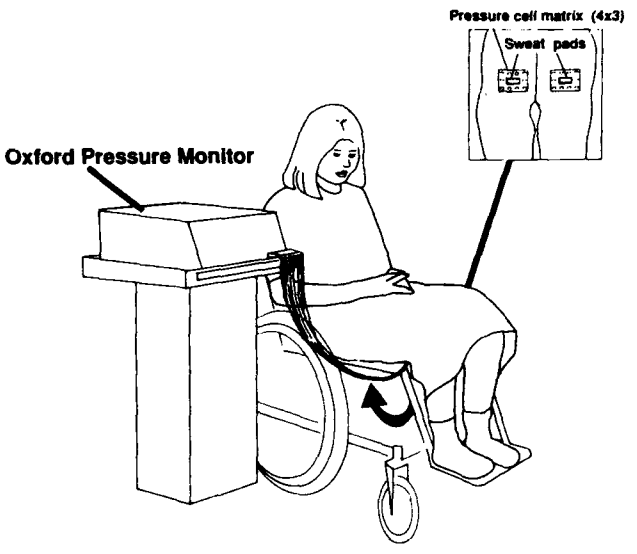

Figure 2.
A subject seated directly on the canvas base of a wheelchair, with loading of the ischial tissues.

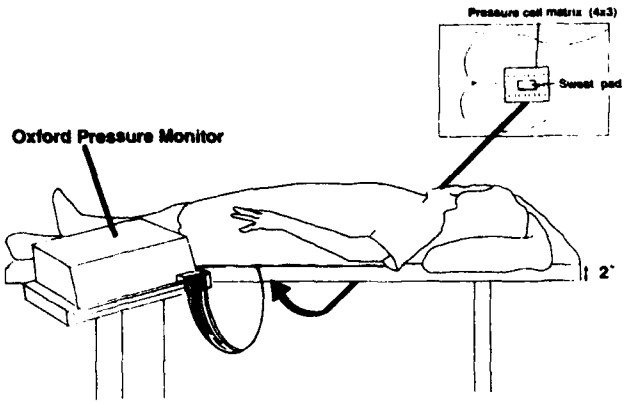

Figure 3.
A subject lying supine on an examination bed, with loading of the sacral tissues.

ously measured by the Oxford Pressure Monitor. This support was maintained for a period of 45 minutes—sufficient time to create minimal ischemia. Upon completion of this stage, the sweat pad was removed and replaced by a fresh pad, while the subject reattained the prone position. After about 25 minutes, sufficient sweat had been collected at the test site during this reperfusion stage. The pad was then removed and placed in a container and the test was terminated.

The analysis involved the measurement of the levels of six metabolites in the collected sweat. Both sets of measurements were performed on a total of 13 able-bodied subjects (9 males and 4 females), in the age range of 22 to 29 years, with no underlying medical problems.

Biochemical Analysis

Following the trial, the 30 ml plastic containers (Universal, Sterilin Ltd., Hounslow, UK) were reweighed to obtain the net sweat weight by difference, and the samples subsequently stored at −20°C prior to chemical analysis. The collected sweat was eluted by adding five times the volume of distilled water. The diluted sweat samples were quantitatively analyzed using established methods for serum and urine analysis, all of which required modification for the low analyte concentrations or sweat volumes available. Lactate, urate, urea, and chloride assays were performed on a Cobas FARA automated centrifugal analyzer (Roche Diagnostic Systems, Welwyn Garden City, UK). For each analyte, all samples from each patient in an experiment were analyzed in the same analytical run to minimize analysis error.

Lactate was measured by a lactate dehydrogenase spectrophotometric method from NADH production at 340 nm (12). Urate was measured by a uricase method (Sigma Chemical Co. Ltd., Poole, UK) by measurement of allantoin production at 292 nm. Urea was measured by a urease method as the decrease in absorbance at 340 nm (13). Reagents were from Technicon (Bayer Diagnostics Ltd., Basingstoke, UK). Chloride was measured by the mercuric thiocyanate method (14) with reagents from Nycomed (UK) Ltd, Birmingham, UK.

Sodium and potassium were measured using a Corning 455 flame photometer (Ciba Corning Diagnostics Ltd., Halstead, UK) with lithium internal standard. The filter paper eluate was centrifuged and aspirated directly without further dilution.

Within run imprecisions, as estimated from the coefficient of variation, at the specified concentrations were as follows:

lactate 1.9% at 4.90 mmol/L, n = 21;
urea 2.3% at 1.98 mmol/L, n = 21;
sodium 2.0% at 4.79 mmol/L, n = 22;
urate 8.6% at 24.0μmol/L, n = 21;
chloride 0.7% at 4.22 mmol/L, n = 21,
potassium 4.3% at 0.81 mmol/L, n = 22

Data Analysis

A mean value and a standard deviation were calculated for each set of data. In the first study, statistical analysis was performed to examine any differences in the levels of lactate and chloride found in sweat when comparing sample values between the three distinct collection periods. For each subject, a paired Student's *t*-test was employed. For the second study, involving six metabolites measured in sweat, an unpaired Student's *t*-test was employed. The criterion level of significance was set at $P \leq 0.05$.

RESULTS

Effects of Different Loading Regimes on Tissues of the Forearm

A comparison of the effects of hydrostatic loading with uniaxial loading is presented in **Figure 4.**

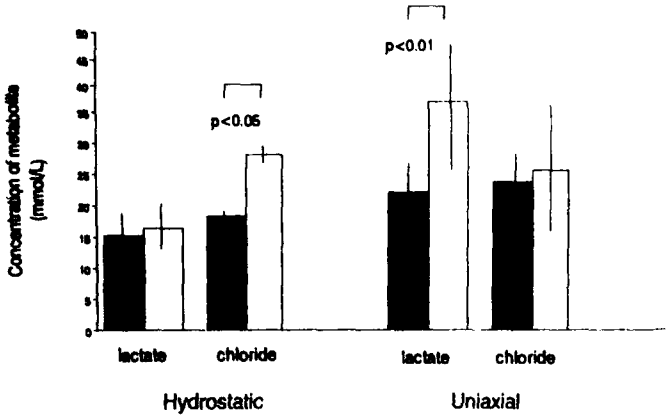

Figure 4.
Sweat lactate and chloride changes under the different loading regimes. Black bar = sweat collected in unloaded state; white bar = sweat collected during ischemia. Only statistically significant levels are indicated.

Ischemic loading produced a statistically significant increase in chloride levels compared to control values, but no difference between lactate levels. By comparison, uniaxial loading produced a statistically significant increase in lactate levels compared to control samples, but no difference between chloride levels. **Figure 5** indicates the levels of lactate and chloride during the three distinct collection periods of the indenter trial. Following the removal of uniaxial loading, the lactate levels decreased rapidly toward basal levels, while the chloride levels appeared to increase only slightly during this reperfusion phase. A summary of the findings with appropriate statistical test results are presented in **Table 1**. It can be seen that the sweat rate decreased during the ischemic phase for both hydrostatic and uniaxial loading, although the decrease was only significant for the latter case. **Table 1** also compares present findings with the results of previous work related to hydrostatic (8), and uniaxial loading (9).

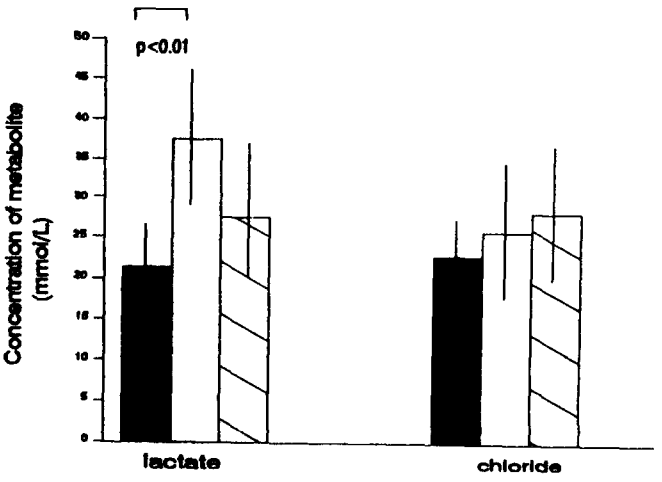

Figure 5.
Sweat lactate and chloride changes under the indenter. Black bar = sweat collected in unloaded state; white bar = sweat collected during ischemia; striped bar = sweat collected during reperfusion. Only statistically significant levels are indicated.

Effects of Wheelchair Sitting and Supine Lying on Soft Tissues

The biochemical composition of sweat collected at tissue sites as a direct result of either sitting in a wheelchair or lying supine on an examination bed is illustrated in **Figure 6** and **Figure 7**, respectively. These changes were associated with mean interface pressures of 7.6 ± 1.2 kPa (57 ± 9 mmHg) at the ischium during wheelchair sitting, and 5.2 ± 1.5 kPa (39 ± 11 mmHg) at the sacrum during support by the examination bed. In the wheelchair test, there was an increase in lactate and urea levels during ischemia, of 24 percent and 27 percent, respectively; these values returning toward basal levels during the reperfusion phase. There was an increase in both sodium and chloride levels during ischemia and this continued during the reperfusion phase to a total increase of 56 percent and 44 percent, respectively. Urate levels showed a statistically significant increase during tissue ischemia, but this increase was reduced during reperfusion. Potassium levels changed little throughout the three phases of the experiment. The study involving the supine position demonstrated similar increases in chloride, sodium, and urea, but no significant increases in lactate and urate were observed in the ischemic phase.

DISCUSSION

This study reports on the use of a simple, robust, inexpensive collection system, which provides a reliable and repeatable measurement of localized metabolite levels in sweat. It can also be used at the loaded interface between the soft tissues and the support surface without disturbing the surface characteristics. Thus, it has many of the design specifications of an ideal system discussed by Ferguson-Pell and Hagisawa (9). It also has the advantage of being sensitive to thermal sweating, as

Table 1.
Comparative results of sweat rate and sweat lactate under different loading regimes.

AUTHOR (Time, pressure site of load test conditions collection area)		Sweat Parameter in Collection Period					
		Sweat rate (μL/min)			Sweat lactate (mmol/L)		
		Ischemic	Control	Reperfusion	Ischemia	Control	Reperfusion
		UNIAXIAL LOADING					
PRESENT STUDY	Mean	9.1	15.6	15.1	37.4	21.2	27.1
(30 min, 150 mm Hg	SD	7.4	9.1	6.1	13	5.7	10.3
forearm	n	11	11	9	6	5	5
thermal to 30°C	p	<0.01	NS		<0.01	NS	
1600 mm^2)		<0.05			NS		
FERGUSON-PELL and HAGISAWA (9)	Mean	0.62	1.2	1.1	9.2	6.7	7.3
(30 min, 150 mm Hg	SD	0.52	0.7	0.5	1.4	1.1	1.1
forearm	n	9	9	9	9	9	9
electrical stimulation	p	<0.05	NS		<0.001	NS	
500 mm^2)							
		HYDROSTATIC LOADING					
PRESENT STUDY	Mean	10.4	12.5		16.4	15.1	
(10 min, 150 mm Hg	SD	2.5	3.4		5.3	4.3	
biceps	n	3	3		3	3	
thermal to 30°C	p	NS			NS		
1600 mm^2)							
VAN HEYNINGEN and WEINER (8)	Mean	130	1000		30.2	17.2	
(25 min, 200 mm Hg	SD	42	395		2.8	2.5	
biceps	n	2	2		2	2	
thermal to 32°C	p	—			—		
with continual exercise							
whole arm)							

opposed to sweat collected by iontophoresis or excessive exercise regimes.

There were clear differences between the tissue responses to the two distinct loading regimes (**Figure 4** and **Table 1**). Ischemic loading as a result of the sphygmomanometer cuff did not produce a significant increase in lactate concentration in sweat when compared to unloaded conditions. This would suggest that severe hypoxia, as a result of ischemia and subsequent accumulation of products of anaerobic metabolism, and typified by increased lactate levels (15), was not achieved. This may be explained by the

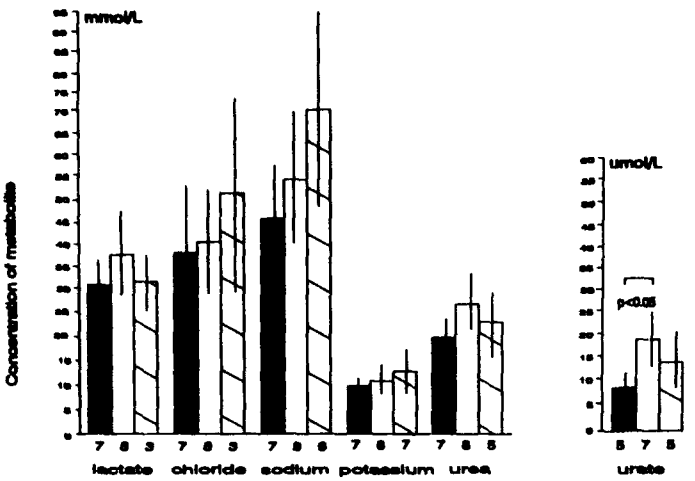

Figure 6.
Sweat analysis of normal subjects under the ischium. During load the subject sat in a wheelchair.
Black bar = sweat collected in unloaded state; mean sweat rate 8.9 ± 4.1 μl/min.
White bar = sweat collected during ischemia; mean sweat rate $= 3.4 \pm 1.2$ μl/min.
Striped bar = sweat collected during reperfusion; mean sweat rate $= 4.9 \pm 3.1$ μl/min.
Values under individual columns indicate subject numbers. Only statistically significant levels are indicated.

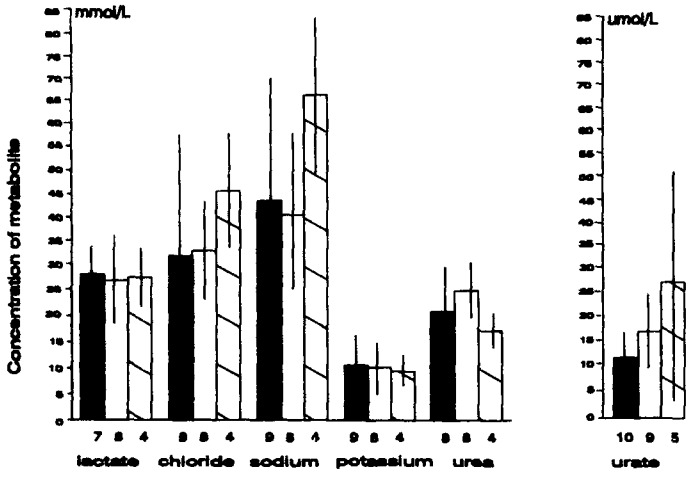

Figure 7.
Sweat analysis of normal subjects under the sacrum. During load the subject lay supine on an examination bed.
Black bar = sweat collected in unloaded state; mean sweat rate $= 9.3 \pm 7.5$ μl/min.
White bar = sweat collected during ischemia; mean sweat rate $= 7.5 \pm 4.0$ μl/min.
Striped bar = sweat collected during reperfusion; mean sweat rate $= 5.0 \pm 1.7$ μl/min.
Values under individual columns indicate subject numbers. Only statistically significant levels are indicated.

lack of pressure differential between the internal tissues and the applied pressure. This would produce a uniform pressure on normal healthy tissues which, in itself, would not produce tissue distortion and subsequent damage. By comparison, lactate levels were significantly elevated in tissue under the uniaxial compression regime. This would strongly imply the achievement of tissue hypoxia and ischemia with associated tissue distortion.

There were also differences between the chloride concentrations measured in sweat collected from tissues subjected to the two distinct loading regimes (**Figure 4**). The chloride levels in sweat are influenced by several factors, including sweat rate and mechanical stress. Thus, a decrease in sweat rate is associated with a decrease in sweat chloride levels (16). In addition, sweat rate, and therefore chloride concentration, has been shown to be directly correlated with skin temperature (16). Conversely, a stress gradient within the loaded tissues can drive the transport of osmotically active molecules, such as sodium chloride, from interstitial fluid into the lumen of the sweat coils (17). Therefore, loaded tissues would be expected to excrete larger amounts of chloride. This may explain the increase in chloride in tissues subjected to hydrostatic loading, where the sweat rate remained relatively unchanged from control values (**Table 1**). However, with uniaxial loading, the chloride levels remained unchanged from control values, which may be explained by the significantly decreased sweat rate during ischemia.

Figure 5 shows that lactate measured in samples from reperfused tissues had returned to basal levels after the period of tissue ischemia. This indicated that oxygenation of tissues induced a rapid return to aerobic respiration of tissues. With respect to chloride levels measured during reperfusion, their values were not significantly different from control values, where the sweat rate was unchanged, and from ischemic values, where the sweat rate was reduced. These findings reaffirm the suggestion that the level of sweat chloride is a function of both sweat rate and the mechanical state of the tissues.

The present results generally follow trends observed in previous studies (**Table 1**). The sweat rate decreased significantly during ischemia and returned to basal levels on reperfusion, in accord with previous reports. However, there are clear differences, for example, when comparing the abso-

lute sweat rates (8,9). These could be attributable to the means of sweat induction, area of sweat collection, and the fact that in the Van Heyningen and Weiner study subjects were tested during a period of physical exercise (8,9).

Both the wheelchair and bed support surfaces provided mean interface pressures at the ischium and sacrum respectively, which were representative of the clinical setting. The condition of pressure ischemia was more extreme in the case of wheelchair sitting. The metabolites measured showed different patterns of response to ischemia and reperfusion (**Figure 6** and **Figure 7**). The trends in lactate and urea levels exhibited during the three phases were similar. The use of sweat lactate has recently been suggested as a good indicator in the evaluation of the severity of peripheral occlusive arterial disease and in assessing the efficiency of vasoactive drug treatment (15). The mechanisms underlying the changes in urea concentrations are unclear. It is known to be inversely related to sweat rate (18) and may, therefore, prove to be a useful additional indicator of tissue ischemia.

In addition, sodium and chloride values showed similar trends for both support surfaces. The complexity of the factors influencing chloride and sodium would render the interpretation of changes difficult in the assessment of tissue damage.

The only statistically significant difference involved the levels of sweat urate. Thus, there was a significant increase in sweat urate in the ischemic phase during wheelchair sitting. During ischemia, urate production may be increased as a result of degradative loss of high energy phosphate metabolites (19). There is also a link between urate and the production of oxygen free radicals in tissue damage (5). This may be relevant to the reperfusion period. Sweat urate may well prove an important marker in future investigations as an indicator of tissue damage.

There were no obvious differences in the response of soft tissues between the male and female subjects, although numbers were small in both groups. Previous studies have shown similar levels of sodium in thermal sweat (20) for both sexes, although changes in sweat rate as a result of aging have recently been reported (21).

Further work is now in progress using this methodology to analyze sweat samples collected from tissues subjected to varying amounts of pressure ischemia. This technique is also being employed to study the sweat characteristics of a range of subjects, during both surgical and rehabilitation procedures, who are at specific risk of developing pressure sores.

REFERENCES

1. Scales JT. Pathogenesis of pressure sores. In: Bader DL, ed. Pressure sores—clinical practice and scientific approach. London: Macmillan Press, 1990:15-26.
2. Bader DL. The recovery characteristics of soft tissues following repeated loading. J Rehabil Res Dev 1990:27(2):141-50.
3. Reswick JB, Rogers JE. Experience at Rancho Los Amigos Hospital with devices and techniques to prevent pressure sores. In: Kenedi RM, Cowden JM, Scales JT, eds. Bedsore biomechanics. London: Macmillan Press, 1976:301-10.
4. Romanus M, Stenqvist O, Svensjo E, Ehira T. Microvascular changes due to repeated local pressure-induced ischemia: intravital microscopic study on hamster cheek pouch. Arch Phys Med Rehabil 1983:64:553-5.
5. Michel CC, Gillott H. Microvascular mechanisms in stasis and ischaemia. In: Bader DL, ed. Pressure sores—clinical practice and scientific approach. London: Macmillan Press, 1990:153-63.
6. Bader DL, Hawken MB. Pressure distribution under the ischium of normal subjects. J Biomed Eng 1986:8:353-7.
7. Bader DL, Gant CA. Changes in transcutaneous oxygen tension as a result of prolonged pressures at the sacrum. Clin Phys Physiol Meas 1988:9:33-40.
8. Van Heyningen R, Weiner JS. The effect of arterial occlusion on sweat composition. J Physiol 1952:116:404-13.
9. Ferguson-Pell MW, Hagisawa S. Biochemical changes in sweat following prolonged ischaemia. J Rehabil Res Dev 1988:25(3):57-62.
10. Sato K, Dobson RL. Glucose metabolism of the isolated eccrine sweat gland. II: The relationship between glucose metabolism and sodium transport. J Clin Invest 1973:52:2166-74.
11. Johnson AT. Thermal responses. In: Johnson AT, ed. Biomechanics and exercise physiology. New York: Wiley Interscience, 1991:405-6.
12. Gutmann I, Wahlefeld AW. L-(+)-lactic determination with lactic dehydrogenase and NAD. In: Bergmeyer HU, ed. Methods of enzymatic analysis, 2nd ed. Verlag Chemie/AP, 1974:1464-8.
13. Tiffany TO, Janson JM, Burtis CA, et al. Enzymatic kinetic rate and endpoint analyses of substrate, by use of a GeMSAEC fast analyzer. Clin Chem 1972:18:829-37.
14. Frey MJ. A quantitative colorimetric method for the determination of serum chloride using the Technicon RA 1000 system. Clin Chem 1983:29:1255, Abs 529.

15. Fellman N, Fabry R, Courdet J. Calf sweat lactate in peripheral occlusive disease. Am J Physiol 1989:257:H395-8.
16. Cage GW, Wolfe S, Thompson RH, Gordon RS. Effects of water intake on composition of thermal sweat in normal human volunteers. J Appl Physiol 1970:29:687-90.
17. Cage GW, Dobson RL. Sodium secretion and reabsorption in the human eccrine sweat gland. J Clin Invest 1965:44:1270-6.
18. Emrich HM, Stoll E, Friolet B, Colombo JP, Richterich R, Rossi E. Sweat composition in relation to site of sweating in patients with cystic fibrosis of the pancreas. Paediat Res 1968:2:464-78.
19. Fox IH, Palella TD, Kelley WN. Hyperuricaemia: a marker for cell energy crisis. N Engl J Med 1987:2:111-2.
20. Brown G, Dobson RL. Sweat sodium excretion in normal women. J Appl Physiol 1967:23:97-9.
21. Cable NT, Green JH. The influence of bicycle exercise, with or without hand immersion in cold water, on forearm sweating in young and middle-aged women. Exp Physiol 1990:75:504-15.

Department of Veterans Affairs

Journal of Rehabilitation Research and Development Vol. 30 No. 2, 1993
Pages 260–266

CLINICAL REPORT

Report on the Evaluation of the VA/SEATTLE Below-Knee Prosthesis

Prepared by Wijegupta Ellepola, BS Eng, CPO, and Saleem J. Sheredos, BEE, MHCA, Rehabilitation Engineer, Program Manager, Technology Transfer Section, Rehabilitation Research and Development Service, Department of Veterans Affairs, Baltimore, MD 21202-4051

Abstract—The Department of Veterans Affairs (VA), Rehabilitation Research and Development (Rehab R&D) Service, Technology Transfer Section (TTS) with collaboration from the Prosthetic and Sensory Aids Service (PSAS) managed clinical trials to evaluate the VA/Seattle Below-Knee (BK) Prosthetic System. The clinical trials were held at the Prosthetic Treatment Center (PTC), VA Medical Center, Hines, Illinois. Five other VA medical centers participated in the outreach program of the trials as satellite stations, with PTC Hines as the central fabrication facility. The VA/Seattle BK system is the first complete prosthetic system designed and developed by the Department of Veterans Affairs. It consists of a socket designed and fabricated using computer-aided, automated technology, and off-the-shelf modular components: a lightweight pylon and an ankle unit, and a lightweight, energy-storing foot. The computer-based socket design software, the modular components, and the prosthetic foot were developed with funds from the VA Rehab R&D Service. The evaluation trials were conducted to determine the efficacy of the VA/Seattle prosthesis, its reliability, and acceptance by veterans. The clinical trials began in April 1991 and were completed in August 1992. Forty-six BK amputee veterans were fitted with the VA/Seattle prosthesis. Their progress with the prosthesis was followed for a period of 6 months and data were gathered at intervals of 2 weeks, 3 months, and 6 months. Forty sets of subject data instruments were collected. In order to maintain the accuracy of the results, TTS used the 22 sets that were complete for data analysis.

The VA/Seattle below-knee prosthesis was well accepted by all the subjects participating in the evaluation trials and confirmed that it is comfortable to wear, safe and reliable. "Previous wearers" preferred it to their former prosthesis both in comfort and overall acceptability.

To optimize the technological advantages of the computerized prosthetic socket design and fabrication system, Automated Fabrication of Mobility Aids (AFMA), the VA should provide a complete and thorough orientation and training program to the VA prosthetists as it introduces the AFMA system into the Healthcare Delivery System.

Key words: *below-knee amputees, clinical evaluation, computer-aided design, computer-aided manufacturing, prosthesis.*

INTRODUCTION

The methods of prosthesis design and fitting have remained relatively unchanged over the past 20–30 years, even though materials have changed. Traditional methods of prosthesis design, fabrica-

For further information, contact: Wijegupta Ellepola, Program Analysis and Review Section, Rehabilitation Research and Development Service, 103 S. Gay St., Baltimore, MD 21202-4051. Phone: 410-962-2578.

The evaluation of the VA-Seattle Below-Knee Prosthesis was sponsored by the Department of Veterans Affairs, Rehabilitation Research and Development Service, Washington, DC.

tion, and fitting are laborious and time-consuming. The mold of the residual limb taken for fabricating a prosthesis must be relieved over areas that cannot tolerate pressure, and decreased in areas over other strategic locations, to accommodate biomechanical considerations of gait. Such modifications are presently made by hand; several diagnostic sockets are fabricated using manual methods until a comfortable-fitting socket is achieved before a final prosthesis is fabricated. This artisan-like process is time-consuming, labor-intensive and expensive; therefore, it delays the timely delivery of prostheses to veterans. To improve timely delivery, the Department of Veterans Affairs (VA) Rehabilitation Research and Development (Rehab R&D) Service funded a long-term project to design and develop the VA/Seattle Below-Knee (BK) Prosthesis **Figure 1**. This new prosthetic system consists of a socket designed and fabricated using computer-aided design technology and interlocking, lightweight, modular components. This method of design, fabrication, and fitting of prostheses will enable the prosthetist to perform more fittings and improve the quality of care to the veteran.

The components of the VA/Seattle BK prosthesis were designed and developed by the Prosthetic Research Study (PRS), Seattle, Washington, with funds from the VA Rehab R&D Service. The computer-aided socket design and computer-aided manufacturing (CASD/CAM) system was tested and evaluated through a collaborative effort directed by Ernest Burgess, MD, between PRS, Seattle, WA; Prosthetics Research Laboratory, Northwestern University, Chicago, IL; and the Department of Rehabilitation Medicine, New York University Medical Center, New York, NY.

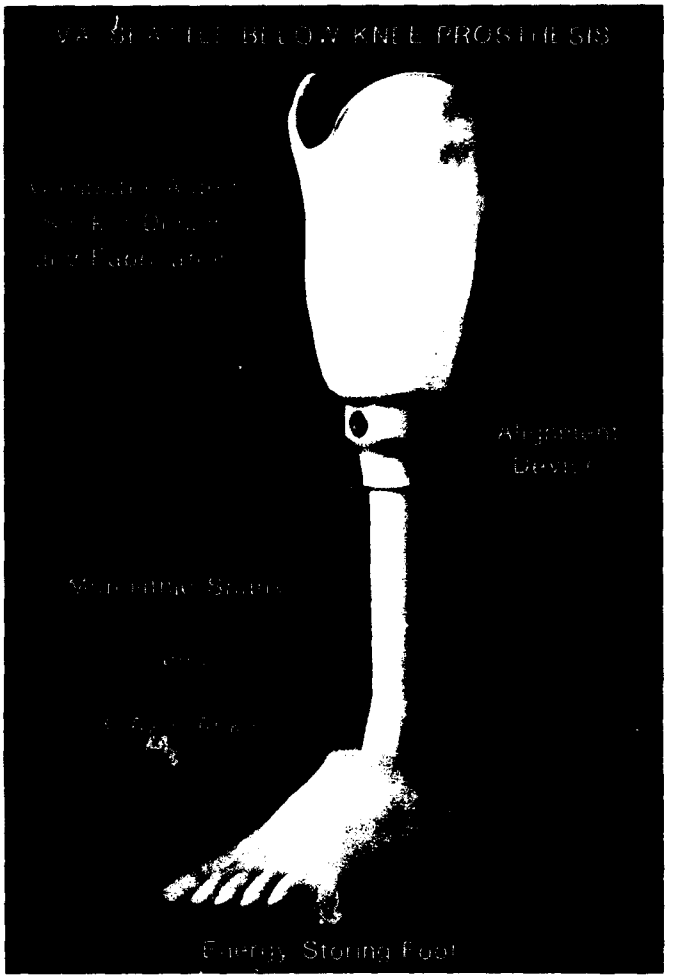

Figure 1.
The VA/Seattle Below-Knee Prosthesis.

PURPOSE

The purpose of this evaluation was to: 1) demonstrate that fabricating the VA/Seattle BK prosthesis using CASD/CAM technology is an efficacious, cost-effective plan for providing well-fitting prostheses to veterans in a timely manner; 2) provide an effective, expedient method to accommodate stump volume changes in cases of edema and/or residual limb tissue shrinkage; 3) provide a better system to manage immediate fittings of a prosthesis; 4) provide the capability to store modified "models" of successful fitting sockets in the computer for fabricating duplicate or new sockets without the need for storing plaster molds; 5) provide prosthetists, physicians, and therapists with quantitative, readily retrievable records of the physiological and anthropometric data of their patients; 6) ascertain whether it is safe and reliable; 7) determine patient acceptability; and, 8) facilitate the technology transfer of VA Rehab R&D funded research to clinical use.

DESCRIPTION

Function

The function of the VA/Seattle BK prosthesis is similar to other BK prosthetic systems. It differs by

system integration in the method and technology used in the design and fabrication of the socket and the use of all plastic, modular components.

Physical Appearance

The VA/Seattle BK prosthesis consists of: a computer-designed, thermoformed socket; a lightweight, modular, plastic, socket attachment/alignment coupling; and, a one-piece, flexible shank/ankle. The shank/ankle is capable of providing 10–15 degrees of ankle dorsi/plantar flexion, and 2 degrees of axial rotation. The prosthesis is complete with a lightweight, energy-storing foot and weighs between 2 and one-half to 3 pounds.

METHODS

Evaluation Sites

Prosthetic Treatment Centers at VA Medical Centers (VAMCs) Hines, Milwaukee, Kansas City, Minneapolis, and Louisville participated in the clinical evaluation trials. Hines was the designated central fabrication site for the "outreach" program.

Subject Selection

Unilateral or bilateral BK amputees prescribed by a physician to receive a patellar-tendon-bearing BK prosthesis with cuff suspension, soft-liner (Pelite), and a Seattle Light Foot were selected to participate in the evaluation trials. The subjects were required to be reasonably active, alert, cooperative, and willing to participate in the trials. Candidates with significant clinical problems such as ulcers, difficult neuromas, etc., in the residual limb, were excluded from this evaluation.

Laboratory Testing

Since the socket design and fabrication system and the modular components were previously evaluated independently and demonstrated to be reliable and safe, the Technology Transfer Section (TTS) determined that cyclic laboratory tests to document durability and reliability over long-term usage of each component of the VA/Seattle prosthesis was not necessary.

Prosthesis Fittings

Anatomical measurements, physical characteristics of the residual limbs, ranges of motion of the knee joint, physical activity, and previous prosthesis use were obtained from the subjects. An unmodified plaster of Paris wrap cast of the residual limb was taken during the subjects' initial visits to the clinic. The plaster wrap casts were digitized and prosthetic sockets were designed using ShapeMaker socket design computer software. Diagnostic sockets were fabricated on a replica model of the residual limb using the computer-aided, automated process and fitted on subjects to determine the accuracy of fit. Prosthetists were allowed to fabricate and fit a maximum of six diagnostic sockets to optimize socket fit.

The complete prosthesis was assembled using the modular components after obtaining a well-fitting socket. The prosthesis was then dynamically aligned for each subject for optimum gait. Established standards of alignment criteria were followed during static and dynamic alignment of the prosthesis. Subjects were instructed in gait training and the proper use of their prostheses. They were evaluated at 2-week, 3-month, and 6-month intervals. Data regarding the subject's experience with the prosthesis were collected at each visit.

The satellite sites in the outreach program selected the candidates, casted the residual limbs, and then sent the casts to Hines VAMC for socket fabrication and assembly of the prosthesis. Satellite stations collected the same data as Hines and the data were provided to TTS. The subjects were allowed to keep the prostheses they had received during the evaluation trials and have since chosen to use them as their permanent prosthesis.

Documentation and Data Collection

Data regarding each subject's experience with the prosthesis and the delivery system were collected using the following data instruments: Subject's Background and Initial (pre-fitting); 2 weeks, 3 months, and 6 months post-fitting; and Prosthetist-Initial and 3 months post-fitting.

RESULTS

A total of 46 subjects were fitted with VA/Seattle BK prostheses during the clinical trials. PTC, Hines (the lead center), fitted 28 subjects and the outreach satellite clinics fitted 18. Of the 46 subjects fitted, 22 fully participated in the study and

provided complete sets of data instruments to TTS; 11 did not provide complete data sets, and 13 withdrew for medical and other reasons not related to the evaluation trials. Four of the 18 subjects fitted at the satellite clinics provided complete sets of data instruments.

All 46 subjects in the trials were males and were mostly World War II veterans. Eighty-five percent of the amputations were non-service-connected; 15 percent were service-connected. Sixty-two percent of the subjects were above the age of 60 years; the youngest was 41, and the oldest was 83 years old. Fifty-two percent had left-leg amputations, 46 percent had right-leg amputations, and 2 percent were bilateral amputees. Forty-three and one-half percent of the subjects were amputated due to diabetes; 30.4 percent due to peripheral vascular disease (other than diabetes); 8.7 percent due to trauma; 2.2 percent due to cardiovascular disease; and 15.2 percent for other reasons (**Figure 2**). Forty-three percent of the amputations due to diabetes were performed in 1991.

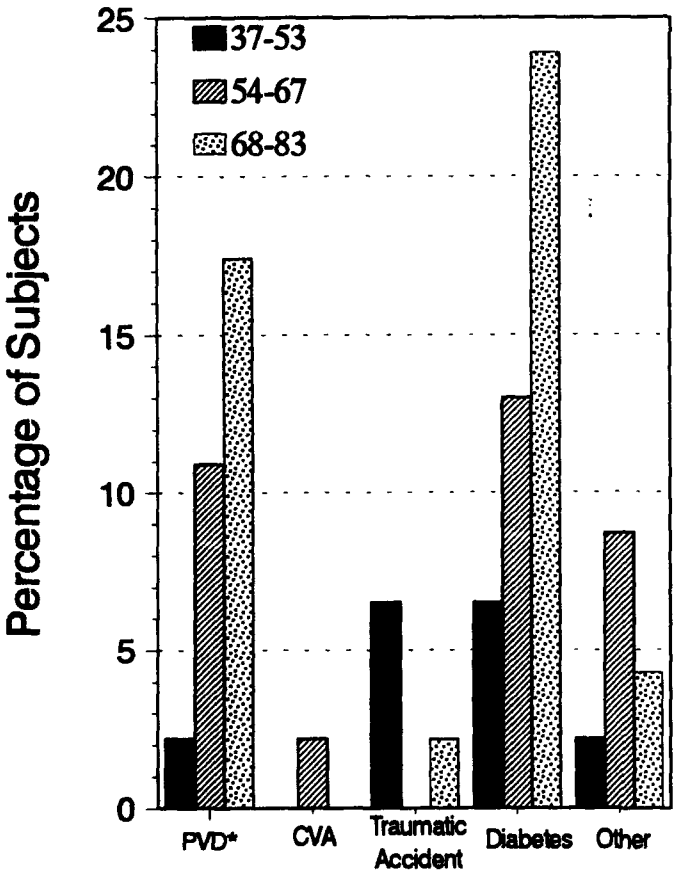

Figure 2.
Subject's Age/Cause of Amputation (other than diabetes).

Ninety-five and one-half percent of the 46 subjects identified walking as the primary reason for needing a prosthesis, and 4.5 percent indicated standing as the second most important function. Running was consistently chosen as a low priority by all subjects; it is assumed that the advanced ages of the subjects in the clinical trials might account for this low rating.

In order to compare the attributes of the VA/Seattle prosthesis with that of other BK prostheses, the 46 subjects in the trials were classified into two groups: subjects who had never worn a prosthesis previous to the evaluation trials were identified as "new wearers," and subjects who had been wearing a prosthesis at the time of the trials were identified as "previous wearers." According to these categories, 63 percent of the subjects were new wearers and 37 percent were previous wearers. The previous wearers, at their initial visit to the evaluation clinic, rated the quality of fit and comfort of their previous prosthesis according to a set of preselected attributes. At the end of 6 months of using the VA/Seattle prosthesis, both new wearers and previous wearers rated the VA/Seattle prosthesis according to the same above set of attributes.

Of the 46 subjects fitted with the VA/Seattle prosthesis, 22 fully participated in the 6-month evaluation trial period. The results reported are therefore based on the data instruments from these 22 subjects and are described in **Figure 3** through **Figure 6**. In rating the "satisfaction" with the VA/Seattle prosthesis, 100 percent of the 22 subjects said they were satisfied. In contrast, 65 percent of the 17 previous wearers, prior to receiving the VA/Seattle prosthesis, said that they were satisfied with their previous prosthesis, 29 percent were dissatisfied, and 6 percent had no opinion (**Figure 3**).

Ninety-five and one-half percent of the subjects said the fit of the VA/Seattle prosthesis socket was "very good" and 4.5 percent said it was "good" (**Figure 4**). In contrast, 41 percent of the previous wearers rated the fit of their previous prosthetic socket as very good, 18 percent good, 17 percent adequate, 12 percent poor and very poor, respectively (**Figure 5**).

Ninety-one percent selected the quality of suspension of the VA/Seattle prosthesis to be very

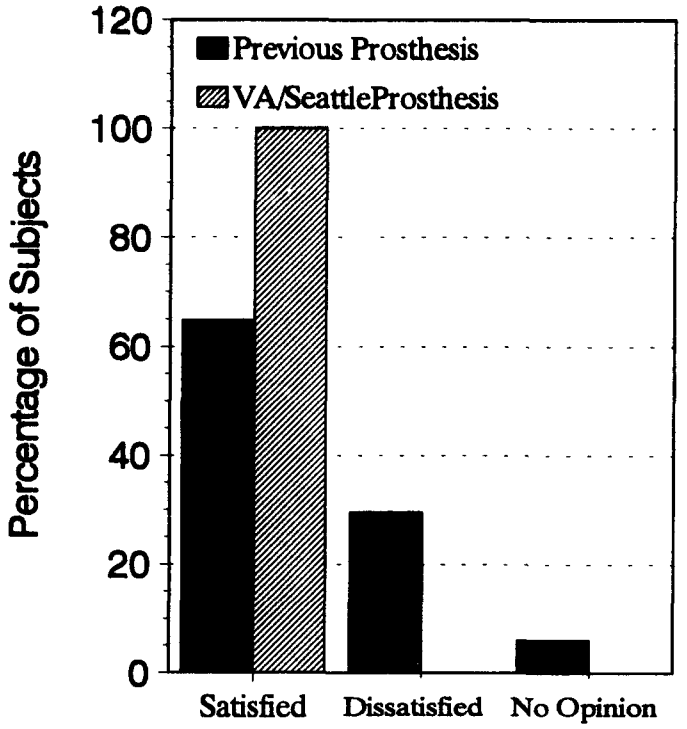

Figure 3.
Prosthesis Satisfaction Rating.

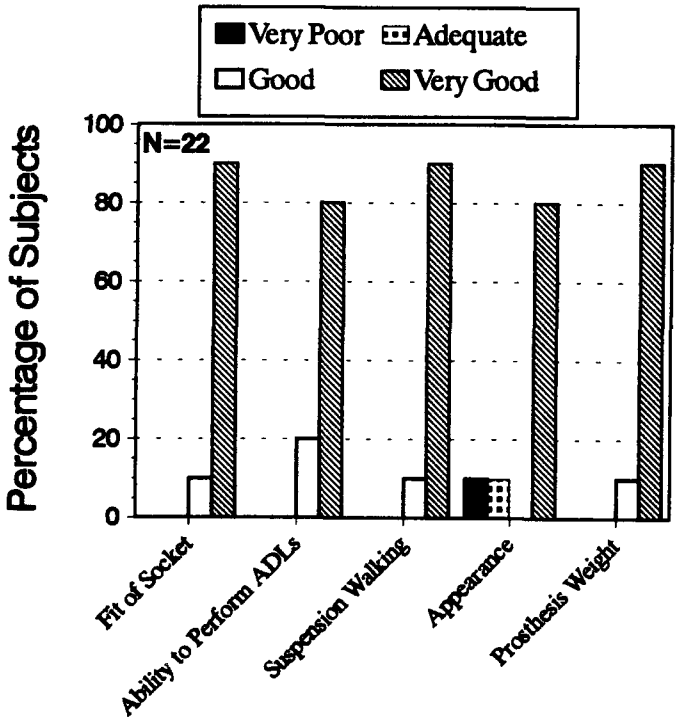

Figure 4.
Features of VA/Seattle Prosthesis.

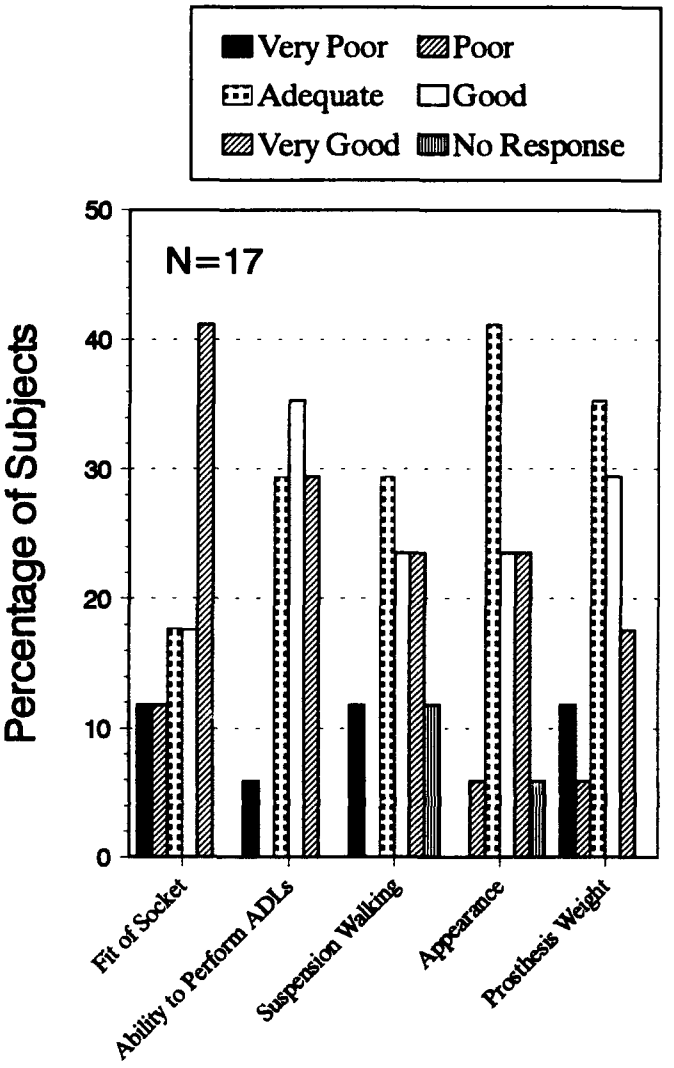

Figure 5.
Features of Previous Prosthesis.

good and the remaining 9 percent rated it as adequate. In comparison, only 23.5 percent of the previous wearers felt that their previous prosthesis suspension was very good, 23.5 percent rated them as good, 29 percent as adequate, and 12 percent as very poor; 12 percent had no response (**Figure 5**).

Ninety percent of the 22 subjects considered the weight of the VA/Seattle prosthesis to be very good and 10 percent said it was good (**Figure 4**). Rating the same attribute, 18 percent of the 17 previous wearers rated the weight of the previous prosthesis as very good, 29 percent as good, 35 percent as adequate, 6 percent as poor, and 12 percent as very poor (**Figure 5**).

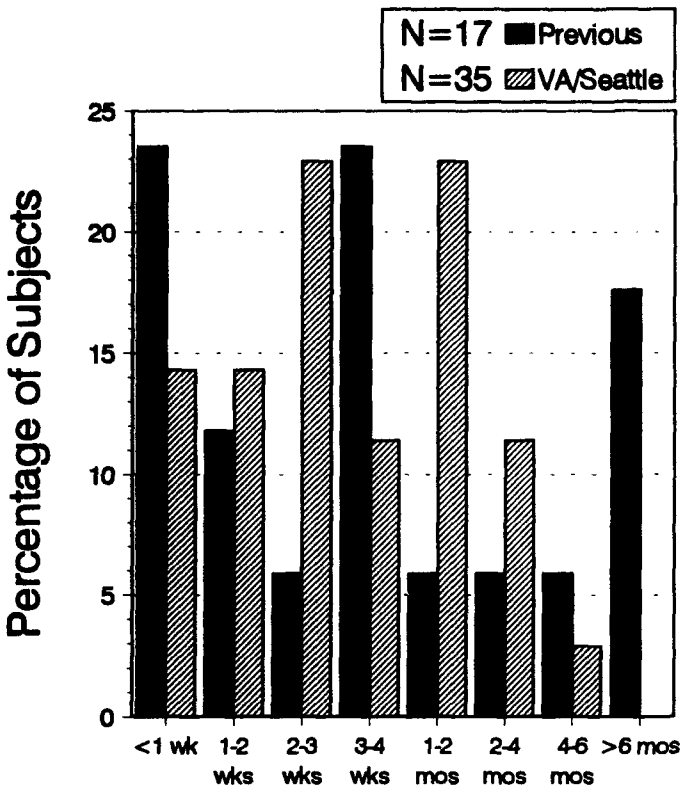

Figure 6.
Time Casting and Receiving Prosthesis.

Eighty percent of the 22 subjects agreed that their ability to perform activities of daily living (ADL) was very good with the VA/Seattle prosthesis, while only 29 percent of the previous wearers considered the same to be true with their previous prosthesis.

One of the important goals of the evaluation trials was to verify the claim that the VA/Seattle prosthesis could be delivered to a patient "sooner" than conventional practice. To determine this, TTS collected subjects' recollections of the casting and delivery dates of the previous prosthesis from the 17 previous wearers, and compared them with those of the 35 subjects who received a VA/Seattle prosthesis. The comparison was made of 35 subjects, because records of 11 out of the 46 subjects fitted with the VA/Seattle BK prosthesis were not available to TTS.

Analysis of the data from the 17 previous wearers revealed that 23 percent of the subjects received their prosthesis in less than 1 week, 12 percent received theirs in from 1 to 2 weeks, 6 percent from 2 to 3 weeks, 23 percent from 3 to 4 weeks, 6 percent from 1 to 2 months, 12 percent from 2 to 6 months, and 18 percent waited longer than 6 months. In comparison, 14 percent of the 35 subjects received their VA/Seattle prosthesis in less than 1 week, 14 percent in from 1 to 2 weeks, 23 percent from 2 to 3 weeks, 11 percent from 3 to 4 weeks, 23 percent from 1 to 2 months, and 15 percent from 2 to 6 months (**Figure 6**). These results indicate that the prosthesis delivery time did not improve during the evaluation trials using the VA/Seattle prosthesis. The percentage of subjects who received their previous prosthesis in less than 1 week decreased by approximately 50 percent in the clinical trials using the VA/Seattle prosthesis. In contrast, the 3- to 4-week group using the VA/Seattle prosthesis improved by nearly 50 percent.

DISCUSSION

The clinical evaluation trials were designed to determine the acceptability of the VA/Seattle prosthesis by BK amputees and to demonstrate its safety, reliability, and efficacy as a cost-effective plan for providing well-fitting prosthesis to veterans.

The evaluation results clearly indicated that this prosthesis was well accepted by all of the subjects who fully participated in the trials and that it was comfortable to wear. It was confirmed that due to its having fewer parts, the VA/Seattle prosthesis is easy to assemble, adjust, service, and replace, and requires less maintenance.

The results indicated that although the computer-aided technology and modular components allowed for quicker fabrication of sockets and assembly of a prosthesis, the actual delivery time of a prosthesis was not reduced. Previous studies clearly proved that the use of computer technology for designing and fabricating a prosthesis did improve the delivery time by reducing the time between casting and delivery of the final prosthesis. Therefore, the VA/Seattle prosthesis evaluation findings point out the critical need for education and training of staff using the new technology in order to maximize its use for improving the prosthesis delivery time to veterans.

CONCLUSIONS

The VA/Seattle BK prosthesis was well accepted by all subjects participating in the evaluation trials and the users confirmed that it is comfortable to wear, safe, and reliable. Previous wearers preferred it to their former prosthesis both in comfort and overall acceptability. To optimize the technological advantages of the CASD/CAM system for automated fabrication of mobility aids (AFMA), the VA should provide a complete and thorough orientation and training program to the VA prosthetists as it introduces the AFMA system to the Healthcare Delivery System.

AVAILABILITY

All components of the VA/Seattle prosthesis are commercially available. Veterans interested in being fitted with a VA/Seattle BK prosthesis are encouraged to contact the Chief, Prosthetic and Sensory Aid Service (PSAS) at their local VA Medical Center.

ACKNOWLEDGMENTS

We express sincere appreciation for the invaluable collaboration of the Central Office, PSAS, throughout the evaluation trials, and in particular, to Frederick Downs, Jr., Director, PSAS, and John Clements.

We acknowledge the PTC, Hines staff: Wanda Hathaway, Chief, PTC; Phillip Tirimacco, CP, Chief, Orthotic Laboratory; and Richard M. Sakols, CP, for their enthusiastic assistance and professional participation in the evaluation trials; and Michael Pinzur, MD, Chief, STAMP Program, Hines VAMC, for helping to coordinate the clinical trials at Hines.

We especially thank Vivian Taha, TTS, for computer data management and report presentation, and Anne Greek, TTS, for providing administrative support throughout this evaluation. Their untiring efforts and patience contributed significantly to the accomplishment of this project.

The contribution of Barry Taylor, OT, in identifying data management needs was timely and facilitated the evaluation's progress.

ABSTRACTS OF RECENT LITERATURE

by
Joan E. Edelstein, M.A., P.T.
Director, Program in Physical Therapy, Columbia University, New York, NY

Abstracts are drawn primarily from the orthotics and prosthetics literature. Selections of articles were made from these journals:

Archives of Physical Medicine and Rehabilitation
Assistive Technology
Journal of Prosthetics and Orthotics
Physical Occupational Therapy for Geriatrics
Physical Therapy
Prosthetics and Orthotics International

Body Composition of Sedentary and Physically Active Spinal Cord Injured Individuals Estimated from Total Body Electrical Conductivity. Olle MM, Pivarnik JM, Klish WJ, Morrow JR, reprinted from *Arch Phys Med Rehabil* 74:706-710, 1993. (©1993 by the American Congress on Rehabilitation Medicine and the American Academy of Physical Medicine and Rehabilitation.)

Reliability and evidence of construct validity of Total Body Electrical Conductivity (TOBEC) for estimating body composition in spinal cord injured subjects evaluated using 17 males with C6L2 spinal cord transections. Subjects reporting regular exercise were categorized as active ($n=12$); nonexercisers were considered sedentary ($n=5$). Measures included body weight, length, circumferences, skinfolds, and three TOBEC readings. Reliability for percent fat of both single and multiple TOBEC trials ($t=3$) ranged from .994 to .999. Average percent fat values were significantly ($p<.009$) higher in sedentary ($23.2\pm4.7\%$) compared to active ($15.6\pm4.8\%$) subjects. Fat mass was also significantly ($p<.02$) higher in sedentary subjects. Sum of seven skinfolds was significantly correlated ($r[15]=0.73, p<.01$) with percent fat measured by TOBEC. Results suggests TOBEC is reliable ($r^{tt}>0.99$) in estimating body composition in spinal cord injured individuals. High reliability estimates for single and multiple trials indicate use of a single trial will provide reliable body fat estimates. Construct validity evidence infers that TOBEC measured body composition discriminates between active and sedentary paraplegics.

Clinical Assessment of Human Gait. Fish DJ, Nielsen J-P, reprinted from *J Prosthet Orthot* 5:39-48, 1993.

The mechanics of human gait involve synchronization of the skeletal, neurological and muscular systems of the human body. This article will enhance the gait assessment abilities and processes of the novice clinician by providing a brief overview of normal gait followed by identification of pathological and pathomechanical gait patterns. Also presented is a systematic approach to clinical gait assessment that emphasizes the need for the development of clinically cost- and time-effective tools to document and quantify data in the assessment of human gait.

A Clinical Experience with a Hierarchically Controlled Myoelectric Hand Prosthesis with Vibrotactile Feedback. Reprinted from *Prosthet Orthot Int* 17:56-64, 1993.

Improved performance of externally powered myoelectric hands is possible when the direct control of the digit flexion and grip force are given over to an electronic controller which frees the operator to concentrate on other demands. *Design:* A commercial myoelectric hand was modified to take the new touch and slip sensors and novel control method. *Subject:* An adult male with a traumatic midforearm amputation. *Outcome measure:* The range and ease of use of the prosthetics system. *Result:* The hand

was easily and usefully operated in the home and work environment. *Conclusion:* Hierarchical control of a hand is possible using sensory feedback to a sophisticated electronic controller. Such a control method reduces the demands on the user's concentration and enhances the hand's range.

Clinical Measurement of Normal and Shear Stresses on a Trans-tibial Stump: Characteristics of Wave-form Shapes During Walking. Sanders JE, Daly CH, Burgess EM, reprinted from *Prosthet Orthot Int* 17:38-48, 1993.

Stresses on the surface of a stump within a prosthetic socket during walking can potentially traumatise stump tissues. To gain insight into stresses and design parameters that affect them, normal and shear interface stresses were measured on three unilateral trans-tibial amputee subjects during walking trials. During stance phase repeated characteristics in wave-form shapes from different subjects were apparent. They included "loading delays", "high frequency events (HFE's)", "first peaks", "valleys", "second peaks", and "push-off". Characteristics did not necessarily occur at the same time from one step to the next but their timings matched well with events in shank force and moment data which were collected simultaneously. For "plantarflexion" and "dorsiflexion" alignment changes, the above wave-form characteristics were still present but their timings within the stance phase changed. The physical meaning and relevance of the characteristics to stump tissue mechanics are discussed.

Comparative Study of Mechanical Characteristics of Plastic AFOs. Yamamoto S, Ebina M, Iwaski M, Kubo S, Kawai H, Hayashi T, reprinted from *J Prosthet Orthot* 5:59-64, 1993.

Ankle-foot orthoses (AFOs) are categorized four ways with respect to their shape: posterior spring, anterior spring, side-stay and spiral. In this article the flexibility of these types of AFOs fitted to the limb is measured using a muscle training machine. A comparison of the flexibility of different types of AFOs is made.

Countertransference and the Multiple Amputee Patient: Pitfalls and Opportunities in Rehabilitation Medicine. Laatsch L, Rothke S, Burke WF, reprinted from *Arch Phys Med Rehabil* 74:644-648, 1993. (©1993 by the American Congress on Rehabilitation Medicine and the American Academy of Physical Medicine and Rehabilitation.)

Current psychoanalytic literature on countertransference broadly defines the term as a helping professional's overall response to an individual patient. Reaction of rehabilitation professionals to their traumatically injured patients can significantly impact on the patient's treatment as well as the individual therapist's and entire rehabilitation team's effectiveness. In this paper, a case is presented illustrating countertransference toward a multiple amputee patient. Implications for the rehabilitation team are also described. The analysis of a single case demonstrates how countertransference interpretation might be used as a vehicle to enhance understanding the patient and promote team effectiveness.

Distance Education Technology for Prosthetic CAD/CAM Instruction. Lemaire ED, reprinted from *J Prosthet Orthot* 5:82-87, 1993.

A 96-hour course was created to instruct prosthetic and orthotic clinicians on computer-aided design/computer-aided manufacturing (CAD/CAM) principles and techniques. This course was presented using distance education technology to link the instruction site (Toronto, Canada) with the student site (Ottawa, Canada).

Through interactive computer graphics and standard telecommunications, course participants studied the CASDaM, CANFIT-PLUS, Shapemaker and University of Texas CAD/CAM systems. A qualitative evaluation of each software package was submitted by each participant during course evaluation. This education method was endorsed by course participants and instructors as a viable technique for clinical CAD/CAM instruction.

Dundee Revisited: 25 Years of a Total Amputee Service. Stewart CPU, Jain AS, reprinted from *Prosthet Orthot Int* 17:120, 1993.

The Dundee Limb Fitting Centre has provided an integrated rehabilitation programme for the amputee since 1965. A review of 1,846 primary amputees is discussed.

During this period a dramatic change in the above-knee/below-knee (AK/BK) ratio has been achieved with 71% BK and 26% AK occurring in 1989. Over 80% of all amputees, the majority being elderly with peripheral vascular disease, were successfully fitted with a prosthesis.

Final discharge home or to a residential home for the elderly was achieved in 76.2% of cases with 3.6% dying in the Unit. Bilateral amputation occurred in 18% of cases of whom 48% were BK-BK. Overall 66% were successfully fitted with a prosthesis. The results demonstrate the advantages of an integrated approach to the amputation and consequent rehabilitation.

The Effect of Marker Placement Deviations on Spinal Range of Motion Determined by Video Motion Analysis. O'Connor PD, Robinson ME, Shirley FR, MacMillan M, reprinted from *Phys Ther* 73:478-483, 1993.

Background and Purpose. Spinal range of motion (ROM) is an important indicator of spinal function and is used in the determination of disability and compensation. One technology that has been used to assess spinal ROM is video motion analysis. No studies, however, have been done to investigate the effects of marker placement on ROM. The purpose of this study was to investigate the effect of deviations in reflective marker placement on ROM measurements obtained via video motion analysis. **Methods.** A model of the spine was constructed and used to obtain ROM measurements from three segments of the model to isolate error from marker placement without the confounding effects of subject error. A standard placement and six altered placements were used to determine the effect of moving reflective markers on ROM. **Results.** Results indicated statistically significant effects of marker placement for a number of flexion/extension and lateral side-bending ROM measurements. When the mean differences were compared with data obtained in human test-retest studies with the same equipment, the differences from a 2.5-cm marker deviation did not appear to be clinically meaningful. **Conclusion and Discussion.** We conclude that small marker deviations (2.5 cm) are not likely to adversely affect clinical information obtained when using this type of apparatus.

Effects of Exercise on Hip Range of Motion, Trunk Muscle Performance, and Gait Economy. Godges JJ, Ma[illegible]e PG, Engelke KA, reprinted from *Phys Ther* 73:468-477, 1993.

Background and Purpose. The purposes of this study were (1) to examine the effects of a passive hip extension stretching exercise program on hip extension range of motion (ROM), (2) to examine the effects of a trunk flexor exercise program on trunk flexor muscle performance, and (3) to examine the effects of passive hip extension stretching or trunk flexor exercises on walking and running economy. ("Gait economy" is defined as the steady-state oxygen consumption per unit of body weight required to walk or run at a specified velocity.) **Subjects.** Twenty-five healthy, athletic, male college students ($\bar{X}$ age = 21 years, $\bar{X}$ weight = 75kg, $\bar{X}$ height = 172cm) were randomly assigned to one of three groups: a control group (n = 7), a hip extension stretching group (n = 9), or a trunk flexor exercise group (n = 9). **Methods.** Before and after 3 weeks of intervention, the following measurements were obtained: right and left hip extension ROM, trunk flexor muscle performance, and walking and running economy. A three × two-way (groups × test sessions) analysis of variance (ANOVA) for repeated measures for unequal subject numbers was performed on each of the five dependent measures, with analysis of simple main effects applied when significant interactions were found. **Results.** The ANOVA on right and left hip extension ROM revealed a significant interaction. Analyses of simple main effects showed that 3 weeks (six sessions) of passive hip extension stretching significantly improved right hip extension ROM (pretest = −20.4°, posttest = −8.3°) and left hip extension ROM (pretest = −16.8°, posttest = −7.0°). There also was a significant interaction for trunk flexor muscle performance. The analysis of simple main effects revealed that 3 weeks of daily trunk flexor exercises significantly improved trunk flexor muscle performance (pretest = 41.5°, posttest = 60.4°). The 3-week intervention program of hip extension stretching or trunk flexion exercises, however, did not produce significant changes in walking or running economy. **Conclusion and Discussion.** The results suggest that (1) six treatment sessions of passive stretching were sufficient to improve hip extension ROM; (2) 3 weeks of exercises performed daily improved trunk

flexor muscle performance; and (3) training of isolated tasks, such as hip flexibility or trunk strengthening activities, did not produce the desired outcome in the economy of walking or running. Possible reasons for the results are discussed.

Gait Patterns of Elderly Men with Transtibial Amputations. Lemaire ED, Fisher FR, Robertson DGE, reprinted from *Prosthet Orthot Int* 17:27-37, 1993.

Gait patterns for the non-amputated leg of eight elderly men with trans-tibial amputations were assessed using kinematic and kinetic measures. Kinematically, the subject's walking speed was faster than expected but less than normative non-amputee data. The stride length was also less than non-amputee norms. Net joint moment and power analyses showed various discrepancies between the amputee subjects and non-amputees. The amputees required a concentric ankle dorsiflexor moment just after heel-strike to help move the lower leg into mid-stance position. The concentric plantarflexor moment at push-off was much larger than comparative data. A large eccentric flexor moment was also found at the hip during late mid-stance. Most of these discrepancies could be explained by the lack of an ankle moment generator on the amputated side of the body.

The ICEROSS Concept: A Discussion of Philosophy. Kristinsson O, reprinted from *Prosthet Orthot Int* 17:49-55, 1993.

Prefabricated ICEROSS (Icelandic Roll On Silicone Socket) sockets have been in use in Iceland since early 1986. Use of custom-made silicone sockets began several years earlier, and a paper devoted to the subject was presented at the 1984 AOPA Assembly by the author of this article.

The ICEROSS system is primarily used for suspension. At the same time the author believes it considerably improves the weightbearing capability of the prosthesis and the interface, between prosthesis and user. After being turned inside out and rolled over the stump, the silicone sleeve forces skin in a distal direction, stabilising soft tissue and minimising pistoning. Both prosthetist and user may experience some problems initially, although most can be overcome by careful socket design and skin care.

Incidence and Prognosis of Dysvascular Amputations in Okayama Prefecture (Japan). Nagashima H, Inoue H, Takechi H, reprinted from *Prosthet Orthot Int* 17:913, 1993.

This survey analysed the clinical characteristics of subjects who first underwent major amputation of lower limbs necessitated by dysvascular disease during the 5 year period from 1984 to 1988. All were residents of Okayama Prefecture, Japan, and have been issued with a Physically Disabled Person's Certificate.

In total, 114 dysvascular amputees, representing 58.2% of all lower limb amputations performed in the resident population during the study period, were surveyed. The underlying diagnosis was arteriosclerotic obstruction in 64.9% of the subjects, diabetic gangrene in 22.8%, acute embolism in 7.0% and Buerger's disease in 5.3%. The yearly incidence of new dysvascular amputees per 100,000 people was estimated to be 1.2 among the general population and 5.7 among those aged over 65 years.

At three years after primary amputation, the survival rate was 52.3% in arteriosclerotic obstruction, and 66.7% in diabetic gangrene. Secondary amputation was performed in 17.0% of the entire group. The concurrent incidence of hemiplegic stroke was 19.8%

Among 36 amputees due to arteriosclerotic obstruction, who survived 3 years postoperatively, 10 (27.8%) were fitted with prosthetic limbs.

A Model for Integrating Technology Into a Multi-Agency Community Service Delivery System. Schoech D, Cavalier A, Hoover B, reprinted from *Assist Technol* 5:23, 1993.

This article presents the results of a 4-year project to develop and test a model for integrating technology into a multi-agency community human services delivery system. "Technology" in this sense refers to both information technology and assistive technology. The project focused on systems change rather than on the creation of comprehensive assistive technology services. Several strategies of the model were developed and tested by the project. The project developed an information/communication tier that lay on top of the existing service delivery system. The information/communication tier was provided to agencies through an electronic

network and searchable database, assistive technology advicegiving software, a public awareness campaign, and professional training. The results of these strategies are used to illustrate the Community Assistive Technology Services Network (CATSN) model. The model consists of five modules: 1) client assessment and technology examination, 2) professional and client training and technical assistance, 3) information and referral and needs analysis, 4) special projects, and, 5) central coordination and facilitation—the hub. This model is important given recent nationwide initiatives for using assistive technology to provide people with disabilities opportunities for maximum independence, productivity, and integration.

Movement Dysfunction following Central Nervous System Lesions: A Problem of Neurologic or Muscular Impairment? Carey JR, Burghardt TP, reprinted from *Phys Ther* 73:538-547, 1993.

In most of the scientific literature that discusses the common problem of resistance to passive movement in patients with central nervous system lesions, this clinical problem is ascribed to a mechanism involving uninhibited neural activity. This article reviews the literature related to an alternative explanation of stiffness in such patients, an explanation involving the mechanical orientation of myosin crossbridges. The conventional view of the crossbridge is that it is detached from actin filaments during the relaxed state of muscle. Information is presented, however, from animal studies indicating that a certain proportion of crossbridges bind weakly to actin even in the relaxed state. The muscles of patients with hypertonicity may undergo an adaptation that involves formation of a higher proportion of binding crossbridges. This results in abnormal stiffness in the muscle and impairs movement. Such crossbridge stiffness may be particularly elevated immediately after a previous contraction.

Movement of the Tibial End in a PTB Prosthesis Socket: A Sagittal X-Ray Study of the PTB Prosthesis. Lilja M, Johansson T, Oberg T. reprinted from *Prosthet Orthot Int* 17:21-26, 1993.

To investigate the movement of the tibial end in the sagittal plane in the PTB prosthetic socket during a gait cycle, 7 patients with a median age of 72 years were examined using X-ray technique. The gait cycle was reduced to four different static positions heel contact, mid-stance, push-off and swing phase. The mean value of tibial movement in the socket in the anteroposterior direction was 2.2 cm, in proximodistal direction 2.8 cm, and the total sagittal movement during the whole gait cycle was 7.5 cm. The results indicate that one factor affecting the magnitude of the movement was the prestretching of soft tissues. All the patients who experienced a good prosthetic fitting had their soft tissues prestretched. The extreme dorsal and proximal positions of the tibial end during the gait cycle was in the swing phase position. The extreme distal position occurred somewhere between mid-stance and push-off. The extreme anterior position of the tibial end was seen during heel contact. This study has shown the magnitude of the movements in a PTB socket during a simulated gait cycle. The study has given hints on factors affecting prosthetic fitting, and further research within this field might provide indications of how to optimise socket shape to give maximal patient comfort.

Multichannel Cochlear Implantation in the Rehabilitation of Post-traumatic Sensorineural Hearing Loss. Coligado J, Wiet RJ, O'Connor CA, Ito V, Sahgal V. reprinted from *Arch Phys Med Rehabil* 74:653-657. (© 1993 by the American Congress on Rehabilitation and the American Academy of Physical Medicine and Rehabilitation.)

Although there is a 17% to 56% incidence of sensorineural hearing loss following head injury, to our knowledge cochlear implants have not been used in treatment of this problem in patients with cognitive deficits and aphasia. We report our experience with multichannel cochlear implantation in one such patient. The patient is a 26-year-old man with bitemporal lobe damage and T11 paraplegia. The clinical profile showed emotional lability, perseveration of thought, impulsivity, good visuospatial orientation, and adequate use of oral and written language in conveying basic needs. Audiologic evaluation showed profound sensorineural hearing loss. Middle latency responses suggested intact thalamocortical pathways. The patient was provided with a multichannel cochlear implant with improvement in his speech recognition and

functional skills. We conclude that the cochlear implant should be considered in patients with traumatic sensorineural hearing loss with relatively intact cognitive skills.

Occupational and Educational Achievements of Head Injured Vietnam Veterans at 15-year Follow-up. Kraft JF, Schwab KA, Salazar AM, Brown HR. reprinted from *Arch Phys Med Rehabil* 74:596-601, 1993. (© 1993 by the American Congress on Rehabilitation and the American Academy of Physical Medicine and Rehabilitation.)

Little is known about the long-term effects of head injury on achievement. The post-injury educational and occupational achievements of 520 survivors of penetrating head injury in Vietnam (and 85 uninjured controls) were examined 15 years after injury. Most patients (82%) had used Veterans Administration educational benefits to return to school, and many of those (64%) had achieved degrees. Return to work was strongly related to level of educational achievement, particularly among the most severely disabled. Though only 56% of the head injured were gainfully employed, the occupational distribution of those who were working differed little from uninjured controls, or the male labor force. Severity of injury affects educational achievement and return to work, but not the occupational distribution of those who do manage to return. Even the most severely injured can sometimes achieve high educational and occupational levels.

Physical Condition, Activity Pattern, and Environment as Factors in Falls by Adult Care Facility Residents. Fleming BE, Pendergast DR. reprinted from *Arch Phys Med Rehabil* 74:627-630, 1993. (© 1993 by the American Congress on Rehabilitation and the American Academy of Physical Medicine and Rehabilitation.)

This study surveyed 294 fall incident reports made over a three-year period concerning 95 residents in an adult care facility. We determined the frequencies of fall location, time of day or night, and assessed the precipitating factors from fall descriptions made by residents and/or their care givers. We found that 57% of the falls occurred in the resident's rooms, with private or shared bathrooms as the next most frequent locus. Precipitating factors were surveyed; 50.3% of the fall descriptions implicated environmental features (pieces of furniture were most frequently mentioned), the physical condition of the resident contributed to 24.3% of the falls, and specific physical activities were implicated in 7.9% of the falls. Multiple factors accounted for 65% of the total falls. In 17% of the cases, no clear indication of cause was found. Unsafe environments have been implicated as a fall risk factor. Despite adaptations to lessen environmental hazards, a large number of reportable falls occurred in this facility, which was for elderly individuals who were in relatively good health commensurate with their age.

Predictors of Assistive Technology Abandonment. Phillips B, Zhao H. reprinted from *Assist Technol* 5:36-45, 1993.

Technology abandonment may have serious repercussions for individuals with disabilities and for society. The purpose of this study was to determine how technology users decide to accept or reject these devices. Two hundred twenty-seven adults with serious disabilities responded to a survey on device selection, acquisition, performance, and use. Results showed that 29.3% of all devices were completely abandoned. Mobility aids were more frequently abandoned than other categories of devices, and abandonment rates were highest during the first year and after 5 years of use. Four factors were significantly related to abandonment—lack of consideration of user opinion in selection, easy device procurement, poor device performance, and change in user needs or priorities. These findings suggest that technology-related policies and services need to emphasize consumer involvement and long-term needs of consumers to reduce device abandonment and enhanced consumer satisfaction.

Predictors of Falls Among Right-Hemisphere Stroke Patients in the Rehabilitation Setting. Rapport W, Webster JS, Flemming KL, Lindberg JW, Godlewski MC, Brees JE, Abadee PS. reprinted from *Arch Phys Med Rehabil* 74:621-626, 1993. (© 1993 by the American Congress on Rehabilitation and the American Academy of Physical Medicine and Rehabilitation.)

The purpose of the study was to examine neuropsychological and general medical risk factors

for falls among a high-risk patient group in an inpatient rehabilitation setting. The sample consisted of 32 nonambulatory males who had sustained a right-hemisphere stroke (R-CVA). The Fall Assessment Questionnaire (FAQ) was introduced as a measure of known risk factors for falls in an inpatient setting. Neuropsychological assessment included measures of attention, perceptual deficits, hemispatial neglect, and impulsivity. A predictive model generated using multiple regression found that the FAQ combined with a measure of behavioral impulsivity successfully predicted fall status in 78% to 81% of cases, depending upon the cutting score used ($p < .003$). R-CVA patients who fell were more impulsive ($p < .001$) and received higher FAQ scores ($p < .001$). Perceptual deficit as measured by the Rey Osterreith Complex Figure and general inattention as measured by Digit Span (reverse) were associated with falls ($p < .04$); however, they did not add to the model predicting which of the R-CVA patients would fall. It was suggested that impulsivity may act as an important mediating factor in determining individual risk for fall.

Quantitative Assessment of Four Men Using Above-Elbow Prosthetic Control. Popat RA, Krebs DE, Mansfield J, Russell D, Clancy E, GillBody KM, Hogan N. reprinted from *Arch Phys Med Rehabil* 74:720-729, 1993. (© 1993 by the American Congress on Rehabilitation and the American Academy of Physical Medicine and Rehabilitation.)

We studied the relationship between kinematically unconstrained activities of daily living (ADL) tasks and a kinematically constrained task in above-elbow (AE) amputee subjects using myoelectrically controlled prostheses. Four men, 24 to 49 years old, with unilateral AE amputation wore a prosthesis interfaced to a programmable controller to emulate two different elbow control schemes, conventional velocity and a new "natural" controller. Subjects were timed during three ADL tasks—cutting meat, donning socks, and rolling dough—both with controllers. The prosthesis emulator was then connected to a crank device with a handle, and the subjects turned the crank from bottom to top positions in a vertical plane using each controller. Synergistic shoulder-elbow joint coordination required for crank turning was quantified as the maximum slope of the change in elbow torque versus the change in crank-angle. Performance between the two controllers differed significantly for the crank test but not for ADL tasks. One subject did not complete all crank tuning tests. Positive canonical correlation of 0.77 was found between time and crank domain measures. We conclude that biomechanical assessments should be integrated with time-based clinical tests to comprehensively evaluate performance of AE amputee subjects with a myoelectric device.

Relationships Among Cane Fitting, Function, and Falls. Dean E, Ross J. reprinted from *Phys Ther* 73:494-504, 1993.

Background and Purpose. Although canes are among the most commonly used mobility aids, little is known about the relationship between cane prescription and effectiveness. The purpose of this study was to examine the relationships among cane fitting (ie, cane fitter, cane hand, and cane length), reported improvements in function, and reduction in falls. **Subjects and Methods.** Cane users living in the community (86 women and 58 men with a median age distribution of 61 to 80 years) and sampled from seven urban shopping centers in British Columbia, Canada, participated in the study. The primary reasons cited for using a cane were joint problems (39%), general balance difficulties (30%), and a combination of joint and balance problems (15%). Measures included appropriateness of cane length and responses to closed-ended questions related to qualifications of the canefitter, cane hand, functional ability with a cane, and falling frequency. **Results.** Overall, cane use was associated with improved confidence and functional ability. Canes fitted by health care workers approximated the clinically recommended length compared with canes fitted by non-health care workers, which tended to be greater than this length. There was no relationship, however, among cane fitter, cane hand, and appropriateness of cane length or between functional ability with a cane and falling frequency. **Conclusion and Discussion.** We concluded that health care workers need to reconsider the variables for optimal cane prescription and their specifications for a given individual. The notion of a correct length and cane hand, for example, may be less important than factors such as the indications for cane use, comfort, and enhanced confidence.

Relationships Between Impairment and Physical Disability as Measured by the Functional Independence Measure. Heinemann AW, Linacre JM, Wright BD, Hamilton BB, Granger C. reprinted from *Arch Phys Med Rehabil* 74:566-573, 1993. (© 1993 by the American Congress on Rehabilitation and the American Academy of Physical Medicine and Rehabilitation.)

This study was conducted to scale the Functional Independence Measure (FIM) with Rasch Analysis and to determine the similarity of scaled measures across impairment groups. The results show that the FIM contains two fundamental subsets of items: one measures motor and the second measures cognitive function. Rasch Analysis of the Uniform Data System for Medical Rehabilitation patient sample yielded interval measures of motor and cognitive function. The validity of the FIM was supported by the patterns of item difficulties across impairment groups. Adequate clinical precision of the FIM was demonstrated, though suggestions for improvement emerged. The frequency of misfit between patients and the performance scales varied across impairment groups, but was acceptable. The results of this project will enable clinicians and researchers to plan cost-effective treatment by providing a valid measure of disability.

Seating Assessment and Management in a Nursing Home Population. Krasilovsky G. reprinted from *Phys Occup Ther Geriatr* 11:25-38, 1993.

This paper reports the findings of assessing body alignment and seating of residents in a nursing home. A total of 67 residents were referred for assessment, with the objective of obtaining optimal body alignment and positioning in a wheelchair or other preferred seating device. Intervention was required in 54 percent to improve faulty posture and alignment. The most common sitting problem was pelvic obliquity while sitting on sling seat upholstery in a wheelchair. A solid seat insert with a cushion was the most common recommendation made (31%). An ambulation program was recommended for 13%, and three customized wheelchairs were recommended.

The SMART® Wrist-Hand Orthosis (WHO) for Quadriplegic Patients. Makaran JE, Dittmer DK, Buchal RO, MacArthur DE. reprinted from *J Prosthet Orthot* 5:73-76, 1993.

The SMART® Wrist-Hand Orthosis (WHO) is a new method of providing grasping function for quadriplegic patients. The use of shape memory alloy (SMA) actuators in rehabilitation technology (SMART) allows for a new type of actuator in addition to traditional actuators such as Bowden cables, pneumatic cylinders, electric motors and linear ratchets. It provides excellent function and ease of use.

The Syme Prosthesis Revisited. Doyle W, Goldstone J, Kramer D. reprinted from *J Prosthet Orthot* 5:95-99, 1993.

Surgically successful Syme amputations have often been followed by use of less successful prostheses. A unique design for medial-opening Syme prostheses has been developed to address issues of comfort, flexibility, strength, lightness and durability. Parallel goals of reducing fabrication complexity, and therefore time, as well as providing ease of adjustment were also achieved.

The design employs carbon graphite material in conjunction with a construction technique that is compatible with commonly used plastic fabrication methods. The procedure is designed to be readily adaptable to advances in materials technology. This article details the fabrication procedures for this medial-opening Syme prosthesis.

Using Seat Contour Measurements During Seating Evaluations of Individuals with SCI. Sprigle S, Schuch JZ. reprinted from *Assist Technol* 5:24-35, 1993.

Measuring the shape of the buttock-cushion interface has been used successfully in research to study tissue loading and as a means to fabricate custom contoured cushions. Seat contours are also able to provide useful clinical information on the weight-bearing surface of the cushion, which can be used to address posture. This article offers specific case

studies that demonstrate how the analysis of seat contours can be used to identify pelvic tilt, pelvic obliquity, and areas of high loading. Seat contour measurements complement other clinical measures, such as seat interface pressures and general postural assessments, to form a more complete picture of the buttock-cushion interface. They have become useful in the clinical management of various pressure and posture problems experienced by individuals with spinal cord injury and other wheelchair users.

A Volume-Adaptable Prosthesis for Ankle Disarticulation. Pinzur MS, Angelico JA, Quigley MJ. reprinted from *J Prosthet Orthot* 5:77-78, 1993.

Ankle disarticulation amputation in patients with peripheral vascular disease is sometimes complicated by delayed healing or residual limb volume fluctuation. This change in shape and contour presents several challenges to the prosthetist charged with producing a static prosthesis that must meet the demands of a constantly changing residual limb.

This article describes a method of producing a preparatory ankle disarticulation prosthesis that can be quickly and inexpensively fabricated, and can adapt to changing residual limb size and shape.

BOOK REVIEWS

by
Paul Beattie, Ph.D., P.T., O.C.S. and Mary Rodgers, Ph.D., P.T.

Clinical Efficacy and Outcome in the Diagnosis and Treatment of Low Back Pain. Edited by James N. Weinstein. New York: Raven Press, 1992. 293 pp. Illustrated.

Reviewed by Paul Beattie, Ph.D., P.T., O.C.S., University of New Mexico, Albuquerque, NM

The evaluation and treatment of people with low back pain (LBP) remains one of the most costly and poorly understood areas of health care delivery in the United States. Despite the high incidence of people with LBP and the numerous methods by which they are evaluated, classified, and treated, there remains a paucity of information by which clinicians can judge the efficacy of their procedures and measure their long-term outcomes. In *Clinical Efficacy and Outcome in the Diagnosis and Treatment of Low Back Pain,* an attempt has been made to address these issues using multiple authors. This text results from an orthopaedic symposium sponsored by the Bristol-Myers Squibb Company and the Zimmer Subsidiary.

The implied purpose of this text is to discuss the relative efficacy and outcomes of a variety of diagnostic and therapeutic procedures used for people with LBP. However, the scope of this text also allows the individual authors a forum to discuss their opinions and philosophies regarding their given topic, which can be quite thought-provoking for the reader.

This text begins with a discussion of the issues that relate to physician practice patterns and clinical decision-making. The sections on tracking physician practice and research support are briefly presented. The discussion of clinical decision analysis by Kent and Weinstein is, however, quite detailed and includes a literature review, theoretical construct, and clinical examples.

The second major portion of this text is "Nonoperative Care for Low Back Pain." Author Nortin M. Hadler presents a compelling argument for a "common sense" approach to the management of backache, while Liang and Fortin very briefly discuss the efficacy of selected nonsurgical treatments of LBP. Modic and Ross give an overview of the uses of Magnetic Resonance Imaging for the evaluation of people with LBP. This is followed by a detailed discussion of CT scanning by Herzog. The efficacy of functional muscle testing is presented and discussed in separate articles by Andersson, Pope, and Mooney.

Lumbar disc herniation and its relative surgical interventions and costs are presented by Frymoyer and Hanley, respectively. These authors discuss these issues with Nachemson. Following this, pedicle fixation is discussed at great length by Garfin and Ozanne, and by Kane. The remainder of the text is devoted to the history, indications for, and scientific basis of the Artificial Disc. The Steffee and Kostuik Artificial Discs are presented.

The list of contributing authors for this text is quite impressive and the presentation of a wide variety of topics is attempted. It should be noted, however, that one-half of this text is devoted to pedicle fixation and the Artificial Disc. While these important and interesting topics are presented and discussed in great detail, other topics such as the efficacy of nonoperative treatments are presented very superficially.

This would appear to be an invaluable text for those who are interested in the surgical issues relative to pedicle fixation and the Artificial Disc. In addition, this text is useful for clinicians and researchers who are interested in clinical decision-making, imaging, and quantitative muscle testing.

Gait Analysis Laboratory: An Interactive Book and Software Package. Christopher L. Vaughan, Brian L. Davis, and Jeremy C. O'Connor. Champaign, IL: Human Kinetics Publishers, 1992. 160 pp. Illustrated, includes software.

Reviewed by Mary Rodgers, Ph.D, P.T., Institute for Rehabilitation Research and Medicine, Wright State University, Dayton, OH

This interactive, IBM-compatible software and accompanying software manual and textbook provide a valuable learning tool for the study of human walking. The package includes over 250 variables involved in human gait, and enables the user to examine these variables in three dimensions (3-D). In order to study the theory and tools of gait analysis provided, the reader needs a basic knowledge of mechanics and anatomy along with access to a personal computer.

The GaitLab software contains three separate programs—Gaitmath, Gaitplot, and Animate—that help users to input data and apply the theoretical information contained in the accompanying text, *Dynamics of Human Gait*. Gaitmath allows users to input data to calculate five sets of parameters for gait-body segment parameters, linear kinematics, centers of gravity, angular kinematics, and dynamics of joints. Gaitplot plots these parameters graphically in many combinations. It also includes an animation program that models data from Gaitmath into a simple moving figure. Users can input the sample data provided or use their own data for the Gaitplot or Gaitmath programs. However, data must have been collected using specific instrumentation criteria in order to be used with the other two programs. In order to create new date files: 1) the first frame must be right heel strike on the first force plate; 2) 15 markers in specified locations must be used; 3) 8 muscles must be used for the electromyographic data; 4) the reference frame must be the same as in the manual; 5) data must be captured at 50–60 Hz; and, 6) a maximum of 150 frames can be used. Another limitation is that only one file can be viewed at a time. Therefore, director comparisons of data such as normal and clinical cases or pre- and post-intervention studies are not possible with the package. The Animate program illustrates gait patterns by showing the way muscle activity, joint moments, and ground reaction forces are integrated. A freeze-frame function allows users to stop and look at any phase of gait cycle.

The companion text provides a theoretical introduction to the 3-D and cyclic nature of human gait. Although the text is considered introductory, it assumes the reader already has a background with basic mechanics and anatomy. Chapters 1 through 4 describe the anthropometric, kinematic, and force-plate data that form a 3-D analysis of gait. A clinical case study of the gait patterns of a person with a movement disability is presented in Chapter 5. Animation sequences that show how muscle activity, joint moments, and ground reaction forces are integrated are included in the appendix. Also included in the appendix are brief descriptions of commercial equipment currently available for gait analysis. This summary would be helpful to those setting up a gait laboratory.

As a whole, the package would be more useful to students and teachers in physical education and physical therapy, and clinicians in a variety of areas (i.e., orthopaedic surgery, physical therapy, podiatry, rehabilitation, neurology, and sports medicine) than to researchers. If the program allowed more flexibility for input of the user's data and allowed the direct comparison of data to "normal" databases, it would be more valuable to a researcher. But, the *Gait Analysis Laboratory* provides an excellent, interactive way for those new to the area to learn about gait analysis.

PUBLICATIONS OF INTEREST

This list of references offers *Journal* readers significant information on the availability of recent rehabilitation literature in various scientific, engineering, and clinical fields. The *Journal* provides this service in an effort to fill the need for a comprehensive and interdisciplinary indexing source for rehabilitation literature.

All entries are numbered so that multidisciplinary publications may be cross-referenced. They are indicated as *See also* at the end of the categories where applicable. A listing of the periodicals reviewed follows the references. In addition to the periodicals covered regularly, other publications will be included when determined to be of special interest to the rehabilitation community. To obtain reprints of a particular article or report, direct your request to the appropriate contact source listed in each citation.

AMPUTATIONS and PROSTHETICS

1. Assessment of Patient Function After Limb-Sparing Surgery. Frieden RA, et al., *Arch Phys Med Rehabil* 74(1):38-43, 1993.
Contact: Richard A. Frieden, MD, Mount Sinai Medical Center, 1 Gustave L. Levy Place, Box 1240, New York, NY 10029

2. Energy Expenditure During Walking in Subjects with Tibial Rotationplasty, Above-Knee Amputation, or Hip Disarticulation. van der Windt DAWM, et al., *Arch Phys Med Rehabil* 73(12):1174-1180, 1992.
Contact: Jan W. van der Eijken, MD, PhD, Academical Medical Centre/Emma Kinderziekenhuis, Dept. of Orthopaedic Surgery, Meibergdreef 9, 1105 AZ Amsterdam-Z.O., The Netherlands

3. Energy Storing Property of So-Called Energy-Storing Prosthetic Feet. Ehara Y, et al., *Arch Phys Med Rehabil* 74(1):68-72, 1993.
Contact: Yoshihiro Ehara, BS, The Rehabilitation Engineering Dept., The Kanagawa Rehabilitation Center, Nanasawa 516, Atsugi-City, Kanagawa, 243-01, Japan

4. How are Physiotherapists Using the Vessa Pneumatic Post-Amputation Mobility Aid? Lein S, *Physiotherapy* 78(5):318-322, 1992.
Contact: Susan Lein, Disablement Services Centre, Medway Hospital, Windmill Rd., Gillingham, Kent ME7 5YX, UK

5. Level of Lower Limb Amputation in Relation to Etiology: An Epidemiological Study. Ebskov LB, *Prosthet Orthot Int* 16(3):163-167, 1992.
Contact: Lars Bo Ebskov, Anyvej 10, DK-3500 Vaerloese, Denmark

6. Phantom Sensation, Phantom Pain, and Stump Pain. Davis RW, *Arch Phys Med Rehabil* 74(1):79-91, 1993.
Contact: Roger W. Davis, MD, c/o Archives of Physical Medicine and Rehabilitation, Suite 1310, 78 East Adam St., Chicago, IL 60603-6103

7. Social Discomfort and Depression in a Sample of Adults with Leg Amputations. Rybarczyk BD, et al., *Arch Phys Med Rehabil* 73(12):1169-1173, 1992.
Contact: Bruce Rybarczyk, PhD, Dept. of Psychology and Social Sciences, 3-Rawson, Rush-Presbyterian-St. Luke's Medical Center, 1653 West Congress Pkwy., Chicago, IL 60612-3864

8. A Standardised Trans-Tibial Amputation Method Following Chronic Occlusive Arterial Disease. Bruckner L, *Prosthet Orthot Int* 16(3):157-162, 1992.
Contact: Doz. Dr. sc. med. Lutz Bruckner, Klinik fur Orthopadie der Universitat Leipzig, Phillip-Rosenthal Str. 53, 0-7010 Leipzig, Germany

9. Tissue Expansion to Cover Amputation Stumps: A Case Report. Berg A, Jonsson CE, *Acta Orthop Scand* 63(5):566-567, 1992.
Contact: Agnes Berg, Dept. of Plastic and Reconstructive Surgery, Karolinska Hospital, S-104 01 Stockholm, Sweden
See also 127

BIOENGINEERING

10. Development and Validation of a New Transducer for Intradiscal Pressure Measurement. McNally DS, Adams MA, Goodship AE, *J Biomed Eng* 14(6):495-498, 1992.
Contact: Dr. D.S. McNally, Comparative Orthopaedic Research Unit, Dept. of Anatomy, University of Bristol, Park Row, Bristol BS1 5LS, UK

11. Three-Dimensional Finite Element Modelling of Bone: Effects of Element Size. Keyak JH, Skinner HB, *J Biomed Eng* 14(6):483-489, 1992.
Contact: Dr. Harry B. Skinner, Dept. of Orthopaedic Surgery, Room U-471, University of California, San Francisco, CA 94143-0728
See also 97, 106, 110

BIOMECHANICS

12. Biomechanical Analyses of Rising from a Chair. Schultz AB, Alexander NB, Ashton-Miller JA, *J Biomech* 25(12):1383-1391, 1992.
Contact: Albert B. Schultz, Dept. of Mechanical Engineering, University of Michigan, Ann Arbor, MI 48109-2125

13. Examining Motion in the Cervical Spine I: Imaging Systems and Measurement Techniques. Roozmon P, et al., *J Biomed Eng* 15(1):5-12, 1993.
Contact: P. Roozmon, Diagnospine Research Inc., 800 Rene Levesque Blvd. West, Suite 2637, Montreal, Quebec, Canada

14. Examining Motion in the Cervical Spine II: Characterization of Coupled Joint Motion Using an Opto-Electronic Device to Track Skin Markers. Roozmon P, et al., *J Biomed Eng* 15(1):13-22, 1993.
Contact: P. Roozmon, Diagnospine Research Inc., 800 Rene Levesque Blvd. West, Suite 2637, Montreal, Quebec, Canada

15. The Forces Acting on the Human Calcaneus. Yettram AL, Camilleri NN, *J Biomed Eng* 15(1):46-50, 1993.
Contact: Prof. A.L. Yettram, Dept. of Mechanical Engineering, Brunel University, Uxbridge, Middlesex, UK

16. Forces and Moments on the Human Leg in the Frontal Plane During Static Bipedal Stance. Carmines DV, MacMahon EB, *J Orthop Res* 10(6):917-925, 1992.

Contact: Dr. David V. Carmines, The Catholic University of America, Dept. of Mechanical Engineering, Pangborn Hall, Rm. G-32, Washington, DC 20064

17. The Functional Standing Test: Development and Standardization of a Clinical Evaluation of Standing Function. Triolo RJ, et al., *IEEE Eng Med Biol Mag* 11(4):32-34, 1992.
Contact: B.W.B. Reilley, Biomedical Engineering Institute, Drexel University, Philadelphia, PA 19104

18. Kinematics of Walking Frame Ambulation. Crosbie J, *Clin Biomech* 8(1):31-36, 1993.
Contact: Jack Crosbie, PhD, Faculty of Health Sciences, The University of Sydney, East St., Lidcombe, NSW 2777, Australia

19. Reliability of Hindfoot Goniometry When Using a Flexible Electrogoniometer. Ball P, Johnson GR, *Clin Biomech* 8(1):13-19, 1993.
Contact: G.R. Johnson, PhD, CEng FIMechE, Dept. of Mechanical, Materials and Manufacturing Engineering, Stephenson Bldg., University of Newcastle upon Tyne, Newcastle upon Tyne NE1 7RU, UK

20. Role of Ground Reaction Torque and Other Dynamic Measures in Postural Stability. Soutas-Little RW, et al., *IEEE Eng Med Biol Mag* 11(4):28-31, 1992.
Contact: R.W. Soutas-Little, Biomechanics Evaluation Laboratory, Michigan State University, Lansing, MI 48823

21. Role of the Calcaneal Heel Pad and Polymeric Shock Absorbers in Attenuation of Heel Strike Impact. Noe DA, et al., *J Biomed Eng* 15(1):23-26, 1993.
Contact: Dr. M.J. Askew, Musculoskeletal Research Laboratory, Dept. of Orthopaedic Surgery, Akron City Hospital, Akron, OH
See also 68, 81, 104, 106, 107

COMMUNICATION AIDS—HEARING

22. Combining Cognitive Learning Theory and Computer Assisted Instruction for Deaf Learners. Mertens DM, Rabiu J, *Am Ann Deaf* 137(5):399-403, 1992.
Contact: Donna M. Mertens, Dept. of Educational Foundations and Research, Gallaudet University, Washington, DC 20002

23. Effects of Speech Output Type, Message Length, and Reauditorization on Perceptions of the Communicative Competence of an Adult AAC User. Hoag LA, Bedrosian JL, *J Speech Hear Res* 35(6):1363-1366, 1992.
Contact: Linda A. Hoag, Kansas State University, Manhattan, KS 66502

24. Electrical Stimulation of the Auditory Nerve: Effects of Pulse Width on Frequency Discrimination. Barretto RL, Pfingst BE, *Hear Res* 62(2):245-249, 1992.
Contact: Bryan E. Pfingst, Kresge Hearing Research Institute, 1301 East Ann St., University of Michigan Medical Center, Ann Arbor, MI 48109-0506

25. Modifications in Sign Under Conditions of Impeded Visibility. Naeve SL, Siegel GM, Clay JL, *J Speech Hear Res* 35(6):1272-1280, 1992.
Contact: Susan L. Naeve, Dept. of Communication Disorders, University of Minnesota, Minneapolis, MN 55403
See also 88

COMMUNICATION AIDS—OTHER

See 90

COMMUNICATION AIDS—VISION

26. Barriers to Acquiring Assistive Technology: Cost and Lack of Information. Uslan MM, *J Visual Impairm Blindn* 86(9):402-407, 1992.
Contact: Mark M. Uslan, MA, MS, Technical Evaluation Services, National Technology Center, American Foundation for the Blind, 15 West 16th St., New York, NY 10011

27. The Externalization of Spatial Representation by Blind Persons. Huertas JA, Ochaita E, *J Visual Impairm Blindn* 86(9):398-402, 1992.
Contact: Juan Antonio Huertas, PhD, Facultad de Psicologia, Universidad Autonoma de Madrid, Cantoblanco, 28049, Madrid, Spain

28. Use of the Alternating Treatment Design to Evaluate Intervention in Low Vision Rehabilitation. LaGrow SJ, Murray S, *J Visual Impairm Blindn* 86(10):435-439, 1992.
Contact: Steven J. LaGrow, EdD, Massey University, Private Bag, Palmerston North, New Zealand

29. Visually Impaired Persons' Comprehension of Text Presented with Speech Synthesis. Hjelmquist E, Dahlstrand U, Hedelin L, *J Visual Impairm Blindn* 86(10):426-428, 1992.
Contact: Erland Hjelmquist, PhD, Dept. of Psychology, University of Goteborg, Box 14158, S-40020, Goteborg, Sweden

COMPUTERS

See 142

FUNCTIONAL ASSESSMENT

30. Perspectives on Functional Assessment: Its Use for Policy Making. Frattali CM, *Disabil Rehabil* 15(1):1-9, 1993.
Contact: Carol M. Frattali, Director, Health Services Division, American Speech-Language-Hearing Association, 10801 Rockville Pike, Rockville, MD 20852
See also 1, 43, 63, 95, 96, 143

FUNCTIONAL ELECTRICAL STIMULATION

31. Functional Electrical Stimulation Leg Cycle Ergometer Exercise: Training Effects on Cardiorespiratory Responses of Spinal Cord Injured Subjects at Rest and During Submaximal Exercise. Faghri PD, Glaser RM, Figoni SF, *Arch Phys Med Rehabil* 73(11):1085-1093, 1992.
Contact: Pouran D. Faghri, MD, MS, Clinical Studies, Rehabilitation Institute of Ohio, Miami Valley Hospital, One Wyoming St., Dayton, OH 45409

32. Hip and Trunk Stability in Paraplegic Electrically Augmented Gait. Marsolais EB, Mansour JM, *IEEE Eng Med Biol Mag* 11(4):64-67, 1992.
Contact: E. Byron Marsolais, Veterans Affairs Medical Center, Cleveland, OH 44106

33. Torque History of Electrically Stimulated Human Quadriceps: Implications for Stimulation Therapy. Lieber RL, Kelly MJ, *J Orthop Res* 11(1):131-141, 1993.
Contact: Dr. Richard L. Lieber, Dept. of Orthopaedics and Biomedical Sciences Graduate Group (V-151), University of California, San Diego, School of Medicine, 3350 La Jolla Village Dr., San Diego, CA 92161
See also 24, 139

GAIT ANALYSIS

34. Adaptations in Gait Resulting from Unilateral Ischaemic Block of the Leg. Dickey JP, Winter DA, *Clin Biomech* 7(4):215-225, 1992.
Contact: Prof. David A. Winter, PhD, PEng, Dept. of Kinesiology, University of Waterloo, Waterloo, Ontario N2L 3G1, Canada

35. The Control of Genu Recurvatum by Combining the Swedish Knee-Cage and an Ankle—Foot Brace. Isakov E, et al., *Disabil Rehabil* 14(4):187-191, 1992.
Contact: Dr. Eli Isakov, Dept. of Orthopaedic Rehabilitation, Loewenstein Hospital, Ra'anana, Israel

36. The Effect of Foot Orthotics and Gait Velocity on Lower Limb Kinematics and Temporal Events of Stance. McCulloch MU, Brunt D, Vander Linden D, *J Orthop Sports Phys Ther* 17(1):2-10, 1993.
Contact: Marina U. McCulloch, MSc, PT, Dept. of Physical Therapy, School of Health Related Professions, University of Florida, Gainesville, FL 32601

37. Gait in Relation to Ageing and Idiopathic Parkinsonism. Bowes SG, et al., *Scan J Rehabil Med* 24:181-186, 1992.
Contact: Drs. R.J. and S.M. Dobbs, Therapeutics in the Elderly Clinical Research Centre, Northwick Park Hospital, Watford Rd., Harrow, HA1 3UJ Middlesex, UK

38. Measurement of Gait by Accelerometer and Walkway: A Comparison Study. Currie G, et al., *Med Biol Eng Comput* 30(6):669-670, 1992.
Contact: G. Currie, Dept. of Clinical Physics & Bio-Engineering, West of Scotland Health Boards, 11 West Graham St., Glasgow, G4 9LF, UK

39. A Neural Network Representation of Electromyography and Joint Dynamics in Human Gait. Sepulveda F, Wells DM, Vaughan CL, *J Biomech* 26(2):101-109, 1993.
Contact: Christopher L. Vaughan, Motion Analysis Laboratory, Dept. of Orthopaedic Surgery, University of Virginia, Charlottesville, VA 22908

40. An Overhead Harness and Trolly System for Balance and Ambulation Assessment and Training. Harburn KL, et al., *Arch Phys Med Rehabil* 74(2):220-223, 1993.
Contact: Karen L. Harburn, PhD, Dept. of Occupational Therapy, Faculty of Applied Health Sciences, Elborn College, The University of Western Ontario, London, ON N6G 1H1, Canada

41. Reliability of Ground Reaction Force Measurements During Dynamic Transitions from Bipedal to Single-Limb Stance in Healthy Adults. Hanke TA, Rogers MW, *Phys Ther* 72(11):810-816, 1992.
Contact: Mark W. Rogers, PhD, PT, Northwestern University Medical School, 345 E. Superior St., Room 1323, Chicago, IL 60611
See also 2, 3, 16, 18, 21, 32, 81, 94, 95, 98, 102, 139

GENERAL

42. Advanced Materials for Assistive Devices. Koeneman JB, *Top Geriatr Rehabil* 8(2):20-28, 1992.
Contact: James B. Koeneman, PhD, Harrington Arthritis Research Center, Phoenix, AZ 85012

43. The Assessment of Disability in Patients on an Acute Medical Ward for Elderly People. Stone SP, et al., *Disabil Rehabil* 15(1):35-37, 1993.
Contact: Dr. S.P. Stone, Academic Dept. of Geriatric Medicine, Royal Free Hospital Medical School, Pond St., London NW3 2QG, UK

44. Behavioral Screening in the Hypertension Clinic: A Descriptive Study. Starker S, *Med Psychother* 5:65-72, 1992.
Contact: Steven Starker, Portland VA Medical Center, Portland, OR 97201

45. Challenging the Biomedical Model. Radmacher SA, *Med Psychother* 5:21-28, 1992.
Contact: Sally A. Radmacher, Missouri Western State College, St. Joseph, MO 64507

46. Characteristics of Self-Help Book Readers Among VA Medical Outpatients. Starker S, *Med Psychother* 5:89-94, 1992.
Contact: Steven Starker, Portland VA Medical Center, Portland, OR 97201

47. A Clinical Study of Degenerative Spondylolisthesis: Radiographic Analysis and Choice of Treatment. Satomi K, et al., *Spine* 17(11):1329-1336, 1992.
Contact: Kazuhiko Satomi, Dept. of Orthopaedics, School of Medicine, Keio University, Tokyo, Japan

48. Computer Solutions to Identify EMG Latency of Automatic Postural Reactions. Moffroid M, et al., *IEEE Eng Med Biol Mag* 11(4):48-51, 1992.
Contact: Mary Moffroid, Vermont Rehabilitation Engineering Center, University of Vermont, Burlington, VT 05401

49. Cost and Complications During In-Hospital Transport of Critically Ill Patients: A Prospective Cohort Study. Hurst JM, et al., *J Trauma* 33(4):582-585, 1992.
Contact: James M. Hurst, MD, Division of Trauma and Critical Care, Dept. of Surgery, University of South Florida, Tampa, FL 33620

50. CTSS: An Interactive Microcomputer Program for the Clinical Screening of Carpal Tunnel Syndrome. II. Statistical and Computational Aspects. Rudolfer SM, *Electromyogr Clin Neurophysiol* 32(10-11):483-489, 1992.
Contact: S.N. Rudolfer, Statistical Laboratory, Mathematics Dept., University of Manchester, Manchester M13 9PL, England

51. Developing Clinical Reasoning Competencies. Higgs J, *Physiotherapy* 78(8):575-579, 1992.
Contact: Dr. Joy Higgs, Head, School of Physiotherapy, Faculty of Health Sciences, University of Sydney, PO Box 170, Lidcombe, 2141, Australia

52. Dynamic Posturography: Analysis of Error in Force Plate Measurement of Postural Sway. Barin K, *IEEE Eng Med Biol Mag* 11(4):52-56, 1992.
Contact: Kamran Barin, Dept. of Otolaryngology, The Ohio State University, Columbus, OH 43210

53. Early Ambulation and Discharge in 100 Patients with Burns of the Foot Treated by Grafts. Grube BJ, Engrav LH, Heimbach DM, *J Trauma* 33(5):662-664, 1992.
Contact: David Heimbach, MD, Dept. of Surgery ZA-16, Harborview Medical Center, 325 Ninth Ave., Seattle, WA 98104

54. The Effects of Auditory and Visual Interference on Speech and Sign. Siegel GM, Clay JL, Naeve SL, *J Speech Hear Res* 35(6):1358-1362, 1992.
Contact: Gerald M. Siegel, University of Minnesota, Minneapolis, MN 55404

55. Effects of Cervical Collars on Standing Balance. Burl MM, Williams JG, Nayak USL, *Arch Phys Med Rehabil* 73(12):1181-1185, 1992.
Contact: Margaret M. Burl, MSc, MCSP, DipTP, School of Physiotherapy, Royal Orthopaedic Hospital, Birmingham, England

56. Effects of High-Frequency (500–1,000 Hz), Indirect Stimulation on Slow and Fast Muscle Relevant to Orthotic Applications. Eldred E, Solomonow M, *J Electromyogr Kinesiol* 2(3):150-159, 1992.
Contact: Dr. E. Eldred, Dept. of Anatomy and Cell Biology, University of California at Los Angeles, Los Angeles, CA 90024-176818

57. Electrophysiological Findings in Poliomyelitis Patients at the Subacute Phase. Keren O, et al., *Electromyogr Clin Neurophysiol* 32(10-11):547-554, 1992.
Contact: Dr. Zeev Groswasser, MD, Loewenstein Rehabilitation Hospital, PO Box 3, Ra'anana 43100, Israel

58. Force- and Moment-Generating Capacity of Lower-Extremity Muscles Before and After Tendon Lengthening. Delp SL, Zajac FE, *Clin Orthop* 284:247-259, 1992.
Contact: Scott L. Delp, PhD, Rehabilitation Institute of Chicago, Room 1406, 345 East Superior St., Chicago, IL 60611

59. Impedance Plethysmography for Blood Flow Measurements in Human Limbs. Part 2: Influence of Limb Cross-Sectional Area. Yamamoto Y, Yamamoto T, Oberg PA, *Med Biol Eng Comput* 30(5):518-524, 1992.
Contact: Y. Yamamoto, Dept. of Electrical Engineering, Okayama University, Tsushima-Naka 3-1-1, Okayama 700, Japan

60. Improved Preservation of Skeletal Muscle in Amputated Limbs Using Pulsatile Hypothermic Perfusion with University of Wisconsin Solution: A Preliminary Study. Gordon L, et al., *J Bone Joint Surg* 74A(9):1358-1366, 1992.
Contact: Leonard Gordon, MD, Hand and Microsurgery Medical Group, California Pacific Medical Center, Clay at Buchanan, San Francisco, CA 94120

61. Interrater Reliability of the Cybex EDI-320 and Fluid Goniometer in Normals and Patients with Low Back Pain. Chiarello CM, Savidge R, *Arch Phys Med Rehabil* 74(1):32-37, 1993.
Contact: Cynthia M. Chiarello, PhD, PT, Dept. of Rehabilitation Medicine, Program in Physical Therapy, College of Physicians and Surgeons, Columbia University, 630 W. 168th St., New York, NY 10032

62. The Intra-Observer Reliability of the Hand-Held Myometer in the Measurement of Isotonic Muscle Strength in Chronic Spasticity. Livesley E, *Physiotherapy* 78(12):918-921, 1992.
Contact: Elizabeth Livesley, MCSP, 54 Chatsworth Dr., Mansfield, Nottinghamshire NG18 4QT, UK

63. Issues Involved in the Evaluation of Assistive Devices. Eblen C, *Top Geriatr Rehabil* 8(2):6-11, 1992.
Contact: Cristobal Eblen, PhD, Research and Statistical Analyst III, Arizona Dept. of Health Services, Phoenix, AZ 85012

64. A Method for Obtaining Repeatable Measurements of the Tensile Properties of Skin at Low Strain. Mansour JM, et al., *J Biomech* 26(2):211-216, 1993.
Contact: J.M. Mansour, Dept. of Mechanical and Aerospace Engineering, Case Western Reserve University, Cleveland, OH 44106

65. Objective Parameters in Magnetic Resonance Imaging (MRI) for Neuromuscular Diagnosis: Preliminary Findings. Tsubahara A, et al., *Disabil Rehabil* 14(4):163-167, 1992.

Contact: Akio Tsubahara, Dept. of Rehabilitation Medicine, Keio University Tsukigase Rehabilitation Center, 380-2 Tsukigase, Amagiyugashima-cho, Tagata-gun, Shizuoka 410-32, Japan

66. On-Scene Helicopter Transport of Patients with Multiple Injuries—Comparison of a German and an American System. Schmidt U, et al., *J Trauma* 33(4):548-555, 1992.
Contact: Scott B. Frame, MD, FACS, Dept. of Surgery, Division of Trauma/Critical Care, University of Tennessee, Graduate School of Medicine, 1924 Alcoa Hwy./U11, Knoxville, TN 37920

67. Optimization of Single Electrode Tactile Codes. Szeto AYJ, Farrenkopf GR, *Ann Biomed Eng* 20(6):647-665, 1992.
Contact: Andrew Y.J. Szeto, Dept. of Electrical and Computer Engineering, San Diego State University, San Diego, CA 92182-0190

68. Physiological Cross-Sectional Area of Human Leg Muscles Based on Magnetic Resonance Imaging. Fukunaga T, et al., *J Orthop Res* 10(6):926-934, 1992.
Contact: Dr. R.R. Roy, Brain Research Institute, UCLA School of Medicine, Center for the Health Sciences, 10833 Le Conte Ave., Los Angeles, CA 90024-1761

69. Porous Polyurethane Vascular Prostheses with Variable Compliances. Liu SQ, Kodama M, *J Biomed Mater Res* 26(11):1489-1502, 1992.
Contact: Shu Qin Liu, Biomaterial Laboratory, Research Institute for Polymers and Textiles, Higashi 1-1-4, Tsukuba, Ibaraki 305, Japan

70. Posttraumatic Disablement: A Prospective Study of Impairment, Disability, and Handicap. Maurette P, et al., *J Trauma* 33(5):728-736, 1992.
Contact: Pierre Maurette, MD, Dept. d'anesthesie et de reanimation I, Hopital Pellegrin, Place Amelie Raba Leon, 33076 Bordeaux Cedex, France

71. A Quantitative Comparison of Four Experimental Axillary Crutches. LeBlanc MA, Carlson LE, Nauenberg T, *J Prosthet Orthot* 5(1):20-28, 1993.
Contact: Maurice LeBlanc, MSME, CP, Packard Children's Hospital, 725 Welsh Rd., Palo Alto, CA 94304

72. Skin Blood Flow Measurements—A Review of Noninvasive Methods. Bukhari ARS, *J Clin Eng* 18(1):53-65, 1993.
Contact: Abdul R.S. Bukhari, PO Box 10219, Riyadh 11433, Saudi Arabia

73. Some Conceptual Remarks About Supraspinal Mechanisms in the Control of Voluntary and Reflex Motor Activities. Jergelova M, Podivinsky F, *Electromyogr Clin Neurophysiol* 32(10-11):537-546, 1992.
Contact: M. Jergelova, MD, PhD, Institute of Normal and Pathological Physiology, Slovak Academy of Sciences, Sienkiewiczova 1, 813 71 Bratislava, Czech and Slovak Federal Republic

74. The Spatial Integration Effect of Surface Electrode Detecting Myoelectric Signal. Helal J-N, Bouissou P, *IEEE Trans Biomed Eng* 39(11):1161-1167, 1992.
Contact: Jean-Noel Helal, Laboratoire de Biomecanique et de Physiologie, Institut National du Sport et de l'Education Physique, F-75012 Paris, France

75. Surface Myoelectric Signals During Ergocycle Exercises at Various Mechanical Powers and Pedalling Rates. Helal J-N, et al., *J Electromyograph Kinesiol* 2(4):242-251, 1993.
Contact: Dr. J. Van Hoecke, Laboratoire de Biomecanique et de Physiologie, Institut National du Sport et de l'Education Physique, 11 avenue du Tremblay, F-75012 Paris, France

76. A Technique to Analyse the Kinetics and Energetics of Cane-Assisted Gait. Winter DA, et al., *Clin Biomech* 8(1):37-43, 1993.
Contact: David A. Winter, PhD, PEng, Dept. of Kinesiology, University of Waterloo, Waterloo, ON, N2L 3G1, Canada

77. Tibial Shaft Fractures: A Biomechanical and Clinical Approach: Thesis Summary. Shah KM, *Clin Biomech* 7(4):247-248, 1992.
Contact: Khalid M. Shah, PhD, Dept. of Orthopaedic Surgery, National University of Singapore, National University Hospital, 5 Lower Kent Ridge Rd., Singapore 0511, Republic of Singapore

78. Tinel's Sign and Phalen's Test in Carpal Tunnel Syndrome. Kuschner SH, et al., *Orthopedics* 15(11):1297-1302, 1992.
Contact: Stuart H. Kuschner, MD, 9001 Wilshire Blvd., Ste 200, Beverly Hills, CA 90211
See also 6, 7, 19, 33, 39, 40, 69, 80, 83, 86, 100, 103, 109, 112, 113, 120, 135, 145

GERIATRICS

79. Aging and the Binaural Advantage in Reverberation and Noise. Helfer KS, *J Speech Hear Res* 35(6):1394-1401, 1992.
Contact: Karen S. Helfer, University of Massachusetts, Amherst, MA 01003

80. Assistive Devices for Home-Based Elderly Persons with Cognitive Impairments. Mann WC, et al., *Top Geriatr Rehabil* 8(2):35-52, 1992.
Contact: William C. Mann, OTR, PhD, Rehabilitation Engineering Center on Aging, State University of New York at Buffalo, Buffalo, NY 14260

81. Clinical and Laboratory Measures of Postural Balance in an Elderly Population. Berg KO, et al., *Arch Phys Med Rehabil* 73(11):1073-1080, 1992.
Contact: Katherine O. Berg, School of Physical and Occupational Therapy, 3654 Drummond St., Montreal, PQ, H3G 1Y5, Canada

82. A Comprehensive Neuropsychology Program in Geriatric Long-Term Care. Lichtenberg PA, et al., *Med Psychother* 5:39-52, 1992.
Contact: Peter A. Lichtenberg, Rehabilitation Institute of Michigan, Detroit, MI 48226

83. Energy Expenditure in Elderly Patients Using Assistive Devices. Waters R, Torburn L, Mulroy S, *Top Geriatr Rehabil* 8(2):12-19, 1992.
Contact: Sara Mulroy, MS, PT, Pathokinesiology Laboratory, Rancho Los Amigos Medical Center, 760 E. Imperial Hwy., Downey, CA 90242

84. Modulation Detection, Modulation Masking, and Speech Understanding in Noise in the Elderly. Takahashi GA, Bacon SP, *J Speech Hear Res* 35(6):1410-1421, 1992.
Contact: Gail A. Takahashi, Arizona State University, Tempe, AZ 85287

85. Postural Steadiness and Ankle Joint Compliance in the Elderly. Prieto TE, Myklebust JB, Myklebust BM, *IEEE Eng Med Biol Mag* 11(4):25-27, 1992.
Contact: Thomas E. Prieto, Laboratory of Sensory-Motor Performance, Zablocki VA Medical Center, 5000 W. National Ave., Milwaukee, WI 53295

86. Predictors and Prognosis of Inability to Get Up After Falls Among Elderly Persons. Tinetti ME, Liu W-L, Claus EB, *JAMA* 269(1)65:-70, 1993.
Contact: Mary E. Tinetti, MD, Dept. of Medicine, Yale University School of Medicine, 333 Cedar St., PO Box 3333, New Haven, CT 06510-8056

87. Rehabilitation of Elderly Patients with Multiple Fractures Secondary to Falls. Weatherall M, *Disabil Rehabil* 15(1):38-40, 1993.
Contact: Mark Weatherall, Consultant Geriatrician, Dept. for the Elderly, Waikato Hospital, Hamilton, New Zealand

88. Sustained Benefits of Hearing Aids. Mulrow CD, Tuley MR, Aguilar C, *J Speech Hear Res* 35(6):1402-1405, 1992.
Contact: Cynthia D. Mulrow, Audie L. Murphy Memorial VA Hospital, 7400 Merton Minter Blvd., San Antonio, TX 78284
See also 154

HEAD TRAUMA and STROKE

89. Assessment of Stroke. Langton Hewer R, *Scand J Rehabil Med* Suppl 26:91-96, 1992.
Contact: Richard Langton Hewer, MD, Dept. of Neurology, Frenchay Hospital, Bristol BS16 1LE, Great Britain

90. Brainstem Infarct with Pharyngeal Dysmotility and Paralyzed Vocal Cord: Management with a Multidisciplinary Approach. Saltzman LS, Rosenberg CH, Wolf RH, *Arch Phys Med Rehabil* 74(2):214-216, 1993.
Contact: Lois S. Saltzman, MD, 89-06 135th St., Jamaica, NY 11418

91. Evaluating Outcome in Stroke Rehabilitation (Quality Control and Clinical Audit). Wade DT, *Scand J Rehabil Med* Suppl 26:97-104, 1992.
Contact: Derick T. Wade, MD, Rivermead Rehabilitation Centre, Oxford OX1 4XD, Great Britain

92. Evaluation of Long-Term Functional Status in First-Ever Stroke Patients in a Defined Population. Johansson BB, et al., *Scand J Rehabil Med* Suppl 26:105-114, 1992.
Contact: Barbro Johansson, MD, PhD, Dept. of Neurology, Lund University Hospital, S-221 85 Lund, Sweden

93. A European Head Injury Evaluation Chart. Truelle JL, et al., *Scand J Rehabil Med* Suppl 26:115-125, 1992.
Contact: J.L. Truelle, MD, Dept. of Neurology, CMC Foch, BP 36 F 92151 SURESNES CEDEX, France

94. Increasing Standing Tolerance and Posture Quality Following Severe Brain Injury Using a Behaviour Modification Approach. Alderman N, Shepherd J, Youngson H, *Physiotherapy* 78(5):335-343, 1992.
Contact: Nick Alderman, Clinical Psychologist, The Kemsley Unit, St. Andrew's Hospital, Northampton NN1 5DG, UK

95. Kinetic Analysis of Dynamic Transitions in Stance Support Accompanying Voluntary Leg Flexion Movements in Hemiparetic Adults. Rogers MW, Hedman LD, Pai Y-C, *Arch Phys Med Rehabil* 74(1):19-25, 1993.
Contact: Mark W. Rogers, PhD, PT, Programs in Physical Therapy, Northwestern University Medical School, 345 East Superior St., Room 1323, Chicago, IL 60611

96. Poor Functional Status of Stroke Patients After Hospital Discharge: Scope for Intervention? Corr S, Bayer A, *Br J Occup Ther* 55(10):383-385, 1992.
Contact: Susan Corr, DipCOT, SROT, Llandough Hospital, Penarth, South Glamorgan CF6 1XX, UK

97. A Radiological Measure of Shoulder Subluxation in Hemiplegia: Its Reliability and Validity. Boyd EA, et al., *Arch Phys Med Rehabil* 74(2):188-193, 1993.
Contact: Elizabeth A. Boyd, MS, Occupational Therapy Dept., The Rehabilitation Centre, 505 Smyth Rd., Ottawa, ON, K1H 8M2, Canada

98. Relationship Between Weight-Bearing Characteristics in Standing and Ambulatory Independence in Hemiplegics. Gruendel TM, *Physiother Can* 44(4):16-17, 1992.
Contact: Thomas M. Gruendal, PT, Clinical Specialist Neurology, Kelowna General Hospital, Rehabilitation Dept., 2268 Pandosy St., Kelowna, BC, V1Y 1T2, Canada

99. Suggestions for the Next Generation of Cognitive Rehabilitation Software: Part I: Memory Software. Lynch WJ, *J Head Trauma Rehabil* 7(4):109-111, 1992.
Contact: William J. Lynch, PhD, Brain Injury Rehabilitation Unit, Veterans Affairs Medical Center, 3801 Miranda Ave., Palo Alto, CA 94304

100. Torque Fluctuations During Maximal Voluntary Knee Extension Efforts After Stroke. Bohannon RW, Puharic T, *Clin Rehabil* 6(4):305-310, 1992.
Contact: Richard W. Bohannon, School of Allied Health, U-101, University of Connecticut, Storrs, CT 06269

101. The Use of a Balance Performance Monitor in the Treatment of Weight-Bearing and Weight-Transference Problems After Stroke. Sackley CM, et al., *Physiotherapy* 78(12):907-912, 1992.
Contact: C.M. Sackley, PhD, Research Office, Chartered Society of Physiotherapy, 14 Bedford Row, London WC1R 4ED, UK

102. Use of an Intensive Task-Oriented Gait Training Program in a Series of Patients with Acute Cerebrovascular Accidents. Malouin F, et al., *Phys Ther* 72(11):781-793, 1992.
Contact: Francine Malouin, PhD, Neurobiology Research Center, Hopital de l'Enfant-Jesus, 1401, 18e Rue, Quebec City, QC G1J 1Z4 Canada

103. Validation of a Cognitive Assessment: Predicting Driving Performance After Stroke. Nouri FM, Lincoln NB, *Clin Rehabil* 6(4):275-281, 1992.
Contact: F.M. Nouri, Stroke Research Unit, City Hospital, Hucknall Rd., Nottingham NG5 1PB, UK

MUSCLES, LIGAMENTS, and TENDONS

104. An Activation-Recruitment Scheme for Use in Muscle Modeling. Hawkins DA, Hull ML, *J Biomech* 25(12):1467-1476, 1992.

Contact: David A. Hawkins, Biomechanics Laboratory, University of Wisconsin-Madison, 2000 Observatory Dr., Madison, WI 53706

105. Estimates of Mechanical Work and Energy Transfers: Demonstration of a Rigid Body Power Model of the Recovery Leg in Gait. Caldwell GE, Forrester LW, *Med Sci Sports Exerc* 24(12):1396-1412, 1992.
Contact: Graham E. Caldwell, Biomechanics Laboratory, Dept. of Kinesiology, University of Maryland, College Park, MD 20742

106. Instrumental Straight-Leg Raising: Results in Healthy Subjects. Goeken LN, Hof AL, *Arch Phys Med Rehabil* 74(2):194-203, 1993.
Contact: Ludwig N. H. Goeken, MD, PhD, Dept. of Rehabilitation Medicine, University Hospital Groningen, Oostersingel 59, 9700 RB Groningen, The Netherlands

107. Isokinetic Trunk Extension Discriminates Uninjured Subjects from Subjects with Previous Low Back Pain. Grabiner MD, Jeziorowski JJ, *Clin Biomech* 7(4):195-200, 1992.
Contact: M.D. Grabiner, PhD, Biomedical Engineering and Applied Therapeutics, The Research Institute, The Cleveland Clinic Foundation, 9500 Euclid Ave., Cleveland, OH 44195

108. Viscoelastic Stress Relaxation in Human Skeletal Muscle. McHugh MP, et al., *Med Sci Sports Exerc* 24(12):1375-1382, 1992.
Contact: Malachy P. McHugh, Nicholas Institute of Sports Medicine and Athletic Trauma, Lenox Hill Hospital, New York, NY 10021
See also 115

NEUROLOGICAL DISORDERS

109. Innervation-Zone Width in Disease and its Changes with Fatigue. Yaar I, *J Electromyograph Kinesiol* 2(4):252-256, 1993.
Contact: Israel Yaar, MD, Neurology Section, VA Medical Center, Davis Park (127A), Providence, RI 02908

110. Objective Parameters in Magnetic Resonance Imaging (MRI) for Neuromuscular Diagnosis: Preliminary Findings. Tsubahara A, et al., *Disabil Rehabil* 14(4):163-167, 1992.
Contact: Akio Tsubahara, Dept. of Rehabilitation Medicine, Keio University Tsukigase Rehabilitation Center, 380-2 Tsukigase, Amagiyugashima-cho, Tagata-gun, Shizuoka 410-32, Japan

111. The Segmental Dorsal Ramus Neuropathy as a Common Cause of Chronic and Recurrent Low Back Pain. Sihvonen T, *Electromyogr Clin Neurophysiol* 32(10-11):507-510, 1992.
Contact: Teuvo Sihvonen, MD, Dept. of Clin. Neurophysiology, University Central Hospital of Kuopio, 70200 Kuopio, Finland

ORTHOPEDICS

112. Acute Effect of Traction, Compression, and Hip Joint Tamponade on Blood Flow of the Femoral Head: An Experimental Model. Naito M, et al., *J Orthop Res* 10(6):800-806, 1992.
Contact: Dr. Masatoshi Naito, Dept. of Orthopedic Surgery, Faculty of Medicine, Kyushu University, 3-1-1, Maidashi, Higashiku, Fukuoka, 812, Japan

113. An Alternative to Screws for Plating Osteoporotic Bone. King TStJ, Cebon D, *J Biomed Eng* 15(1):79-82, 1993.
Contact: D. Cebon, University Engineering Dept., Trumpington St., Cambridge, CB2 1PZ, UK

114. The Anterior Cruciate Ligament-Deficient Knee with Varus Alignment: An Analysis of Gait Adaptations and Dynamic Joint Loadings. Noyes FR, et al., *Am J Sports Med* 20(6):707-716, 1992.
Contact: Frank R. Noyes MD, Cincinnati Sportsmedicine and Orthopaedic Center, Deaconess Hospital, 311 Straight St., Cincinnati, OH 45219

115. A Biomechanical Evaluation of the Iliotibial Tract Screw Tenodesis. Lipscomb AB, Woods GW, Jones A, *Am J Sports Med* 20(6):742-745, 1992.
Contact: A. Brant Lipscomb, Jr., MD, The Lipscomb Clinic, Suite 1000, 4230 Harding Rd., Nashville, TN 37205

116. A Finite Element Model for Evaluation of Tibial Prosthesis-Bone Interface in Total Knee Re-

placement. Rakotomanana RL, et al., *J Biomech* 25(12):1413-1424, 1992.
Contact: R.L. Rakotomanana, Hopital Orthopedique, Lausanne, Switzerland

117. Orthopedic Prosthesis Fixation. Park JB, *Ann Biomed Eng* 20(6):583-594, 1992.
Contact: Joon B. Park, Dept. of Biomedical Engineering, The University of Iowa, Iowa City, IA 52242
See also 10, 11, 18, 76, 87, 97, 122, 138, 140

ORTHOTICS

118. An Adjustable Thermoplastic Knee Brace, Directly Moulded and Colour Coordinated. Cunliffe MW, *Br J Occup Ther* 55(11):430-434, 1992.
Contact: M.W. Cunliffe, DipCOT, SROT, Royal Preston Hospital, Sharoe Green Lane North, Fulwood, Preston, Lancs PR2 4BR, UK

119. Alternative Strategies in Tone-Reducing AFO Design. Lohman M, Goldstein H, *J Prosthet Orthot* 5(1):1-4, 1993.
Contact: Michael Lohman, MEd, CO, OTR/L, Orthopedic Services Inc., 7820 Wakeley Plaza, Omaha, NE 68114

120. The Control of Genu Recurvatum by Combining the Swedish Knee-Cage and an Ankle—Foot Brace. Isakov E, et al., *Disabil Rehabil* 14(4):187-191, 1992.
Contact: Dr. Eli Isakov, Dept. of Orthopaedic Rehabilitation, Loewenstein Hospital, Ra'anana, Israel

121. The Effect of Functional Knee-Braces on Strain on the Anterior Cruciate Ligament in Vivo. Beynnon BD, et al., *J Bone Joint Surg* 74A(9):1298-1312, 1992.
Contact: B.D. Beynnon, PhD, McClure Musculoskeletal Research Center, Dept. of Orthopaedics and Rehabilitation, University of Vermont College of Medicine, Burlington, VT 05405

122. Evaluation of Soft Foot Orthotics in the Treatment of Patellofemoral Pain Syndrome. Eng JJ, Pierrynowski MR, *Phys Ther* 73(2):62-70, 1993.
Contact: Janice J. Eng, Dept. of Kinesiology, University of Waterloo, Waterloo, ON N2L 3G1, Canada

123. Preliminary Results of Orthotic Treatment for Chronic Low Back Pain. Gavin TM, et al., *J Prosthet Orthot* 5(1):5-9, 1993.
Contact: Michael R. Zindrick, MD, Hinsdale Orthopaedic Associates, Hinsdale, IL 60611
See also 35, 36, 77, 130, 134

PROSTHETICS

124. The All-Terrain Foot. Mathews D, Burgess E, Boone D, *J Prosthet Orthot* 5(1):29-30, 1993.
Contact: David Mathews, CP, Prosthetics Research Study, 720 Broadway, Seattle, WA 98122

125. An Alternative Bent-Knee Prosthesis. Hays RD, et al., *Arch Phys Med Rehabil* 73(11):1118-1121, 1992.
Contact: Ruth D. Hays, MD, Dept. of PM&R, St. Francis Medical Center, 45th & Penn Aves., Pittsburgh, PA 15201

126. A CAD CAM Method for Custom Below-Knee Sockets. Engsberg JR, et al., *Prosthet Orthot Int* 16(3):183-188, 1992.
Contact: Dr. J.R. Engsberg, Human Performance Laboratory, The University of Calgary, 2500 University Dr. N.W., Calgary, AB, T2N 1N4 Canada

127. Function After Through-Knee Compared with Below-Knee and Above-Knee Amputation. Hagberg K, Berlin OK, Renstrom P, *Prosthet Orthot Int* 16(3):168-173, 1992.
Contact: Kerstin Hagberg, Gaskolan, Hjalpmedelscentrum, St. Sigfridsgatan 85, S-41267 Gothenburg, Sweden

128. Functional Evaluation by Gait Analysis of Various Ankle-Foot Assemblies Used by Below-Knee Amputees. Mizuno N, et al., *Prosthet Orthot Int* 16(3):174-182, 1992.
Contact: Mr. N. Mizuno, Dept. of Orthopaedic Surgery, Chubu Rosai Hospital, 1-10-6 Koumei, Minato-ku, Nagoya City, Japan

129. Lower-Limb Proprioception in Above-Knee Amputees. Eakin CL, Quesada PM, Skinner H,

Clin Orthop 284:239-246, 1992.
Contact: Harry B. Skinner, MD, PhD, Dept. of Orthopaedic Surgery, Room U454, University of California at San Francisco, San Francisco, CA 94143-0728

130. Rehabilitation Engineering and Leprosy in Nepal: A Personal View. Meanley S, *J Med Eng Technol* 16(4):165-169, 1992.
Contact: S. Meanley, 53 Northumberland Rd., Leamington Spa, Warks CV32 6HF, UK
See also 3, 116

SPINAL CORD INJURY

131. Assessment of Rehabilitation in Patients with Spinal Cord Injuries: Methodological Considerations. Daverat P, *Paraplegia* 30(11):759-761, 1992.
Contact: P. Daverat, MD, Service de Reeducation Fonctionnelle Neurologique, Hopital Pellegrin, 33076, Bordeaux Cedex, France

132. Bladder Rehabilitation with Dorsal Rhizotomy and Ventral Neuroprosthesis. Baskin LS, Schmidt RA, *Paraplegia* 30(11):783-787, 1992.
Contact: R.A. Schmidt, MD, Dept. of Urology, University of California School of Medicine, San Francisco, CA 94143-0738

133. Computerized Quantitative Radionuclide Assessment of Heterotopic Ossification in Spinal Cord Injury Patients. Kim SW, et al., *Paraplegia* 30(11):803-807, 1992.
Contact: Sun W. Kim, MD, Spinal Cord Injury Service (128), Veterans Affairs Medical Center, 130 W. Kingsbridge Rd., Bronx, NY 10468

134. A Dynamic Pronation Orthosis for the C6 Tetraplegic Arm. Hokken W, et al., *Arch Phys Med Rehabil* 74(1):104-105, 1993.
Contact: Willem Hokken, MD, Dept. of Rehabilitation Medicine, Lichtenberg Hospital, PO Box 4150, 3800 ED Amersfoort, The Netherlands

135. Effect of "Standing" on Spasticity, Contracture, and Osteoporosis in Paralyzed Males. Kunkel CF, et al., *Arch Phys Med Rehabil* 74(1):73-78, 1993.
Contact: Charles Kunkel, MD, VA Medical Center, Rehabilitation Medicine Service (117), 2100 Ridgecrest Dr. SE, Albuquerque, NM 87108

136. The Effect of Surgical Intervention on Rehabilitation Time in Patients with Thoracolumbar and Lumbar Spinal Cord Injuries. Rimoldi RL, et al., *Spine* 17(12):1443-1449, 1992.
Contact: Reynold L. Rimoldi, MD, 12802 Adams St., Garden Grove, CA 92645

137. The Effects of Hyperthermia on the Spinal Cord. Yamane T, et al., *Spine* 17(11):1386-1391, 1992.
Contact: Tomojiro Yamane, MD, Dept. of Orthopedic Surgery, Teikyo University School of Medicine, 2-11-1, Kaga, Itabahi-ku, Tokyo (173) Japan

138. The Force Exerted by the Halo Pin: A Study Comparing Different Halo Systems. Whitesides TE, Mehserle WL, Hutton WC, *Spine* 17(10S):S413-S417, 1992.
Contact: Thomas E. Whitesides, MD, Dept. of Orthopaedics, Emory University School of Medicine, 2165 N. Decatur Rd., Decatur, GA 30033

139. Improving Limb Flexion in FES Gait Using the Flexion Withdrawal Response for the Spinal Cord Injured Person. Granat MH, et al., *J Biomed Eng* 15(1):51-56, 1993.
Contact: Malcolm Howard Granat, Bioengineering Unit, Wolfson Centre, University of Strathclyde, 106 Rottenrow, Glasgow G4 0NW, Scotland, UK

140. Incidence and Risk Factors in the Appearance of Heterotopic Ossification in Spinal Cord Injury. Bravo-Payno P, *Paraplegia* 30(10):740-745, 1992.
Contact: P. Bravo-Payno, MD, Hospital Nacional de Paraplejicos, Toledo, Spain

141. The Mechanical Properties of the Human L4—5 Functional Spinal Unit During Cyclic Loading: The Structural Effects of the Posterior Elements. Asano S, et al., *Spine* 17(11):1343-1352, 1992.
Contact: Satoshi Asano, MD, Dept. of Orthopaedic Surgery, Hokkaido University School of Medicine, Kita-15, Nishi-7, Kita-ku, Sapporo 060 Japan

142. Mouse Emulator for Tetraplegics. Bolton MP, Wytch R, *Med Biol Eng Comput* 30(6):665-668, 1992.

Contact: Dr. M.P. Bolton, Clinical Engineering, R&T Bldg., Withington Hospital, West Didsbury, Manchester M20 8LR, UK

143. A New Scale for the Clinical Assessment of Spinal Cord Function. Botsford DJ, Esses SI, *Orthopedics* 15(11):1309-1313, 1992.
Contact: D.J. Botsford, MD, Toronto Western Hospital, 399 Bathurst St., EC 1-010, Toronto, ON M5T 2S8, Canada

144. Peripheral Nerve Block with Phenol to Treat Spasticity in Spinal Cord Injured Patients. Gunduz S, et al., *Paraplegia* 30(11):808-811, 1992.
Contact: S. Gunduz, MD, Dept. of Physical Therapy and Rehabilitation, Gulhane Military Medical Academy, Etlik, Ankara 06018, Turkey

145. Pin Sensation as a Predictor of Extensor Carpi Radialis Recovery in Spinal Cord Injury. Browne BJ, et al., *Arch Phys Med Rehabil* 74(1):14-18, 1993.
Contact: Stanley R. Jacobs, MD, Dept. of Rehabilitation Medicine, Suite 9420 Gibbon Bldg., Jefferson Medical College, Thomas Jefferson University, 11th & Walnut Sts., Philadelphia, PA 19107

146. Postoperative Wound Infections Following Myocutaneous Flap Surgery in Spinal Injury Patients. Garg M, Rubayi S, Montgomerie JZ, *Paraplegia* 30(10):734-739, 1992.
Contact: M. Garg, MD, Infectious Disease Division, Dept. of Medicine, Rancho Los Amigos Medical Center, 7601 E. Imperial Hwy., Downey, CA 90242

147. Spinal Cord Injury: 10 and 15 Years After. Cushman LA, Hassett J, *Paraplegia* 30(10):690-696, 1992.
Contact: L.A. Cushman, PhD, University of Rochester Medical Centre, Rehabilitation Unit, Box 664, 601 Elmwood Ave., Rochester, NY 14642

148. Spinal Cord Injury: Prognosis for Ambulation Based on Quadriceps Recovery. Crozier KS, et al., *Paraplegia* 30(11):762-767, 1992.
Contact: K.S. Crozier, MD, Dept. of Rehabilitation Medicine, Thomas Jefferson University Hospital, 11th and Walnut Sts., Suite 9604 Gibbon, Philadelphia, PA 19107

149. Suggested MRI Criteria for Surgical Decompression in Acute Spinal Cord Injury. Preliminary Observations. Silberstein M, et al., *Paraplegia* 30(10):704-710, 1992.
Contact: M. Silberstein, FRACR, Dept. of Radiology, Royal Melbourne Hospital, Parkville, Victoria 3001, Australia

150. Sympathetic Skin Response in Spinal Cord Injured Patients: Preliminary Report. Hanson P, et al., *Electromyogr Clin Neurophysiol* 32(10-11):555-557, 1992.
Contact: P. Hanson, MD, University of Mont-Godinne, B-5530 Yvoir, Belgium

151. Upper-Limb Surgery for Tetraplegia. Mohammed KD, et al., *J Bone Joint Surg* 74B(6):873-879, 1992.
Contact: Alastair G. Rothwell, Prof. of Orthopaedic Surgery, Christchurch School of Medicine, Christchurch Hospital, Private Bag 4710, Christchurch, New Zealand
See also 31, 32

SURGERY

See 5, 8, 127, 146, 149

WHEELCHAIRS and POWERED VEHICLES

152. Albatros: An Innovative Low-Cost Wheelchair. Vos R, et al., *Disabil Rehabil* 15(1):44-46, 1993.
Contact: Pieter Fourie, Bureau of Bio-Engineering, PO Box 19063, Tygerberg 7505, Republic of South Africa

WOUNDS and ULCERS

153. Fabrication and Characterization of an Asymmetric Polyurethane Membrane for Use as a Wound Dressing. Hinrichs WLJ, et al., *J Appl Biomater* 3(4):287-303, 1992.
Contact: Prof. Dr. J. Feijen, Dept. of Chemical Technology, University of Twente, PO Box 217, 7500 AE Enschede, The Netherlands

154. A Randomized Trial of Low-Air-Loss Beds for Treatment of Pressure Ulcers. Ferrell BA, Osterweil

D, Christenson P, *JAMA* 269(4):494-497, 1993.
Contact: Bruce A. Ferrell, MD, Sepulveda Veterans Affairs Medical Center (11E), 16111 Plummer St., Sepulveda, CA 91343

See also 146

Periodicals reviewed for
PUBLICATIONS OF INTEREST

Accent on Living
Acta Orthopaedica Scandinavica
Advances in Orthopaedic Surgery
American Annals of the Deaf
American Journal of Occupational Therapy
American Journal of Physical Medicine and Rehabilitation
American Journal of Sports Medicine
American Rehabilitation
Annals of Biomedical Engineering
AOPA Almanac (American Orthotic and Prosthetic Association)
Applied Optics
Archives of Physical Medicine and Rehabilitation
ASHA (American Speech and Hearing Association)
Bio Engineering
Biomaterials, Artificial Cells and Artificial Organs
Biomedical Instrumentation & Technology
British Journal of Occupational Therapy
Caliper (Canadian Paraplegic Association)
Canadian Journal of Occupational Therapy
Canadian Journal of Rehabilitation
Clinical Biomechanics
Clinical Kinesiology
Clinical Orthopaedics and Related Research
Clinical Physics and Physiological Measurement
Clinical Rehabilitation
Communication Outlook
Computer Disability News
CRC Critical Reviews in Biomedical Engineering
DAV Magazine (Disabled American Veterans)
Discover
Electromyography and Clinical Neurophysiology
Electronic Design
Electronic Engineering
Electronics
Ergonomics
Harvard Medical School Newsletter
Headlines: The Brain Injury Magazine
Hearing Journal
Hearing Research
Human Factors: The Journal of the Human Factors Society
IEEE Engineering in Medicine and Biology Magazine
IEEE Transactions in Biomedical Engineering
IEEE Transactions in Systems, Man and Cybernetics
International Disability Studies
International Journal of Rehabilitatic esearch
International Journal of Technolog ng
JAMA
Journal of Acoustical Society of America
Journal of American Optometric Association
Journal of Association of Persons with Severe Handicaps
Journal of Biomechanical Engineering
Journal of Biomechanics
Journal of Biomedical Engineering
Journal of Biomedical Materials Research
Journal of Bone and Joint Surgery—American Ed.
Journal of Bone and Joint Surgery—British Ed.
Journal of Clinical Engineering
Journal of Head Trauma and Rehabilitation
Journal of Medical Engineering and Technology
Journal of Neurologic Rehabilitation
Journal of Optical Society of America A
Journal of Orthopaedic and Sports Physical Therapy
Journal of Orthopaedic Research
Journal of Prosthetics and Orthotics
Journal of Rehabilitation
Journal of Rehabilitation Sciences
Journal of Speech and Hearing Research
Journal of Vision Rehabilitation
Journal of Visual Impairment and Blindness
Laser Focus World
Mayo Clinic Proceedings
Medical and Biological Engineering and Computing
Medical Device and Diagnostic Industry
Medical Electronics
Medical Physics
Medical Progress Through Technology
Medical Psychotherapy Yearbook
Medicine & Science in Sports and Exercise
Military Medicine
New England Journal of Medicine
The Occupational Therapy Journal of Research
Optometry and Vision Science
Orthopaedic Review

Orthopedic Clinics of North America
Orthopedics
Palaestra
Paraplegia
Paraplegia News
Physical and Occupational Therapy in Geriatrics
Physical Medicine and Rehabilitation
Physical Therapy
Physics Today
Physiotherapy
Proceedings of the Institution of Mechanical Engineers—Part H: Journal of Engineering in Medicine
Rehab Management
Rehabilitation Digest
Rehabilitation World
Robotics World
Scandinavian Journal of Rehabilitation Medicine
Science
Science News
Scientific American
SOMA: Engineering for the Human Body
Speech Technology
Spine
Sports 'N Spokes
Technical Aid to the Disabled Journal
Techniques in Orthopaedics
Topics in Geriatric Rehabilitation
VA Practitioner
Vanguard
Volta Review
Worklife

CALENDAR OF EVENTS

NOTE: An asterisk at the end of a citation indicates a new entry to the calendar.

1993

December 7-12, 1993
American Academy of Neurological and Orthopaedic Surgery: 17th Annual Convention, Las Vegas, NV
Contact: Dr. Michael R. Rask, 2320 Rancho Drive, Suite 108, Las Vegas, NV 89102-4592

December 8-12, 1993
Fifth International Symposium on Neural Regeneration, Pacific Grove, CA
Contact: Office of Regeneration Research Programs (151N), VA Medical Center, Portland, OR 97201; Tel: 503-273-5193; FAX: 503-721-7906*

1994

(no date yet), 1994
16th Annual International Conference of the IEEE/EMBS, Baltimore, MD
Contact: Dr. Joshua Tsitlik, Johns Hopkins School of Medicine, Rm 410 Traylor Bldg., 720 Rutland Ave., Baltimore, MD 21205

January 28-29, 1994
Third Annual Symposium on Pathomechanical Conditions of the Human Body, New Orleans, LA
Contact: Deanna Fish, CPO; Tel: 800-866-7522, ext: 23*

January 31-February 4, 1994
Visions in Mobility International Mobility Conference-7, Melbourne, Australia
Contact: Royal Guide Dogs Associations of Australia, Chandler Highway, Kew, Victoria 3101, Australia; Tel: +61-3-860-4444; Fax: +61-3-860-4500

February 17-19, 1994
10th International Seating Symposium, Vancouver, BC Canada
Contact: Seating Symposium, Room 105-2194 Health Sciences Mall, The University of British Columbia, Vancouver, BC Canada V6T 1Z3; Tel: 604-822-4965; Fax: 604-822-4835*

February 24-March 1, 1994
Annual Meeting of American Academy of Orthopedic Surgeons, New Orleans, LA
Contact: 222 South Prospect Avenue, Park Ridge, Ill, 60068*

March 15-20, 1994
American Academy of Orthotists and Prosthetists (AAOP), Annual Meeting and Scientific Symposium, Nashville, TN
Contact: Annette Suriani, AAOP, 1650 King St., Alexandria, VA 22314; Tel: (703) 836-7116

March 16-19, 1994
CSUN'S Ninth Annual International Conference, Technology and Persons with Disabilities, Los Angeles, CA
Contact: Dr. Harry J. Murphy, Center on Disabilities, California State University, Northridge, 18111 Nordhoff Street-DVSS, Northridge, CA 91330; Tel: 818-885-2578; Fax: 818-885-4929*

March 22-27, 1994
Academy Annual Meeting and Scientific Symposium, Nashville, TN
Contact: Annette Suriani; Tel: 703-836-7116*

March 23-26, 1994
AAOP Annual Meeting and Scientific Symposium, Nashville, TN
Contact: Annette Suriani, National Office; Tel: 703-836-7118*

March 27-30, 1994
IFAC Symposium on Modeling and Control in Biomedical Systems, Galveston, TX

Contact: Susan George, IFAC Biomedical Symposium, University of Texas Medical Branch, Box 55176, Galveston, TX 77555-5176; Tel: 409-770-6628; Fax: 409-770-6825*

April 6-12 1994
17th International Conference on Medical and Biological Engineering and 10th International Conference on Medical Physics, Rio de Janeiro, Brazil
Contact: Mr. OZ Roy, Sec Gen Intl, Union for Physical and Engineering Sciences in Medicine, c/o National Research Council, Room 307, Building M-50, Ottawa, Ontario, K1A OR8, Canada

April 7-9, 1994
BME'94 International Conference on Biomedical Engineering, Hong Kong
Contact: BME'94 Conference Secretariat, c/o Rehabilitation Engineering Centre, Hong Kong Polytechnic, Hunghom, Kowloon, Hong Kong; Tel: 852-766-7683; Fax: 852-362-4365

April 9-16, 1994
IRMA VII—Seventh World Congress of the International Rehabilitation Medicine Association: 25th Anniversary of IRMA, Washington, DC
Contact: IRMA VII, 875 Kings Hwy., West Deptford, NJ 08096

April 9-16, 1994
XIIth World Congress of the Rehabilitation Medicine Association, Washington, DC
Contact: Ms. D. Jones, 1333 Moursund, A-221, Houston, TX 77030

April 16-17, 1994
Thirteenth Southern Biomedical Engineering Conference, Washington, DC
Contact: Jafar Vossoughi, PhD, 4401-A Connecticut Avenue, NW, Suite 327, Washington, DC 20008; Tel: 202-282-2388; Fax: 202-282-3677*

April 17-22, 1994
11th International Congress of the World Federation of Occupational Therapists, London, United Kingdom
Contact: Conference Associates and Services Ltd - WFOT, Congress House, 55 New Cavendish Street, London W1M 7RE, UK; Tel: 071-486-0531; Fax: 071-935-7559

April 25-27, 1994
Annual Conference of the American Spinal Injury Association, Philadelphia, PA
Contact: Jane Mulkey, ASIA, 2020 Peachtree Road, Atlanta, GA 30309; Tel: 404-335-9772*

May 31-June 2, 1994
Annual Meeting of International Medical Society of Paraplegia, Kobe, Japan
Contact: Host Organizer, IMSOP 1994 Annual Meeting, Japan Organizing Committee, Orthopedic Department of Tokushima University 3, Kuramoto-cho, Tokushima-shi, 770, Japan; Tel: 0886-31-3111; Fax: 0886-33-0178

June 2-3, 1994
Improving the Quality of Physical Therapy, International Conference, 's-Hertogenbosch, The Netherlands
Contact: Mr. J. Dekker, PhD or Ms. E. Zoer, PO Box 1568, 3500 BN Utrecht, The Netherlands; Tel: 31-30-319946; Fax: 31-30-319290

June 4-8, 1994
Annual Conference of The American Physical Therapy Association, Toronto, Canada
Contact: APTA, 111 N. Fairfax Street, Alexandria, VA 22314; Tel: 703-706-3169*

June 9-10, 1994
Second Annual International Conference,"Virtual Reality and Disabilities," San Francisco, CA
Contact: Dr. Harry J. Murphy, Center on Disabilities, California State University, Northridge, 18111 Nordhoff Street-DVSS, Northridge, CA 91330; Tel: 818-885-2578; Fax: 818-885-4929*

June 17-22, 1994
17th Annual RESNA Conference, Nashville, TN
Contact: RESNA, 1101 Connecticut Avenue NW, Suite 700, Washington, DC 20036; Tel: 202-857-1199*

June 21-24, 1994
10th Congress of the International Society of Electrophysiology and Kinesiology, Charleston, SC
Contact: ISEK Congress, Dr. Richard Shiavi, Biomedical Engineering, Box 6117, Station B, Vanderbilt University, Nashville, TN 37235*

June 29-July 1, 1994
American Control Conference, Baltimore, MD
Contact: Prof. Hassan Khalil, Department of Electrical Engineering, Michigan State University, East Lansing, MI 48823-1226; Tel: 517-355-6689; Fax: 517-353-1980*

July 4-7, 1994
The Second Biennial European Joint Conference on Engineering Systems Design and Analysis (ESDA), London, England
Contact: Dr. Minoo Debestani or Professor P.S. Walker, Department of Biomedical Engineering, Institute of Orthopaedics, Brockley Hill, Stanmore, Middlesex HA7 4LP, England*

July 5-8, 1994
Dundee '94—International Conference on Clinical Gait Analysis, Dundee, Scotland
Contact: Dundee '94 Secretariat, Dundee Limb Fitting Centre, 133 Queen Street, Broughty Ferry, Dundee DD5 1AG, Scotland*

July 10-15, 1994
2nd World Congress of Biomechanics, Amsterdam
Contact: Biomechanics Section, Institute of Orthopaedics, University of Nijmegen, PO Box 9101, 6500 HB Nijmegen, Netherlands*

August 15-19, 1994
Rehabilitation Ergonomics, Toronto, Ontario, Canada
Contact: IEA '94 Secretariat, c/o JPdL Multimanagement Inc., Toronto Dominion Centre, 55 King Street West, Suite 2550, Toronto, ON, Canada M5K 1EZ; Tel: (416) 784-9396; Fax: (416) 784-0808

August 21-26, 1994
World Congress on Medical Physics and Biomedical Engineering, Rio de Janeiro, Brazil
Contact: Conference Secretariat, Rua do Ouvidor, 60/414 Rio de Janeiro, CEP 20040, Brazil; Tel: +55 21 224 6080; Fax: +55 21 231. 1492

September 4-9, 1994
6th European Regional Conference of Rehabilitation International, Budapest, Hungary
Contact: Rehabilitation Secretariat, ISM Limited, The Old Vicarage, Haley Hill, Halifax HX3 6DR, UK; Tel: 44(0)422 359 161; Fax: 44(0)422 355 604

September 19-21, 1994
4th IFAC Symposium on Robot Control (SY.RO.CO.'94), Capri, Italy
Contact: Prof. Salvatore Nicosia, SY.RO.CO.'94 Scientific Secretariat, Departimento di Ingegneria Elettronica, Universita' degli Stidi di Roma "Tor Vergata", Via della Ricerca Scientifica, 00133 Roma, Italy; Fax: +39-81-7683186*

October 11-15, 1994
American Orthotic and Prosthetic Association (AOPA), Annual National Assembly, Washington, DC
Contact: Annette Suriani, AOPA, 717 Pendleton St., Alexandria, VA 22314; Tel: (703) 836-7116

November 8-11, 1994
Third International Conference on Automation, Robotics, and Computer Vision, Singapore
Contact: Prof. N. Sundararajan, c/o UCARCV'94 Conference Secretariat, Institution of Engineers, Singapore, 70 Bukit Tinggi Road, Singapore 1128, Republic of Singapore; Tel: 65-469-5000; Fax: 65-467-1108*

November 18-21, 1994
American Speech-Language-Hearing Association (ASHA), Annual Convention, New Orleans, LA
Contact: Frances Johnston, ASHA, 10801 Rockville Pike, Rockville, MD 20852; Tel: (301) 897-5700

December 7-10, 1994
8th International Conference on BioMedical Engineering, Singapore
Contact: The Secretary, 8th ICBME 1994, Department of Orthopaedic Surgery, National University Hospital, Lower Kent Ridge Road, Singapore 05ll; Tel: (65) 772-4424; Fax: (65) 778-0720*

1995

February 16-18, 1995
11th International Seating Symposium, Pittsburgh, PA
Contact: Elaine Trefler or Jill Bebout, University of Pittsburgh Medical Center, Department of Conference Management, Nese-Barkan Building, Suite 511,

Pittsburgh, PA 15213-2593; Tel: 412-647-8218; Fax: 412-647-8222*

March 27-31, 1995
International Federation of Physical Medicine and Rehabilitation (IFPMR), Sydney, Australia
Contact: Dianna Crebbin Conferences, PO Box 629, Willoughby NSW 2068, Australia; Tel: +61 (02) 417-8525; Fax: +61 (02) 417-8513*

April 2-7, 1995
International Society for Prosthetics and Orthotics (ISPO), 1995 World Congress, Melbourne, Australia
Contact: ISPO, Australian National Member Society, Repatriation General Hospital, Banksia St., Heidelberg, 3081 Victoria, Australia; Tel: +61 (03) 499 6099

July 9-16, 1995
4th World Congress of Neuroscience, Kyoto, Japan
Contact: Host Organizer, Secretariat, 4th World Congress of Neuroscience, c/o International Communications, Inc., Kasho Building, 2-14-9, Nihonbashi, Chuo-ku, Tokyo 103, Japan; Tel: 03-3272-7981; Fax: 03-3273-2445

November 17-20, 1995
American Speech-Language-Hearing Association (ASHA), Annual Convention, Cincinnati, OH
Contact: Frances Johnston, ASHA, 10801 Rockville Pike, Rockville, MD 20852; Tel: (301) 897-5700

*U.S. G.P.O.:1993-343-226:80001

BACK ISSUE ORDER FORM

Back issues/reprints of the *Journal of Rehabilitation Research and Development* and *Rehabilitation R&D Progress Reports* are available on request, free of charge, when in stock. Check any you wish to receive.

_____ Vol. 20 No. 1 (July 1983)
_____ Vol. 20 No. 2 (*Progress Reports 1983*)
_____ Vol. 21 No. 1 (January 1984)
_____ Vol. 21 No. 2 (April 1984)
_____ Vol. 21 No. 3 (*Progress Reports 1984*)
_____ Vol. 22 No. 1 (January 1985) Special Articles: Evaluation [*out of print*]
_____ Vol. 22 No. 2 (April 1985) Index of Rehabilitation Literature [*out of print*]
_____ Vol. 22 No. 3 (July 1985) Special Articles: Low Vision, Wheelchairs [*out of print*]
_____ Vol. 22 No. 4 (*Progress Reports 1985*) [*out of print*]
_____ Vol. 23 No. 1 (January 1986) Sensory Aids for Hearing Impairment [*out of print*]
_____ Vol. 23 No. 2 (April 1986) Special Articles: Wheelchairs [*out of print*]
_____ Vol. 23 No. 3 (July 1986) Special Articles: Spinal Cord Injury, FES
_____ Vol. 23 No. 4 (October 1986)
_____ Vol. 24 No. 1 (*Progress Reports 1986*) [*out of print*]
_____ Vol. 24 No. 2 (Spring 1987) Special Articles: Hearing Impairment, Wheelchairs [*out of print*]
_____ Vol. 24 No. 3 (Summer 1987) Clinical Articles: Microstomia, Hip Replacement
_____ Vol. 24 No. 4 (Fall 1987) Sensory Aids for Hearing Impairment [*out of print*]
_____ Vol. 25 No. 1 (*Progress Reports 1987*) [*out of print*]
_____ Vol. 25 No. 2 (Spring 1988) JRRD Index: 1981-1987
_____ Vol. 25 No. 3 (Summer 1988)
_____ Vol. 25 No. 4 (Fall 1988) Special Articles: Speech Communication
_____ Annual Supplement (*Progress Reports 1988*)
_____ Vol. 26 No. 1 (Winter 1989) Special Articles: Wheelchairs [*out of print*]
_____ Vol. 26 No. 2 (Spring 1989) JRRD Index: Vol. 25-1988 [*out of print*]
_____ Vol. 26 No. 3 (Summer 1989)
_____ Vol. 26 No. 4 (Fall 1989)
_____ Annual Supplement (*Progress Reports 1989*)
_____ Vol. 27 No. 1 (Winter 1990) JRRD Index: Vol. 26-1989
_____ Vol. 27 No. 2 (Spring 1990)
_____ Vol. 27 No. 3 (Summer 1990)
_____ Vol. 27 No. 4 (Fall 1990)
_____ Vol. 28 No. 1 (*Progress Reports 1990*)
_____ Vol. 28 No. 2 (Spring 1991) JRRD Index: Vol. 27-1990
_____ Vol. 28 No. 3 (Summer 1991)
_____ Vol. 28 No. 4 (Fall 1991)
_____ Vol. 29 No. 1 (Winter 1992) JRRD Index: Vol. 28-1991
_____ Vol. 29 No. 2 (Spring 1992)
_____ Vol. 29 No. 3 (Summer 1992)
_____ Vol. 29 No. 4 (Fall 1992)
_____ Vol. 30 No. 1 (1993)

Label ID Number: _____

Name: _____

Address: _____
Street Apt. #

_____
City State Zip Code

Country: _____
Postal Code

Please mail this form with your request to:

Publications Back Order Department
Scientific and Technical Publications Section (117A)
VA Rehabilitation R&D Service
103 South Gay Street
Baltimore, Maryland 21202-4051

Fax orders accepted:
Commercial Users: (410)962-9670
FTS Users: (8)410-962-9670

JRRD On-Line

Selected portions of the *Journal of Rehabilitation Research and Development* (JRRD) are being put on-line via CompuServe. Abstracts of scientific articles, Calendar of Events, and Publications of Interest are available to readers through **JRRD On-Line.**

Subscribers to CompuServe may access **JRRD On-Line** by typing "GO REHAB" (or "GO HUD" and selecting the "Research and Development" menu option).

USING THE EXISTING VA REHABILITATION DATABASE ON COMPUSERVE

I. **What you need: Access to equipment and software.**
- Personal computer
- Modem with communication software
- Subscription to CompuServe (connect time costs range from $6/hour [300 baud] to $12.50/hour [1200 baud], prices vary with baud rate).

II. **You can get help if needed:**
- VA Rehabilitation Database — write or call
  Scientific and Technical Publications Section (117A)
  VA Rehabilitation R&D Service
  103 South Gay Street
  Baltimore, Maryland 21202-4051
  Phone: 410-962-1800

III. **The VA Rehabilitation Database is user friendly:**
- A user friendly system is a central design feature of the database. No previous experience with computers is necessary and very little learning is required. The system makes obtaining information about rehabilitation devices as easy as making a telephone call.

IV. **Eligibility:**
- The VA Rehabilitation Database is available for use by anyone who subscribes to CompuServe.